Adapting Aquaculture for Sisal

Integrating social and environmental design for local context

CEGM3000: Multidisciplinary Project

Group MP402

Delft University of Technology

TU Delft

FAST

TU Delft | University Fund

Adapting Aquaculture for Sisal

Integrating social and environmental design for local context

by

Group MP402

Student Name	Student Number
Ties ter Laan	5170273
Joppe van Hoeve	5109523
Lars Olde Riekerink	6292208
Martijn de Boer	5076706
Silvester den Boer	6318169

Instructors TU Delft: Dr.ing. JA Antolínez, Jan Anne Annema, JO Colomes Gene PhD and Dr.ir. L. van Biert
Instructors UNAM: Dr. A. Torres Freyermuth, Dr. J.A. Kurczyn Robledo and Dr. C. Rosas-Vazquez
Project Duration: Sep, 2025 - Nov, 2025

TU Delft

Preface

This report has been made by Group MP402 as part of the Multidisciplinary Project (MDP) CIEM3000 course at TU Delft. The project was carried out in collaboration with the Universidad Nacional Autónoma de México (UNAM) and the University of Technology Delft. The report focuses on exploring the design and multifunctionality of aquaculture in Sisal, Yucatán.

Working across disciplines and institutions has provided an invaluable opportunity to approach the topic of sustainable aquaculture from both technical and social perspectives. Throughout this project, we have aimed to combine engineering analysis with local context and community engagement, seeking to create a balanced and realistic concept for offshore aquaculture in the region.

We would like to express our gratitude to our supervisors at TU Delft: Dr.ing. J.A. Antolínez, J.A. Annema, J.O. Colomés Gené PhD, and Dr.ir. L. van Biert, for their continuous support and valuable feedback during all stages of the project. Our sincere thanks also go to our UNAM supervisors: Dr. A. Torres Freyermuth, Dr. J.A. Kurczyn Robledo, and Dr. C. Rosas-Vázquez, for their guidance, local expertise, and warm collaboration in Mexico.

We are grateful for the opportunity to take part in this international collaboration, which has allowed us to combine knowledge from different disciplines and cultural contexts. Working together as a team has been both a challenge and a very rewarding experience, teaching us how diverse expertise can come together to solve complex problems. We hope that this report provides useful insights for future studies and contributes to the continued development of sustainable aquaculture in Sisal.

Finally, we would like to thank Fastfund and the Lamminga fund, to make this research financially possible and we would like to thank Aquastructures for providing us a license to use their Aquasim hydrodynamic simulation tool.

Group MP402
Sisal, October 2025

Summary

The outcome of this multidisciplinary project, conducted collaboratively between Delft University of Technology and the Universidad Nacional Autónoma de México (UNAM), is a single, locally grounded model for sustainable, small-scale, community-led aquaculture in Sisal, Yucatán. Sisal's coastal community relies heavily on traditional fishing, which faces economic vulnerability due to seasonal variations, market fluctuations, and regulations. Aquaculture presents an opportunity to diversify income and enhance resilience. This research sought to develop a practical and community-supported aquaculture model by addressing two core questions: first, how the fish farm's design can be adapted for Sisal's local environmental extremes, including energetic waves and currents and second, which additional functions can be integrated to maximize ecological benefit, economic value, and secure social acceptance within the community. The resultant design emphasizes operational efficiency, resilience against storms, and transparency in its purpose and benefits.

The core analysis employed a combined multidisciplinary approach. Hydrodynamic modelling assessed the structural viability of different cage designs under realistic local conditions. Concurrently, a social analysis determined community priorities using the Triple Bottom Line (TBL) framework (Planet, People, Profit). Input was collected through questionnaires administered to local fishers and high school students. A Multi-Criteria Decision Analysis ranked potential multifunctional options based on these stakeholder priorities, followed by an assessment of the practical attainability.

The technical analysis compared standard circular cage geometry against a more novel vessel-shaped configuration. The vessel-shaped cage demonstrated superior hydrodynamic stability, exhibiting reduced deformation and significantly lower mooring line loads, particularly under extreme storm conditions (up to a 23% reduction compared to the circular cage in the 20-year storm scenario). Its streamlined design was also found to offer considerably lower resistance during towing operations, directly addressing the community's need for a system that can be easily relocated using local vessels for maintenance or storm preparedness.

The social analysis revealed a strong consensus among both students and fishers, who ranked ecological protection (Planet) as the highest priority. This clear preference guided the selection of multifunctional options, favouring those that are visible, simple to operate, and encourage community participation. The MCDA consequently ranked artificial reefs around the cages, educational and research visits, and snorkelling/ecotourism as the most desirable additions. Complex, capital-intensive options were deemed less suitable, reinforcing the importance of local ownership and minimizing dependency on external resources or expertise. The attainability assessment confirmed the feasibility of implementing the top choices, specifically recommending locally fabricated Reef Balls for reefs, guided surface snorkelling, integrated educational programs, a spotter buoy and a basic safety kit.

Synthesizing these findings, the final design recommendation proposes a small, vessel-shaped cage. This structure is to be anchored using modular artificial reefs, specifically Reef Balls, fabricated locally. This innovative anchoring approach directly merges the technical requirement for robust mooring with the primary social and ecological priority for visible habitat enhancement. The system incorporates simple, attainable multifunctional features, including a standardized safety kit on the platform and secured environmental sensors, enhancing transparency and safety without adding complexity.

In conclusion, this project offers a defined, replicable model for small-scale, community-led aquaculture specifically tailored to Sisal. It demonstrates how technical resilience can converge with social simplicity. The long-term success of such an initiative is contingent upon aligning robust engineering with sustained social legitimacy, ensuring the system is genuinely owned, valued, and maintained by the community itself. Full-scale deployment, however, should prudently follow the completion of identified next research steps, such as controlled flume validation of the design, further optimization of anchoring configurations, and studies addressing long-term governance and operational responsibilities.

Contents

Nomenclature

Abbreviations

Abbreviation	Definition
ADCP	Acoustic Doppler Current Profiler
EVA	Extreme Value Analysis
RBF	Radial Basis Function
GDP	Generalized Pareto Distribution
HDPE	High-Density Polyethylene
IMTA	Integrated Multi-Trophic Aquaculture
MAE	Mean Absolute Directional Error
MCDA	Multi Functionality Decision criteria
MWDF	Mean Wave Drift Force
POT	Peaks Over Threshold
RBF	Radial Basis Function
TBL	Triple Bottom Line Framework
UNAM	Universidad Nacional Autónoma de México

Symbols

Symbol	**Definition**	**Unit**
A	Area	[m^2]
D_p	Peak wave direction	[$^\circ$]
F_d	Drag force	[N]
g	Gravity	[m/s^2]
H_b	Breaking wave height	[m]
H_s	Significant wave height	[m]
H_{rms}	RMS wave height	[m]
h	Water depth	[m]
Q_{95}	95th percentile	[m] or [m/s]
RL_T	T-year return level	[m]
S	Stress index	[-]
T	Return period	[yr]
T_m	Mean wave period	[s]
T_p	Peak wave period	[s]
U	Current speed	[m/s]
u	POT threshold	[m]
u_c	East–West velocity	[m/s]
v_c	North–South velocity	[m/s]
u_r	Resultant velocity	[m/s]
V	Velocity	[m/s]
ρ	Density	[kg/m^3]
C_d	Drag coefficient	[-]
σ	Standard deviation	[-]
σ_u	GPD scale	[m]
ξ	GPD shape	[-]
λ	Poisson rate	[1/yr]

1

Introduction

Sisal is a small coastal community in the state of Yucatan, Mexico, historically known as an old port and fishing village. It has since evolved into a quiet town centred on fishing, tourism, and marine research. The population relies heavily on small-scale coastal fisheries, which remain a vital part of local livelihoods and cultural identity. Alongside fishing, tourism and services connected to nearby biosphere reserves and marine research centres have become increasingly important sources of employment.

Despite its strong connection to the sea, the economic base of Sisal remains narrow and vulnerable to environmental and market fluctuations. Periods of low catch rates, price instability, and government restrictions on specific species often create financial uncertainty for fishers and their families. For instance, the octopus fishery is subject to an annual closed season to protect stocks, temporarily limiting fishing activities. This illustrates a broader challenge: the community's income is strongly tied to seasonal and ecological variability.

In this context, aquaculture presents an opportunity to diversify income sources and strengthen economic resilience. Developing sustainable fish farming systems can help reduce dependence on wild-capture fisheries, provide year-round employment, and contribute to food security. Moreover, Sisal offers favourable conditions for aquaculture development. Technical expertise and juvenile fish supplies can be supported by the presence of marine research infrastructure, including the Universidad Nacional Autónoma de México (UNAM) coastal station and hatchery facilities.

By introducing aquaculture as a complementary activity to traditional fishing, the community can build a more stable and diversified coastal economy. This approach not only addresses income variability but also aligns with sustainable development goals, balancing environmental care with social and economic benefits for the people of Sisal.

1.1. Goals and Motivation of the Study

The main goal of this study is to explore the potential for developing sustainable aquaculture in Sisal that benefits both the local community and the coastal environment. The research aims to design a fish farming system capable of operating safely under local ocean conditions while fitting within the social and economic reality of Sisal. By combining technical and social perspectives, the project seeks to provide a realistic and community-supported model for aquaculture development.

The motivation for this study arises from the need to diversify local livelihoods and create more stable income opportunities. While fishing remains a central part of Sisal's identity and economy, it does not always ensure consistent earnings throughout the year. External factors such as changing weather patterns, market fluctuations, and management regulations can restrict fishing activity or reduce profitability. Aquaculture offers a complementary activity that can help mitigate these challenges by providing year-round employment and a more predictable source of income.

Beyond economic benefits, aquaculture can also enhance food security and environmental sustainability. Locally produced fish can reduce dependence on wild catches and give options to diversify in-

come, thereby helping to protect marine ecosystems while supplying fresh products to the community. Moreover, aquaculture can foster opportunities for education, research, and eco-tourism, particularly through collaboration with UNAM's coastal research station, which is actively involved in sustainable marine development.

In summary, the aim of this project is twofold: to design an aquaculture system that is technically feasible under Sisal's environmental conditions, and to ensure that it is socially acceptable and beneficial for the local population. By integrating these dimensions, the study seeks to contribute to a more resilient and sustainable future for the community of Sisal.

1.2. Research Questions

To achieve the study's goals, two main research questions have been formulated. These reflect the dual focus of the project, which are combining technical feasibility with social and community perspectives:

- *How can the fish farm's design be adapted for the local environmental conditions of Sisal?*
- *Which additional functions can be integrated into the fish farm to maximize ecological benefit, economic value, and local acceptance in Sisal?*

1.3. Structure of the Report

The remainder of this report is organized into chapters that together address the two main research questions and lead toward an integrated conceptual design for aquaculture in Sisal. The structure reflects the multidisciplinary nature of the study, combining both technical and social perspectives to create a complete understanding of the topic.

Chapter 2, Literature Review: This chapter presents the theoretical background and existing knowledge relevant to the study. It reviews prior research on aquaculture technologies, environmental conditions influencing cage design, and social dimensions of aquaculture development. The literature review provides the foundation for understanding both the technical and community-related challenges that guide this project.

Chapter 3, Problem Analysis: This chapter outlines the key challenges for developing aquaculture in Sisal: community acceptance and engineering feasibility. It defines the scope of both the technical and social studies and explains how they complement each other. The engineering part examines suitable cage designs for local sea conditions, while the social part explores multifunctional uses that could increase community support. The chapter concludes by presenting the research questions that guide the rest of the report.

Chapter 4, Social acceptance through multi-functionality: Focuses on the social dimension of the study by examining how aquaculture can gain community support through multifunctional uses. It explores ways in which aquaculture could provide additional benefits, such as tourism, education, research, or habitat enhancement. This to ensure that the initiative contributes positively to local livelihoods and values.

Chapter 5, Environmental conditions assessment: Will summarize the findings from the environmental data analysis presented in Appendix F, which establishes the environmental design conditions for offshore aquaculture near Sisal. This includes the study of waves and currents, which are key hydrodynamic factors that influence cage stability, mooring design, and operational safety. The chapter will highlight the main results most relevant for the engineering analysis that follows.

Chapter 6, Design optimization: Builds on the environmental findings to evaluate and compare potential fish cage designs. It examines how different configurations perform under local conditions and identifies the most suitable design for safe and practical operation. After this, the findings from the social and technical studies are integrated to propose a first conceptual aquaculture design for Sisal. This design combines engineering feasibility and social insights, ensuring that it is both technically sound and aligned with community needs and multifunctional opportunities.

Chapter 7, Further research: Discusses topics that emerged during the study which require additional investigation. It provides recommendations for future research directions, pilot studies, and technical or social aspects that could strengthen the development and implementation of aquaculture in Sisal.

Chapter 8, Conclusion: At last, the conclusion will be given. This chapter summarizes the main findings of the project, reflects on the research questions, and highlights how the combination of technical and social perspectives has contributed to a holistic understanding of aquaculture development in Sisal. It closes the report by emphasizing the relevance of the results for future sustainable initiatives in the region.

2

Background

2.1. Introduction

This chapter presents an overview of the project background to clarify the problem that this study aims to address. It begins with a brief description of Sisal and its surrounding environment to provide a clearer understanding of the geographical, ecological and social setting in which the project takes place. To complement this, the current state of aquaculture in the region is discussed, outlining both existing practices and the challenges that shape its development.

The chapter then summarises the work conducted last year in Sisal by the MDP group (MP374) Bakker et al. (2024). Reviewing their findings helps to place this study within a broader research context and highlights the progress already made as well as the gaps that remain.

Following this, the remainder of the literature review explores essential elements of offshore aquaculture. Topics such as ecological impacts, the technical and logistical complexity of operating fish farms at sea and the range of potential cage configurations are discussed in greater depth. Finally, attention is given to the acceptance of fish farms within the local community, acknowledging that long-term success depends not only on engineering solutions but also on social support and local participation.

2.2. Sisal

Sisal is a small coastal fishing town in the municipality of Hunucmá in the state of Yucatan, Mexico with approximately 2000 residents [Bakker et al., 2024]. It lies about 53 kilometres north-west of Mérida on the Gulf of Mexico. Historically, Sisal served as an important port until the 1950s. Exporting the so-called Sisal fibres around the world in the form of ropes. Until the invention of synthetic fibres suddenly diminished demand [Fernández, 2024] Today, it remains a fishing community with growing interest in tourism and ecotourism. The area has an interesting coastal environment that includes mangroves, shallow bays and open sea. The coastal system experiences seasonal weather variation and exposure to waves, currents and occasional hurricanes.

No offshore aquaculture farm has yet been successfully implemented along Sisal's coast. About a decade ago, an industrial company attempted to install large cages but failed: the heavy equipment was unsuitable for local conditions, the cages repeatedly broke during storms and, crucially, local fishers had not been involved in planning or maintenance [Bakker et al., 2024].

Despite this history, UNAM considers Sisal a promising site for community-scale aquaculture. Small farms could supplement fishers' seasonal and often unpredictable income, reducing reliance on wild catches and providing greater economic stability for local families. The vision is for modest, low-impact cages that integrate with the marine environment, creating benefits for residents while avoiding large-scale industrial disruption.

A relevant example for Sisal is Celestún; a coastal town west of Sisal that has successfully adopted community-based aquaculture after earlier industrial attempts in the region had failed. Local coopera-

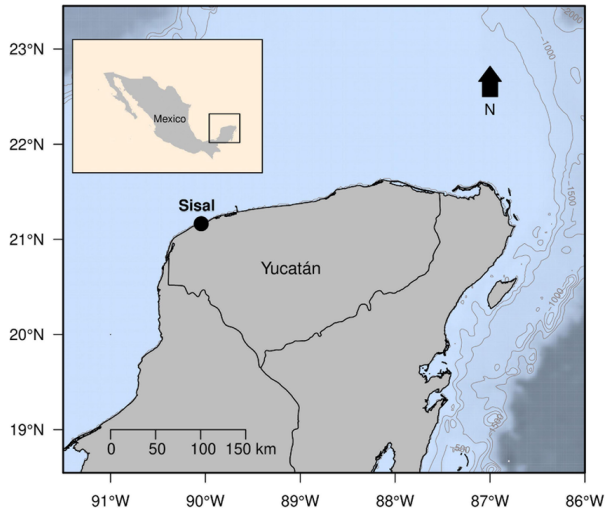

Figure 2.1: Sisal, located in Yucatan [Quijano Quiñones et al., 2021]

tives now operate small, manageable fish farms using designs suited to the shallow seabed and local wave conditions. These farms are maintained and repaired by the fishers themselves, keeping costs low and ensuring local ownership.

However, several challenges remain, as identified by professors at UNAM:

- **Environmental risk:** Harmful algae blooms (red tides) have become more frequent and severe, threatening fish stocks, both inside and outside the fish farms, if a bloom persists nearby.
- **Vandalism:** Offshore monitoring equipment is often stolen, limiting scientific measurements of wave climate and currents. As a result, selecting the most suitable site within approximately 40 km offshore remains uncertain.
- **Community ownership:** Fishers must be able to maintain cages themselves to avoid dependence on outside contractors, which undermined Celestún's early adoption of aquaculture.

Alongside these hurdles, local facilities already offer a foundation for progress. The UNAM hatchery in Sisal maintains stock of several marine species, hatches eggs and raises larvae to juvenile size before releasing them to coastal cooperatives. This continuous supply of juveniles lowers entry barriers for fishers and strengthens participation, providing a practical pathway toward sustainable small-scale aquaculture.

2.3. Prior Work on Aquaculture in Sisal

Bakker et al. (2024) set out to develop a practical concept for offshore fish farming at Sisal with the aim of supporting local fishers affected by seasonal restrictions. Their study covered three main aspects, identifying a suitable offshore distance that fits local environmental and community conditions, designing anchoring and cage layouts that can withstand local wave and current regimes, and evaluating ecological impacts together with community attitudes to maximise local acceptance.

The overall intent was to create a durable and affordable cage system that matches Sisal's environment and can be maintained by the community without outside contractors. To that end the team proposed a deadweight anchoring system and a corresponding structural cage concept. Numerical simulations in ProteusDS explored different diameter-to-depth ratios. Since, Sisal has a limestone seabed, deadweight anchors were judged most feasible since they minimise dependence on external marine contractors. The team also simulated single-cage and multi-cage arrays to compare the robustness of alternative layouts, and for each configuration they sized the required anchor mass. Under a design condition of 3.4 m significant wave height with an 8 second period and a 0.5 ms^{-1} current, multi-anchor layouts aligned to dominant north to north-east waves and east to west currents reduced line tension and improved global stability.

The research considered the optimal offshore distance. The analysis identified a site about 8 km from the coast as a workable compromise. Nearer sites risk lower water quality and greater stress on fish during warm periods, while more distant sites increase fuel use and operational costs.

Ecological sustainability and community acceptance were studied in parallel. Lessons from the Celestún cooperative suggested that small cages, shared upkeep and local repair capacity are important enablers of long-term operation. Interviews indicated that earlier failures by industrial operators had created distrust among fishers. Yet, respondents were open to participation provided the design remained affordable, easy to tow, safe for tourism and manageable with local skills.

The MP374 report concluded with several recommendations: involve fishers more deeply in design and maintenance planning, test alternative anchoring materials and layouts to withstand extreme storms, refine cost estimates with local supply chains, and link aquaculture with eco-tourism to diversify income for cooperatives.

2.4. Elements of Aquaculture

2.4.1. Ecological Impact

Fish farming exerts multiple pressures on marine ecosystems. Nutrient enrichment from uneaten feed and faeces is one of the most documented impacts, with aquaculture recognised as a significant driver of coastal nutrient loading [Bouwman et al., 2013]. Elevated nitrogen and phosphorus levels can lead to eutrophication, harmful algal blooms, and shifts in benthic and microbial communities [Braña et al., 2021]. On the seabed, organic matter accumulation causes oxygen depletion and the loss of sensitive species. In ecosystems dominated by large aquatic plants, such as seagrasses, these effects can result in habitat decline and altered community structure [Boudouresque et al., 2020].

Fish farms also modify ecosystem dynamics by aggregating wild fish. Farms act as feeding hotspots where waste feed attracts large biomasses, reshaping local food webs and increasing the potential for disease or parasite transmission between farmed and wild populations [Dempster et al., 2009]. Such effects can spill over into nearby fisheries and alter natural species behaviour.

The intensity of these impacts generally increases with farm size and density. Larger operations release greater volumes of waste, and ecological responses can be non-linear: systems may remain stable for long periods before abruptly shifting to hypoxia, algal blooms, or seagrass collapse once critical thresholds are crossed [Bouwman et al., 2013]. Recognising these risks, early studies already proposed mitigation through artificial structures such as reefs to distribute pressure and support local biodiversity [Bergan et al., 1991].

In summary, ecological impacts arise from both nutrient release and ecological restructuring around farms. The extent of these effects depends on site conditions, hydrodynamic exchange, and management practices, underscoring the need for scale-appropriate design and monitoring.

2.4.2. Mitigating Measures

Reducing the ecological footprint of aquaculture requires a combination of operational, ecological, and structural approaches. At the farm level, improvements in feed efficiency, lower stocking densities, and periodic fallowing (resting sites to allow recovery) are among the most effective operational measures. These strategies can substantially reduce waste outputs, although some nutrient release remains inevitable in open-water systems [Braña et al., 2021; Bouwman et al., 2013].

Ecological approaches aim to recycle or reabsorb these wastes. Integrated multi-trophic aquaculture (IMTA) combines species at different trophic levels, such as seaweeds that absorb dissolved nutrients and shellfish that filter organic particles [Fang et al., 2016]. Similarly, ecosystem-engineering bivalves such as Atrina Zelandica can enhance nutrient recovery and improve local water quality [Elvines et al., 2023]. While ecologically beneficial, these systems require additional space, infrastructure, and markets for co-farmed species, which limits their suitability for small community operations.

Structural interventions target habitat restoration and ecosystem support. Artificial reefs were first proposed by Bergan et al. (1991) and later developed into modular, low-impact designs [Carral et al., 2017]. They create additional substrate for marine life and can enhance biodiversity in degraded areas. How-

ever, reefs do not directly reduce nutrient loading and may attract wild fish, increasing potential disease transfer if placed too close to cages [Dempster et al., 2009].

Overall, each approach addresses a different aspect of ecological mitigation. Operational measures are cost-effective but partial, ecological systems offer recycling potential but add complexity, and structural solutions restore habitat without solving pollution. The most robust outcomes emerge from combining these strategies and adapting them to local hydrodynamic and social conditions.

2.4.3. Complexity of increased scale

As aquaculture scales up, challenges become more complex rather than simply larger. Ecologically, higher biomass leads to greater waste and impacts escalate once critical thresholds are crossed, resulting in sudden oxygen depletion, harmful blooms or seagrass collapse [Bouwman et al., 2013; Boudouresque et al., 2020]. Larger farms also draw in more wild fish, increasing interactions and the risk for spreading diseases [Dempster et al., 2009; Bøhn et al., 2024].

Technical demands grow as well. Bigger cages and arrays require stronger moorings, careful orientation to waves and currents and more intensive monitoring. Maintenance effort and the risk of equipment failure rise with scale, making engineering design and operational management more demanding.

Social and governance complexity also increases. Large farms occupy more marine space, potentially conflicting with fisheries, conservation or tourism. They trigger stricter regulatory oversight and require detailed environmental monitoring to ensure ecological thresholds are not exceeded [Braña et al., 2021].

In summary, scaling up aquaculture heightens ecological pressure and increases engineering complexity. Mitigation measures such as improved feed efficiency, lower stocking densities and habitat restoration remain important, but they must be adapted and scaled to remain effective in larger systems.

2.4.4. Aquaculture Shape and Configuration

The shape of aquaculture cages has a decisive influence on hydrodynamic stability, rearing volume, fish welfare and the loads transmitted to mooring systems. In regions such as Sisal, where currents and waves are strong and seasonal storms can be severe, the choice of cage geometry is particularly important. The scientific literature distinguishes mainly between circular, vessel-shaped and array-level configurations.

Circular-shape

Circular cages are by far the most common and best studied. Their smooth perimeter distributes loads evenly, avoids stress concentrations and provides a continuous swimming path that matches the natural schooling behaviour of certain species [Lader and Enerhaug, 2013]. Hydrodynamic analyses show that circular cages are more efficient than square cages for maintaining effective rearing volume: under currents above 0.4 m s^{-1}, circular cages lose less usable space and generate less drag per unit volume [Bi et al., 2018]. At the same time, circular systems are not free of challenges. Net deformation under steady currents can reduce available volume by up to 20%, which leads to higher local stocking densities and oxygen demand [Gansel et al., 2015]. To limit such effects, studies recommend conservative ratios between cage height and circumference (keeping cages relatively wide and shallow to reduce bending and net collapse) as well as reinforcement of structural elements. For example, strengthening the floating frame or adding stiffeners to resist bending forces.

Vessel-shape

Vessel-shape cages have emerged more recently as an alternative for high-energy offshore sites. Their bow-like structure reduces the surface area exposed to incoming waves and the use of single-point mooring systems enables the structure to rotate into the prevailing direction of wave and current. This reduces asymmetric loading and allows forces to be distributed more evenly along the floating frame [Zhuo et al., 2024]. Numerical and scaled experiments suggest that vessel-shaped systems can achieve lower mooring tensions and pitch motions under energetic wave conditions. Field deployments have demonstrated survival during typhoon events, indicating that these systems are capable of withstanding extreme environments.

Existing studies often treat the cage frame as rigid and do not fully capture pontoon flexibility or net deformation, both of which are important for long-term biological performance. Moreover, vessel-shaped systems are more complex to build and maintain than gravity-type cages (traditional floating net pens that rely on buoyancy and gravity to maintain their shape), which may limit their applicability in community-based aquaculture projects. Recent dynamic response analyses show that wave diffraction and radiation effects can alter net tensions and connector loads, indicating that simplified models underestimate structural demands [Wang et al., 2024]. For this reason, while vessel-shaped designs show promise, their suitability for Sisal cannot yet be assumed and requires further investigation.

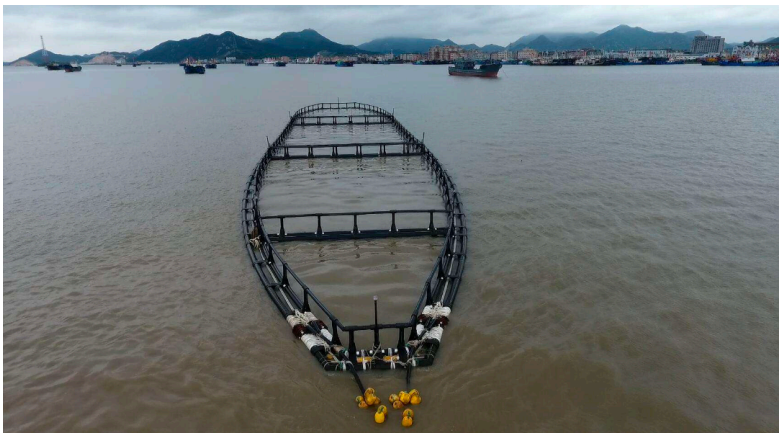

Figure 2.2: Vessel-shape fish farm design as proposed by Zhuo et al. (2024).

Configuration

At the farm scale, configuration adds another layer of complexity. Hydrodynamic studies show that water velocities decrease significantly inside and downstream of cages, which affects oxygen supply and waste dispersion. To counteract this, spacing of at least one to one and at a distance of half cage diameters is generally recommended [Lader and Enerhaug, 2013]. Beyond spacing, the overall layout determines how forces are transmitted through the mooring system. Symmetric and staggered arrays tend to produce more even load distributions than simple rectangular grids, while honeycomb-like configurations may optimise space use but require more advanced anchoring arrangements [Bi et al., 2018; Nasyrlayev et al., 2023]. These trade-offs highlight that configuration choices influence not only the stability of individual cages but also the efficiency and resilience of the farm as a whole.

Array layout also affects water exchange and sediment distribution. Densely packed or poorly oriented farms can reduce flushing, causing local accumulation of organic material. Staggered or offset configurations allow better flow through the array and can therefore help maintain oxygen levels and limit local seabed impact. The orientation of the array relative to dominant wave and current directions is particularly important under Sisal's conditions, where currents shift seasonally and storms can induce high loads on mooring lines.

2.4.5. Acceptance and Social Aspect

Developing fish farms in coastal communities such as Sisal requires careful attention to social acceptance. Long-term success depends not only on technical feasibility but also on gaining and maintaining local trust, participation, and shared benefits.

Community involvement is essential from the design stage onward. When local fishers contribute to planning and operation, the project aligns with local values and knowledge, reducing scepticism and fostering ownership. Cooperative structures are particularly effective in ensuring that economic benefits remain within the community rather than being perceived as externally imposed [Belausteguigoitia et al., 2019; Bañuelos-García et al., 2021].

Transparency and communication further strengthen acceptance. Open sharing of information about objectives, environmental impacts, and management practices helps build credibility and resolve uncertainty. Visible sustainability measures, such as habitat protection and collaboration with research institu-

tions, reinforce public confidence and demonstrate environmental responsibility [Eriksen and Mikkelsen, 2024].

Equitable benefit-sharing also plays a decisive role. Reinvesting profits into local employment, infrastructure, and environmental initiatives links aquaculture success directly to community welfare. Such arrangements promote fairness and long-term support for the project [Bañuelos-García et al., 2021].

Finally, co-management approaches, where fishers and community members share responsibility for decisions and daily operations, have proven effective in similar contexts. This structure cultivates a sense of ownership and continuity, ensuring the farm becomes a sustainable part of the local economy [Bañuelos-García et al., 2021].

2.4.6. Multi-functionality of Fish Farms

The concept of multi-functionality in aquaculture refers to the intentional co-use of ocean space by fish farming structures and other maritime activities. This approach aims to enhance spatial efficiency, improve economic viability and generate wider societal benefits while minimising conflicts between sectors. Schupp et al. (2019) distinguish three main forms of multi-use: co-location (parallel activities within the same maritime zone), shared services (common use of infrastructure) and integrated platforms (systems designed for multiple functions from the outset). These categories provide a useful typology for assessing how fish farms can operate as multifunctional hubs.

Traditional Sea-Based Hubs

Examples from different regions show how offshore structures have long served as multifunctional hubs. In Southeast Asia, lift-net fishing platforms (Bagan) combine fishing activities with lighting, storage and temporary accommodation. Studies of illuminated Bagan demonstrate how the introduction of LED systems can influence catch efficiency and energy use [Puspito et al., 2015]. Anchored fish aggregating devices (FADs) used in small-scale fisheries across the Indian Ocean, Pacific and Southeast Asia similarly provide communal workspaces and navigation aids in addition to supporting tuna and small pelagic fisheries [Beverly et al., 2012]. In the Caribbean, moored FAD fisheries have expanded in several island states, where regional assessments describe the need for clear rules on access, monitoring and maintenance [Wilson et al., 2020]. In Japan, aquaculture rafts for oyster and seaweed farming serve not only as production units but also as platforms for maintenance, storage and environmental monitoring [Murata et al., 2021].

These examples highlight transferable elements such as workspace, storage capacity and attraction effects that can inform the development of multifunctional fish farms in other contexts. Recent innovations such as Spotter buoys extend this concept by combining wave and weather monitoring with real-time data transmission, enabling low-cost environmental observation and supporting research, safety and educational applications [Sofar Ocean, 2025]. These systems illustrate how modern technology can complement traditional multifunctional platforms through added research and community value.

(a) Lift-net fishing platform (bagan) in Southeast Asia.

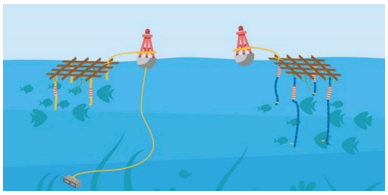

(b) Anchored fish aggregating devices (FADs).

(c) Aquaculture raft for oyster farming in Japan.

Figure 2.3: Examples of traditional sea-based hubs: (a) bagan lift-net platform, (b) anchored FADs and (c) aquaculture raft. Sources: [Puspito et al., 2015; Beverly et al., 2012; Wilson et al., 2020; Murata et al., 2021].

Integration with Renewable Energy

Integrating renewable energy with aquaculture extends beyond power generation; it enables supporting systems that enhance monitoring, safety and environmental management. Photovoltaic systems have been applied in aquaculture to power aerators, automated feeders, pumps and water quality sensors [Vo et al., 2021]. For example, solar-powered aeration can maintain dissolved oxygen levels and reduce dependence on external power sources, while stand-alone photovoltaic–battery systems have been tested for continuous environmental monitoring using smart sensor networks [Jamroen et al., 2023]. In Japan, small-scale aquaculture projects have combined solar modules with existing farming infrastructure to operate pumps and monitor oyster rafts and seagrass ecosystems [Murata et al., 2021].

At larger scales, renewable energy integration has also been explored in commercial settings. The Norwegian company Inseanergy (now Alotta) developed circular floating solar arrays designed to operate alongside salmon cages, reducing the reliance on diesel generators and improving energy autonomy. Such systems demonstrate how renewable energy and aquaculture can be co-designed within the same marine infrastructure [Santos, 2023; Team, 2022]. Although these examples exceed the scale and complexity suitable for Sisal, they illustrate how energy integration can serve as a multifunctional bridge between aquaculture, innovation and environmental awareness.

Together, these cases show that renewable energy can contribute to multifunctionality by supporting environmental monitoring, powering safety and research equipment and demonstrating low-impact marine technology to local communities. Even small autonomous systems can strengthen educational and ecological dimensions without altering the simplicity of the primary fish farming operation.

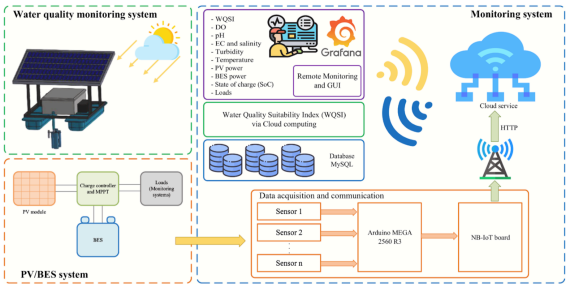

(a) Standalone photovoltaic–battery system powering water quality monitoring equipment [Jamroen et al., 2023].

(b) Circular floating solar array co-located with aquaculture cages (Inseanergy pilot, Norway) [Santos, 2023; Team, 2022].

Figure 2.4: Examples of renewable energy integration with aquaculture: (a) small-scale photovoltaic–battery system for environmental monitoring, (b) large-scale floating solar array integrated with offshore aquaculture.

Freshwater and Desalination Functions

Small amounts of freshwater can be valuable for aquaculture workers operating offshore, for example for drinking, cleaning or basic maintenance. In this context, compact desalination units powered by renewable energy could be integrated into fish farm platforms as a service function rather than as a response to wider regional water scarcity.

Laboratory and field trials have demonstrated the technical feasibility of wave-powered desalination. Reverse osmosis devices linked directly to wave energy converters have produced freshwater at pilot scale without intermediate electricity conversion [Mi et al., 2023]. Government-supported programmes have also tested autonomous desalination buoys. The U.S. Department of Energy's *Waves to Water* programme conducted open-water demonstrations in which multiple devices generated potable water under real ocean conditions [U.S. Department of Energy, 2023].

Commercial pilots illustrate the robustness of this technology. In California, the city of Fort Bragg deployed a Oneka desalination buoy capable of producing up to 50,000 gallons per day [City of Fort Bragg, 2025]. Although designed for municipal supply, this case shows how buoy-based desalination systems can be adapted to meet the modest freshwater needs of offshore aquaculture. Complementary research has also explored solar-based concepts, including floating solar stills built with refractory plasmonic materials that achieve higher evaporation efficiency in nearshore conditions [Margeson et al., 2024].

Figures 2.5a and 2.5b illustrate two approaches to renewable-powered desalination. The Oneka buoy exemplifies wave-driven reverse osmosis, while the solar still demonstrates innovation in compact solar-based systems. Both could be adapted to provide small but valuable freshwater supplies directly at aquaculture hubs. Beyond their practical use, such systems can also serve educational and demonstration purposes, showing how marine infrastructure can integrate low-impact water and energy technologies.

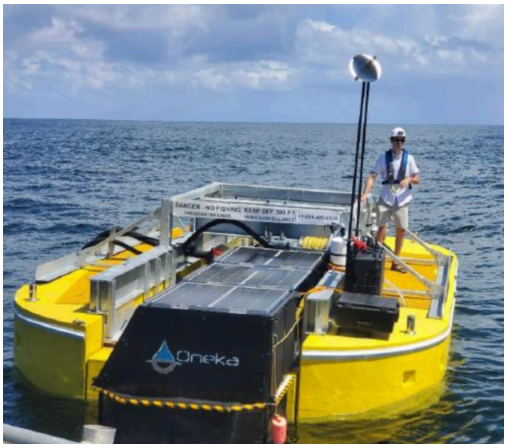

(a) Wave-powered desalination buoy tested in California (Oneka Technologies) [City of Fort Bragg, 2025].

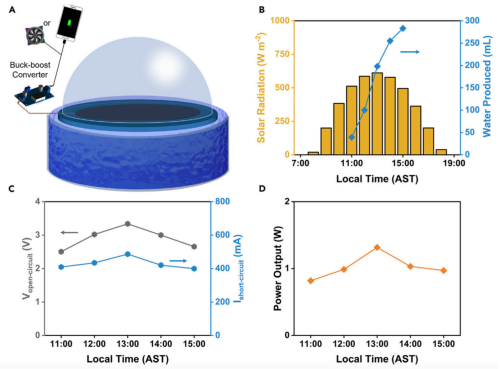

(b) Experimental floating solar still using refractory plasmonic materials [Margeson et al., 2024].

Figure 2.5: Examples of small-scale desalination technologies relevant for integration with fish farms: (a) autonomous wave-powered desalination buoy and (b) experimental solar still design.

Tourism, Research and Biodiversity Co-Benefits

Tourism and education offer promising paths to expand the social and environmental value of aquaculture. Offshore fish farms can host eco-tourism experiences such as guided visits, snorkelling, or recreational fishing, diversifying income streams while promoting public awareness of marine ecosystems. Collaborative projects between aquaculture operators and academic institutions can further transform such sites into living laboratories for water quality monitoring, biodiversity assessment, and training in sustainable production [Cárdenas-Torres et al., 2007; Meza-Osorio et al., 2024].

Ecologically, aquaculture structures can act as artificial reefs, providing hard substrate that supports colonisation by marine flora and fauna. Well-designed installations enhance local biodiversity and productivity, though they may also alter community composition or trophic balance if not properly managed [Hutchison et al., 2020; Miller, 2002]. Integrating nature-inclusive design principles (such as varied substrate materials, textured surfaces, and ecologically shaped anchors) can maximise habitat benefits while maintaining operational safety [Kingma et al., 2024].

Within this framework, hybrid systems that combine education, research, and eco-tourism show particular potential. These models, tested in several coastal regions, enable visitors to experience marine life while learning about sustainable aquaculture and biodiversity restoration. Local cooperatives typically manage snorkelling and environmental interpretation, while research institutions conduct monitoring and training programmes. This collaboration reduces environmental disturbance, creates community employment, and strengthens public trust in aquaculture as a transparent and environmentally responsible activity [Hannak et al., 2011; Ardoin et al., 2020].

For Sisal, a small-scale hybrid model linking snorkelling, environmental interpretation, and reef enhancement could deliver both income and conservation value. Partnerships between the local cooperative, UNAM, and visiting schools would align with existing educational and ecological initiatives, reinforcing the vision of a socially inclusive and environmentally restorative aquaculture system [Falk and Dierking, 1997; Bonney et al., 2009].

In summary, integrating tourism, research, and biodiversity restoration can transform aquaculture platforms into multifunctional hubs that promote environmental stewardship, education, and community engagement.

2.5. Synthesis

The reviewed literature highlights that sustainable aquaculture depends on the integration of environmental, technical and social considerations. Environmentally, fish farms must be designed to operate safely within local wave and current regimes while minimising disturbance to surrounding ecosystems. Technically, cage shape, spacing and orientation strongly influence hydrodynamic stability and operational reliability, with small, modular systems offering clear advantages in maintenance and resilience. Socially, long-term success requires active community participation, transparent communication and shared economic benefits that foster trust and local ownership.

Additionally, multifunctionality emerges as a key strategy to align aquaculture with broader community and ecological goals. Integrating functions such as environmental education, small-scale tourism, reef enhancement and research collaboration can increase acceptance while maintaining low operational complexity.

Together, these insights define the design boundary for community-based aquaculture in Sisal: systems should remain environmentally compatible, technically manageable and socially inclusive. The next chapter builds on these findings to identify the specific challenges and design requirements that must be addressed to realise such a system in practice.

3

Problem Description

This study explores the potential for developing small-scale aquaculture off the coast of Sisal. The idea originates from UNAM's ambition to create a system that strengthens the local economy while providing a stable and sustainable source of income for the fishing community. For this to be viable, cages must be safe, practical to operate, and maintainable by local users, while offering clear value to those who depend on the sea. This chapter outlines the problems that must be addressed and explains why they matter in the context of Sisal.

As noted in the introduction, the project integrates social and engineering perspectives, which are treated separately in the coming chapters. This chapter first identifies the main challenges in both domains and then formulates the guiding research questions that define the project's focus and scope.

3.1. Challenges

Two interlinked challenges shape the feasibility of community-based aquaculture off the coast of Sisal: social acceptance and engineering feasibility under local sea conditions. Together, these determine whether a system can be maintained locally, operated safely throughout the year, and regarded as valuable by the community.

Interviews with UNAM staff indicate that local uptake depends on practical factors such as the ability of fishers to inspect and repair equipment using existing vessels and skills, the clarity of communication about project goals, and the accessibility of sites for regular maintenance. Acceptance is therefore more likely when the technology remains understandable and manageable at the community level (Interview UNAM, 2025, Appendix A). A key task for this study is to examine which multifunctional uses are most valued by local stakeholders and how these can strengthen social acceptance of aquaculture in Sisal.

The northern Yucatán shelf experiences strong seasonal variations in wind and wave conditions. During winter months, cold fronts (Nortes) generate more energetic sea states, while summer periods are dominated by regular sea-breeze cycles (Interview Coastal Engineering, 2025, Appendix A). Although circular cages are the most common in aquaculture, it is not evident that they perform optimally under Sisal's conditions. Recent designs, such as vessel-shaped systems, may behave differently under wave and current forces. Comparing both configurations will clarify whether an alternative form offers advantages in stability or handling and thereby inform future design choices.

Addressing both challenges is essential. A technically sound system without local usability is unlikely to persist, while socially accepted concepts must still demonstrate structural safety and resilience under the prevailing environmental conditions.

3.1.1. Community Acceptance

Community acceptance involves more than technical safety. It also depends on perceived fairness, transparency, and the distribution of benefits and responsibilities. In aquaculture literature, this is referred to as the 'social licence to operate', which develops through early engagement, continuous

dialogue, and evidence that operations respond to local concerns [Whitmore et al., 2022; Olsen et al., 2024; Leith et al., 2014]. In comparable coastal contexts, acceptance increases when communities perceive clear local benefits, when farm operations are understandable to non-experts, and when maintenance tasks can be carried out using local vessels, skills, and materials [Whitmore et al., 2022; Olsen et al., 2024].

Discussions in Yucatán reflect similar conditions. In Celestún, adoption has been limited when maintenance depended on external contractors, which reduced the sense of ownership among local fishers. UNAM professors therefore emphasised the need for systems that fishers can inspect and repair independently (Interview UNAM, 2025, Appendix A). For Sisal, the key challenge is to develop a small-scale, community-based model that can diversify income with minimal ecological disturbance. Offshore sites must remain within a practical distance from shore to limit fuel and time costs, with an upper operational limit of roughly 40 km for routine visits (Interview UNAM, 2025, Appendix A).

Social factors such as trust and communication are equally important. Equipment visible above the water has been identified as vulnerable to theft, which influences how monitoring instruments are designed and secured (Interview UNAM, 2025, Appendix A). Effective communication also requires clear, visual tools to ensure that technical information is shared accurately and understood across different experience levels (Interview Rosas, 2025, Appendix A).

In summary, community acceptance in Sisal depends on developing an aquaculture system that is locally understandable, economically beneficial, and technically manageable, while aligning with community values and practical capacities. These social aspects are as crucial to long-term success as the engineering design itself.

3.1.2. Engineering Challenges

Beyond the social factors that determine whether aquaculture can be accepted and maintained locally, the second major challenge lies in the engineering feasibility of operating fish cages safely in the coastal conditions off Sisal. The northern Yucatán shelf experiences two recurring wind regimes that shape sea states throughout the year. From April to September, regular sea-breeze cycles drive alongshore currents, while from October to March, cold fronts known locally as Nortes generate higher waves and more energetic conditions [Cahuich-López et al., 2020; Torres-Freyermuth et al., 2017]. These patterns define the hydrodynamic forces that any cage and mooring system must withstand.

The main engineering task is to design a system that remains structurally stable and secure under varying and sometimes extreme conditions. Cages must resist continuous loads from waves, currents, and wind, while tolerating occasional storm events without failure. These forces act not only on the cage frame but also on the mooring lines and anchors that hold the system in place. If anchors are undersized or poorly arranged, even moderate waves can cause displacement or line fatigue, compromising both safety and maintenance.

UNAM professors estimated that cages and moorings should be designed to withstand waves of roughly 2.5–3 m during winter events (Interview Coastal Engineer, 2025, Appendix A; Interview UNAM, 2025, Appendix A). This requires an anchoring system capable of resisting significant horizontal and vertical loads while remaining accessible for maintenance using local vessels.

Although circular cages are the most widely used in aquaculture, it is uncertain whether they offer the best performance under Sisal's conditions. Alternative geometries, such as vessel-shaped designs, may distribute forces differently and provide improved stability or handling. Further research is therefore needed to assess which form is most appropriate for local sea states and maintenance capacity.

The professors translated these conditions into concrete design and operational guidelines. They noted that hurricane season extends from June to November and advised that if a major cyclone threatens, one practical option is to remove the cages after harvest to prevent damage. Currents were described as generally persistent and of similar strength in Sisal and Celestún, and routine operations should remain compatible with local vessels and sea states (Interview Coastal Engineer, 2025, Appendix A; Interview UNAM, 2025, Appendix A).

In summary, while the environment defines the external forces at play, the engineering challenge lies in designing a system that is both locally maintainable and capable of withstanding these conditions

throughout the year. Determining which cage form performs best under the prevailing forces will guide future design improvements and support the broader goal of establishing a community-based aquaculture system that is both technically reliable and socially accepted.

3.2. Focus of the Study

Social acceptance and engineering feasibility define the overall focus of this study. Each represents one dimension of the problem: the social side examines how aquaculture can be accepted and valued by the local community, while the engineering side investigates whether the system can safely operate under the physical conditions off the coast of Sisal.

The study therefore focuses on the interaction between these two dimensions. It explores how design choices influence social acceptance and how community priorities, in turn, affect the technical requirements of the system. The objective is not to produce a complete farm design or business plan, but to identify which technical and social factors are most critical to making aquaculture in Sisal both feasible and valuable for the community.

3.2.1. Environmental Boundary Conditions

The environmental conditions of the northern Yucatán coast set the physical limits within which aquaculture systems must operate. Seasonal wind patterns, dominated by sea breezes in summer and cold fronts (Nortes) in winter, create varying wave and current regimes that determine the forces acting on cages and moorings. These site-specific dynamics define the design boundary for structural stability and maintenance feasibility. Understanding these constraints is essential for assessing which cage geometries can perform reliably under local conditions and remain manageable for community operation.

3.2.2. Scope of the Engineering Study

The engineering component focuses on assessing the stability and strength of two cage geometries vessel-shaped and circular under the hydrodynamic conditions off Sisal. The analysis compares how each design responds to waves and currents, examining anchor strength, mooring loads, and cage motion. These evaluations combine hydrodynamic simulations with analytical force calculations to capture both numerical and theoretical perspectives.

The objective is to identify which configuration performs more effectively in terms of safety, durability, and practicality for local operation and maintenance. Although long-term aspects such as corrosion, fatigue, and cost modelling fall outside the present scope, they are recognised as important considerations for future development once a suitable geometry has been determined.

3.2.3. Scope of the Social Study

The social component examines how aquaculture can become more desirable and acceptable to the community of Sisal. This is achieved through a Multi-Criteria Decision Analysis (MCDA) that evaluates which multifunctional uses such as education, tourism, or habitat enhancement are most valuable to local fishers. The MCDA integrates community perspectives with structured evaluation criteria, including economic benefit, ecological impact, and feasibility.

The aim is to identify the combinations of functions that provide the greatest value for local stakeholders and thereby strengthen the social acceptance of aquaculture in Sisal. As detailed in the MCDA chapter, this approach allows for transparent comparison between alternatives and incorporates both qualitative and quantitative perspectives on community value.

3.2.4. Integration, Limitations and Overall Scope

Although the social and engineering components are examined separately, their outcomes are closely connected. The engineering analysis identifies which cage geometry performs most effectively under the environmental conditions defined for Sisal, while the social analysis reveals which multifunctional purposes make aquaculture more meaningful and accepted by the community.

Together, these findings contribute to a conceptual design that balances technical feasibility with social value. The study does not include implementation, large-scale economic modelling, or long-term

environmental assessment, which are identified as directions for future research.

In summary, this research explores how technical design and social context interact in the development of community-based aquaculture in Sisal. The engineering component compares the hydrodynamic performance of vessel-shaped and circular cages using numerical and analytical methods, while the social component applies MCDA to evaluate multifunctional options that enhance local acceptance. Combined, these approaches lay the foundation for a system that is both technically reliable and socially valuable, representing a first step toward sustainable aquaculture development in Sisal.

3.3. Research Questions

Based on the challenges and scope described above, this study is guided by two main research questions: one addressing the engineering feasibility and the other focusing on the social acceptance of aquaculture in Sisal. Together, they define the direction of the project and link the technical and social dimensions into a single research framework.

- **How can the fish farm's design be adapted to the local environmental conditions off Sisal?**
  This question addresses the engineering dimension of the study. It investigates how cage geometry affects structural stability and resistance under local wave and current conditions. The analysis compares vessel-shaped and circular cages using numerical and analytical approaches to evaluate which configuration offers greater robustness and suitability for community-based operation.
- **Which additional functions can be integrated into the fish farm to enhance ecological benefits, economic value, and community acceptance in Sisal?**
  This question represents the social dimension of the study. Through a Multi-Criteria Decision Analysis (MCDA), it identifies which multifunctional uses such as education, tourism, or habitat enhancement are most valued by local stakeholders and how these functions can strengthen the social and ecological contribution of aquaculture in Sisal.

Together, these research questions connect the technical performance of the fish farm to its social relevance. The findings from both analyses will inform a conceptual design for a community-based aquaculture system that is technically reliable, environmentally compatible, and socially supported under the local conditions of Sisal.

4

Social Acceptance Through Multi-Functionality

4.1. Introduction

This chapter examines how a community-led fish farm in Sisal can be better socially accepted by creating value beyond fish production through environmentally and socially integrated functions. In coastal communities such as Sisal, aquaculture projects face not only technical and ecological challenges but also the need for local legitimacy. Social acceptance depends on whether community members perceive the initiative as fair, beneficial, and compatible with their environment and livelihoods. Multi-functionality provides a pathway to achieve this acceptance, as it connects ecological improvement with community participation, education, and public benefits.

To structure this analysis, the Triple Bottom Line (TBL) framework is applied to capture local priorities across Planet, People, and Profit. These priorities are expressed as stakeholder weights within an MCDA that ranks ten potential multifunctional options according to their ecological, social, and economic contributions. This approach links technical performance to community-defined values and produces transparent rankings for both students and fishers.

Since acceptance also depends on practical feasibility, an attainability assessment complements the MCDA by evaluating investment requirements, robustness, required skills, operational simplicity, and community engagement of real life options. Together, these methods identify which multifunctional measures are not only valued in principle but also realistically achievable under the local conditions in Sisal. In this way, stakeholder priorities are translated into design choices that can improve trust, participation, and long-term sustainability of offshore aquaculture.

4.2. Triple Bottom Line Framework

4.2.1. Conceptual and Analytical Approach

To assess community preferences for the multi-functionality of the fish farms, the TBL framework was applied. Introduced by Elkington in 1994, the TBL expands traditional economic evaluation by integrating three equally important dimensions of sustainability: environmental (Planet), social (People), and economic (Profit) performance [Elkington, 1997]. The framework has since been widely adopted in sustainability studies, including in fisheries management, as it enables a balanced consideration of ecological health, community well-being, and economic viability [Fletcher et al., 2010; Anderson et al., 2015].

In the context of Sisal, the TBL framework provided a structured way to link fish farm development to local community values. From interviews conducted with professors (Appendix A), it was concluded that fishers primarily focus on immediate operational challenges, such as fuel consumption or maintenance costs, rather than on long-term ecological and economic interdependence. By translating sustainability into three clear categories that represent benefits, the framework made it possible to discuss priorities

in accessible and familiar terms. This approach ensured that sustainability was evaluated not only in ecological or technical terms but also through the lens of community relevance and social acceptance.

A schematic representation of the TBL framework is shown in Figure 4.1, and the three dimensions are described below.

Figure 4.1: TBL framework.

- **Planet**
  Refers to the protection of the natural environment through healthy ecosystems, reduced pollution, and efficient use of resources. In fish farming, it represents the ecological responsibility of maintaining clean and resilient marine areas.
- **People**
  Relates to the social value of fish farming for the community, including fair working conditions, education, collaboration, and just benefit sharing between the community of Sisal.
- **Profit**
  Represents the economic sustainability of the farms as perceived by the community. It reflects expected cost savings, manageable investment, and stable income generation rather than detailed financial modelling. The Profit dimension captures how stakeholders evaluate the economic attractiveness or affordability of multifunctional measures, which is later complemented by a technical feasibility check in the attainability assessment.

By structuring sustainability according to these three categories, the TBL framework established a clear and theoretically consistent foundation for identifying community priorities in Sisal. These priorities subsequently serve as input for the MCDA presented later in this chapter.

4.2.2. Capturing Community Priorities

To measure how different groups valued the three sustainability dimensions of the TBL framework, a questionnaire was created (Appendix C). Participants were asked to assign importance scores to People, Planet, and Profit, and to answer a set of practical questions on topics such as tourism, technology use, and ecological awareness. The goal was not to test technical knowledge but to reveal which values were considered most relevant for multifunctional fish farms in Sisal.

To support comprehension, a brief explanatory video was created. The video (Appendix C) introduced the concept of multifunctional fish farms and explained the three TBL categories in straightforward and local Spanish dialect. It illustrated how environmental protection could generate indirect social and economic benefits for the community and gave clear instructions on how to fill in the questionnaire.

The questionnaire was administered to two groups: high school students from Sisal and local fisheries

stakeholders, including fishers, technicians, and aquaculture operators. Responses from these two groups allowed comparison between generational perspectives and experience levels. All responses were collected manually and later processed for statistical analysis.

Besides the main TBL rating, the questionnaire contained practical statements about possible activities and facilities around fish farms. These items explored how participants viewed extensions such as combining aquaculture with tourism, adopting simple technologies like sensors or Wi-Fi, and installing freshwater makers. Participants also indicated whether they were willing to change their own behaviour to support environmental improvement. These questions provided qualitative context to the TBL results by showing how participants translated their values into practical attitudes toward innovation and sustainability.

As many locals were unfamiliar with advanced aquaculture concepts, the TBL framework was chosen instead of a detailed survey on specific options. This approach allowed participants to express their values in accessible ecological, social, and economic terms, instead of giving opinions on various technological solutions. The participants' values could then be systematically translated into design preferences through the MCDA. This way, the evaluation of solutions is grounded in community-defined priorities rather than in technical assumptions.

4.2.3. Results and Discussion of Community Preferences

High School Group

The questionnaire was completed by seventeen high school students and their teacher of the 'Telebachillerato Comunitario de Sisal', resulting in eighteen total responses (average age 17.7 years).

On a scale from 0 to 5, Planet scored highest with an average of 4.94, followed by People with 3.89 and Profit with 3.28 (Figure 4.2). This pattern indicates a clear prioritization of environmental protection over social and economic considerations. The high valuation of Planet suggests that ecological sustainability is viewed as the foundation for future fish farm development.

Responses to the additional practical questions provided further insight into local attitudes toward multifunctionality. Participants expressed moderate willingness to diversify into tourism (average 3.22) but showed less interest in continuing traditional fishing practices (2.39). Interest in technological and ecological improvements was higher: Wi-Fi connectivity (4.11), freshwater makers at sea (3.94), and sensors to locate fish (4.00) all received relatively strong support. The statement on willingness to change behaviour to promote ecological improvement also scored highly (4.22).

The open question adds qualitative depth to the survey results. Several respondents explain that fish farms could "help the fishing families" by providing new work opportunities and reducing dependence on wild catches. Others emphasise environmental protection, noting that such projects should "not harm the sea" and should encourage care for local ecosystems. A few students highlight educational potential, describing the farms as opportunities for learning and school visits that could inspire future careers in aquaculture. These remarks can be grouped into three main themes: community and income (People and Profit), protection of nature (Planet), and education and awareness (People).

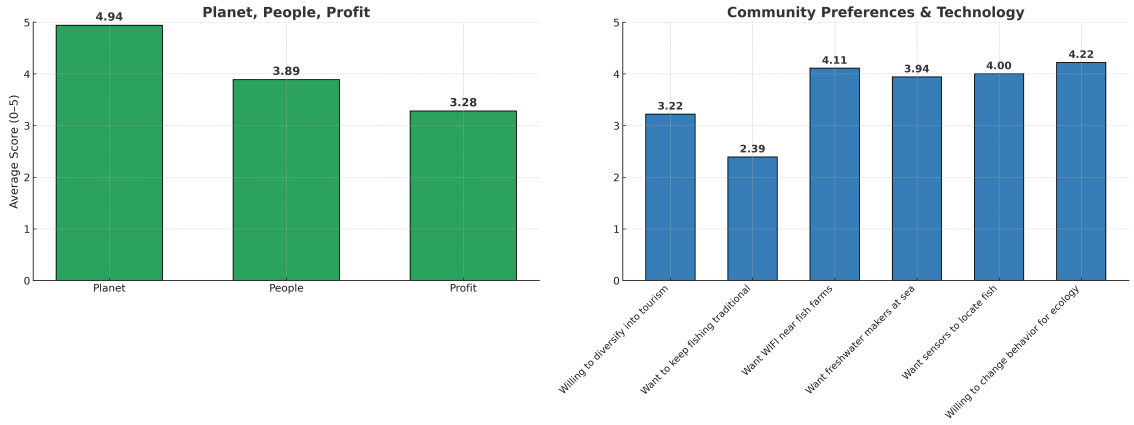

Figure 4.2: Average questionnaire results from high school in Sisal (n=18).

Fisheries Stakeholder Group

The second group included six fisheries stakeholders from Sisal and Celestún: two fishers, one squid farm operator, a technician, a volunteer in ecoculture, and a high school teacher involved in aquaculture projects with an average age of 53 years old. Several participants had direct experience with single-purpose fish farming in Celestún, providing practical perspectives on multifunctional aquaculture.

As shown in Figure 4.3, Planet received the highest average score, followed by People and Profit. A similar pattern compared to the high school students. This confirms that ecological factors are considered most important, while social and economic aspects are seen as complementary. Scores across all three dimensions were relatively high, reflecting shared recognition that sustainable aquaculture can support both environmental recovery and community well-being.

In the practical questions, participants emphasise technologies and safety measures that can improve farm reliability. They show interest in ecological management tools and educational activities, suggesting that multifunctionality is interpreted mainly as a combination of environmental protection, safety, and knowledge sharing rather than commercial expansion.

The open-ended responses, although brief, are practical and grounded in local experience. One technician explains that aquaculture offers “a path to provide a solution to the shortage of marine products and to ensure food security for the nation”. Another participant notes that fish farms should “help people take better care of natural resources” and encourage more community involvement. Several others refer to safety at sea, cooperation among fishers, and the need for reliable equipment. Only one response mentions direct economic gain, indicating that profitability is secondary to ecological and operational considerations. Overall, these remarks reflect a hands-on mindset focused on responsibility, safety, and reliability under the demanding local conditions.

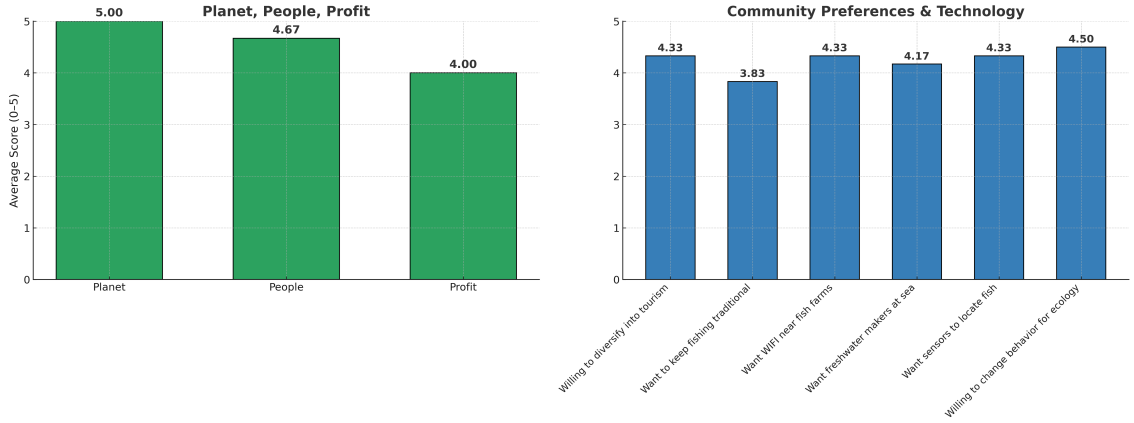

Figure 4.3: Average questionnaire results from fisheries stakeholders in the Sisal region (n=6).

Discussion and Interpretation

The results from both groups indicate that ecological sustainability and social value are central to the acceptance of multifunctional fish farming. In both samples, Planet receives the highest scores, confirming that environmental protection is regarded as the foundation for development. Having said that, the rating patterns differ slightly between the groups.

High school participants display a clear hierarchy of priorities: Planet dominates, followed by People and Profit. Their responses show a selective focus on environmental and educational benefits, while economic considerations receive only moderate attention. This pattern suggests that younger participants perceive sustainability primarily as learning, innovation, and future potential rather than immediate livelihood improvement.

The fisheries stakeholders, by contrast, assign high scores to all three dimensions. Rather than highlighting a single dominant value, they evaluate ecological, social, and economic aspects as interdependent. This balanced pattern reflects practical experience in aquaculture, where environmental care, cooperative effort, and financial viability must operate together. Their comments about safety, maintenance, and cooperation reveal that sustainability is interpreted as reliability and shared responsibility within daily operations rather than as an abstract goal.

The difference between the two groups therefore lies not in what they value but how they prioritise it. Students express aspirational views shaped by education and technological curiosity, while stakeholders adopt a pragmatic outlook grounded in operational experience. Both associate sustainable aquaculture with environmental protection and community benefit rather than profit maximisation.

When interpreting these findings, the composition of the stakeholder group remains important. Participants are drawn from university-linked aquaculture initiatives and are already familiar with sustainability practices, which can bias their responses toward a stronger emphasis on the environment and cooperation compared to the general fishing community.

These observed patterns form the empirical basis for the stakeholder weightings used in the MCDA presented in the following section.

4.3. Identification of Multifunctional Design Options

4.3.1. Overview and Purpose

Building on the priorities identified in the community analysis, ten potential design options are identified through literature review and discussions with local stakeholders and professors (Appendix A). These options represent ecological, social, and operational improvements aligned with the three dimensions of the TBL. Each combines environmental protection, community benefit, and economic potential in different proportions.

The purpose of this section is to describe each option conceptually before its evaluation using the MCDA. The descriptions outline the principal function, expected contribution to one or more sustainability dimensions, and level of technical complexity. Together, these options provide the foundation for the comparative scoring presented in the next section.

4.3.2. Design Options

Artificial reefs around cages

Artificial reef modules placed near fish cages can enhance biodiversity and create new habitats for marine organisms. These structures promote coral settlement and attract fish populations, strengthening natural food chains and supporting local fisheries. The reefs could also function as structural anchors that improve cage stability under rough sea conditions and could be interesting for tourism functions [Bracho-Villavicencio et al., 2023].

Integrated Multi-Trophic Aquaculture (IMTA)

This approach combines species from different trophic levels in one system. Waste from fish production becomes nutrients for lower trophic species, improving water quality and reducing eutrophication. IMTA can increase total yield and ecosystem stability but requires higher technical knowledge and maintenance [Fang et al., 2016; Liu et al., 2022].

Fish aggregation through cage structures
Fish cages naturally act as aggregation devices that attract wild species seeking shelter and food. This process occurs even without active intervention, as the cage frames and mooring components provide structural complexity similar to natural reefs. However, the extent and ecological benefits of aggregation can be influenced by design choices, such as the use of environmentally friendly materials, mesh size, and positioning relative to currents and habitats. When intentionally considered in the design phase, fish aggregation can enhance local biodiversity and nearby fishing opportunities while minimizing ecological disturbance. Nonetheless, it does not directly improve water quality and requires management to prevent overfishing [Dagorn et al., 2013].

Fish health and environmental monitoring
Installing sensors to monitor dissolved oxygen, temperature, and fish behaviour enables early detection of stress or disease. Continuous data collection supports management decisions and reduces losses from poor water quality. However, effective operation depends on maintenance capacity and stable power supply [Flores-Iwasaki et al., 2025].

Snorkelling, diving, and eco-tourism
Designing fish farms for low-impact tourism can combine recreation with environmental education. Underwater structures such as artificial reefs or seaweed lines can attract interesting marine life. This diversification offers additional income but requires strict safety management and monitoring of environmental impact [Hishamunda et al., 2014].

Educational and research visits
Fish farms can function as demonstration sites for schools, universities and non-governmental-organisations. Educational visits raise awareness of sustainable aquaculture, strengthen collaboration between fishers and researchers, and improve social acceptance of aquaculture projects [Stevenson and Irwin, 2018].

Solar energy integration
Solar photovoltaic panels can power aeration systems, feeders, or communication devices, reducing fuel dependence and emissions. Although beneficial for environmental performance, high installation costs and exposure to marine corrosion pose a challenge for integration on small community farms [Han et al., 2022].

Small-scale desalination units
Compact desalination units can produce freshwater at sea, reducing the need for frequent trips to shore for traditional fishers. Renewable-powered systems have been tested for marine use but remain experimental and maintenance-intensive. Their high initial cost limits feasibility under current conditions [U.S. Department of Energy, 2021].

Connectivity systems (Wi-Fi or radio link)
Establishing communication links between fish farms or fishers, and shore can improve coordination and safety at sea. Connectivity enhances real-time contact with families and support services, adding social value. Although with a limited direct ecological effect [Buck and Langan, 2017].

Safe-harbor features on platforms
Basic safety provisions such as first-aid kits, lights, or flotation devices can allow fish farms to serve as temporary shelters for traditional fishers. These measures improve safety and demonstrate collective responsibility among fishers with minimal investment [Michler-Cieluch et al., 2009].

4.3.3. Summary
The ten identified options together illustrate the range of possibilities for multifunctional fish farms in Sisal. They address ecological restoration, social participation, and operational reliability, reflecting the three dimensions of the Triple Bottom Line. The following section applies the MCDA to evaluate these options systematically and determine which best align with the values expressed by the local community.

4.4. MCDA

4.4.1. Conceptual Framework

MCDA provides a structured way to compare options when several criteria must be considered. It combines performance scores of alternatives with the relative importance of sustainability dimensions to generate transparent rankings [Estévez and Gelcich, 2015]. In this chapter MCDA links community priorities, expressed through the Triple Bottom Line, to the assessed performance of ten design options. The approach translates qualitative preferences into a systematic ordering of multifunctional options that reflect local values rather than external assumptions [Sauvé et al., 2022; Li et al., 2023].

4.4.2. Methodology

The MCDA provides the link between community preferences and the technical assessment of design options. It combines two separate inputs: Firstly, the questionnaire results presented in Section 4.2, which express stakeholder priorities, and secondly, the utility scores of design options, introduced later in Section 4.4.3. Which indicate how well each option performs on the TBL framework.

Step 1: Stakeholder weights
Average importance ratings for Planet, People, and Profit from the questionnaire are normalized so their sum equals one. This produces the weight vector $(w_{\text{People}}, w_{\text{Planet}}, w_{\text{Profit}})$ for each stakeholder group, representing the relative importance of the three sustainability dimensions.

Step 2: Utility scores of design options
Each design option receives a utility score from 1 to 5 for each dimension, based on its estimated contribution to ecological, social, and economic outcomes. Higher values represent stronger contributions. The scores per design option are introduced later in Section 4.4.3.

Step 3: Weighted aggregation in MCDA
The combination of stakeholder preferences and design performance takes place in the MCDA calculation. For each design option j, a composite score is calculated as shown in Equation 4.1:

$$S_j = w_{\text{Planet}} \cdot u_{j,\text{Planet}} \; + \; w_{\text{People}} \cdot u_{j,\text{People}} \; + \; w_{\text{Profit}} \cdot u_{j,\text{Profit}} \tag{4.1}$$

where $u_{j,k}$ is the utility score of option j on dimension k, and w_k is the stakeholder weight for that dimension. This produces a composite S_j on a 1–5 scale.

Step 4: Ranking of alternatives
The composite scores are compared to establish a ranked list of design options. The calculation is performed separately for the high school and fisheries stakeholder groups to identify converging or diverging priorities between generations and experience levels.

4.4.3. Scoring of the Preliminary Designs

Each design option was scored on a scale from 1 to 5 across the three dimensions of the TBL. The purpose of this scoring is to quantify how each option performs within the sustainability framework before weighting it with stakeholder preferences in the MCDA. Detailed reasoning for each score is provided in Appendix B.

Scoring Framework
Scores of 1 represent the lowest contribution and 5 the highest. The Profit dimension is adjusted to reflect relative investment, meaning low-cost or cost-saving solutions receive higher Profit scores. The scale definitions are shown below.

Planet

1: No ecological contribution or potential negative impact.

2: Small or indirect ecological benefit.

3: Moderate ecological benefit; helps prevent environmental risks.

4: Strong ecological benefit with measurable improvements.

5: Very high ecological contribution through restoration or significant enhancement.

People

1: No social value or may reduce acceptance.

2: Limited social benefit, affecting few people directly.

3: Moderate social contribution; improves daily work or provides modest community benefit.

4: Strong social benefit; enhances safety, inclusion, or legitimacy.

5: Very high social value; essential for community acceptance or safety.

Profit

1: No economic benefit or investment outweighs returns.

2: Limited financial contribution or high cost with minor savings.

3: Moderate impact; provides supplementary income or manageable investment.

4: Strong impact; reduces costs or generates income with low investment.

5: Very high contribution; low-cost solution with major savings or new market potential.

Utility Scores of Design Options
The resulting scores for all ten options are summarized in Table 4.1. These scores serve as the technical input to the MCDA, which combines them with stakeholder weights to derive composite rankings.

Table 4.1: Utility scores for design options under the Triple Bottom Line (adjusted Profit dimension).

Design option	Planet	People	Profit
Artificial reefs around cages	5	3	2
Integrated Multi-Trophic Aquaculture (IMTA)	4	2	1
Fish aggregation through cage structures	3	2	1
Fish health and environmental monitoring	4	3	2
Educational and research visits	3	4	3
Solar energy integration	3	3	1
Snorkeling, diving, and eco-tourism	2	4	4
Small-scale desalination units	2	4	1
Connectivity systems (WiFi or radio link)	2	4	1
Safe-harbor features on platforms	2	5	2

4.4.4. Results

High School Survey Application

The normalized weights derived from the high school questionnaire were applied directly to the preliminary design scores from Section 4.4.3 using the MCDA procedure. Table 4.2 shows the raw averages and resulting normalized weights for Planet, People, and Profit, while Table 4.3 presents the composite scores and final ranking of all ten design options.

Table 4.2: High school priorities: raw averages and normalised weights.

Dimension	Raw mean (0–5)	Normalised weight
Planet	4.94	0.408
People	3.89	0.321
Profit	3.28	0.271

Table 4.3: MCDA ranking of design options based on high school weights.

Rank	Design option	Composite score
1	Artificial reefs around cages	3.545
2	Educational and research visits	3.321
3	Snorkeling, diving, and eco-tourism	3.184
4	Fish health and environmental monitoring	3.137
5	Safe-harbor features on platforms	2.964
6	Integrated Multi-Trophic Aquaculture	2.545
7	Solar energy integration	2.458
8	Small-scale desalination units	2.372
9	Connectivity systems (Wi-Fi or radio link)	2.372
10	Fish aggregation through cage structures	2.137

Artificial reefs rank first, followed by educational visits and eco-tourism. This reflects a preference for tangible, visible functions that deliver ecological improvement and learning opportunities. Monitoring and safety measures also score relatively high, indicating recognition of their role in reliability and responsible operation. In contrast, options requiring higher investment or technical expertise, such as IMTA and desalination, rank lower, consistent with their limited feasibility under local cooperative conditions. These results show that the economic dimension in the MCDA reflects perceived affordability and cost–benefit balance rather than absolute profitability. Stakeholders favour options that feel financially manageable and avoid high-risk or capital-intensive investments.

Fisheries Stakeholder Survey Application

The normalized weights derived from the fisheries stakeholder questionnaire were applied to the same preliminary design scores from Section 4.4.3 using the MCDA framework. Table 4.4 presents the raw averages and normalized weights, and Table 4.5 lists the resulting composite scores and ranking of design options.

Table 4.4: Fisheries stakeholder priorities: raw averages and normalised weights.

Dimension	Raw mean (0 to 5)	Normalised weight
Planet	5.00	0.366
People	4.67	0.342
Profit	4.00	0.293

Table 4.5: MCDA ranking of design options based on fisheries stakeholder weights.

Rank	Design option	Composite score
1	Artificial reefs around cages	3.439
2	Educational and research visits	3.342
3	Snorkelling, diving, and eco-tourism	3.268
4	Fish health and environmental monitoring	3.073
5	Safe harbour features on platforms	3.025
6	Integrated Multi-Trophic Aquaculture	2.439
7	Solar energy integration	2.415
8	Small-scale desalination units	2.391
9	Connectivity systems (Wi-Fi or radio link)	2.391
10	Fish aggregation through cage structures	2.073

The ranking shows a pattern consistent with the high school results. Ecological and educational functions again score highest, while complex or capital-intensive measures rank lowest. The slightly higher weights for People and Profit among stakeholders raise the relative position of monitoring and safety options, reflecting their operational experience and focus on reliability. Overall, both groups align on

the importance of visible ecological benefits, community involvement, and practical manageability as the defining criteria for multifunctional fish farm development in Sisal.

4.4.5. Conclusion MCDA Results

The MCDA results show strong agreement between the two stakeholder groups in how multifunctional options are prioritised. Both analyses rank artificial reefs, educational visits, and eco-tourism as the most desirable functions, indicating a shared preference for visible ecological enhancement and socially inclusive activities. Options that combine environmental improvement with education or participation achieve the highest composite scores in both cases.

The similarity in results reflects the close correspondence of the Planet, People, and Profit weights across groups. As both groups assign comparable importance to ecological and social dimensions, their final rankings converge, producing almost identical ordering of alternatives. The main difference lies in the range of scores: the high school group shows a wider spread between top and bottom options, suggesting stronger differentiation in perceived value, whereas the fisheries stakeholders produce a narrower range, reflecting more balanced and pragmatic evaluations.

Across both analyses, high-investment or technically demanding measures such as IMTA and desalination consistently occupy the lowest positions. This convergence highlights a shared understanding that multifunctional development in Sisal should focus on attainable, low-complexity measures that deliver tangible ecological and social benefits.

Overall, the MCDA demonstrates that the local community values simplicity, visibility, and participation in multifunctional fish farm design. Principles that together define a coherent foundation for socially accepted aquaculture development in Sisal.

4.5. Attainability of Solutions

4.5.1. Purpose and Approach

The MCDA identifies which multifunctional measures are most valued by local stakeholders, but a high ranking does not necessarily imply that a measure can be implemented under real conditions. The attainability analysis therefore examines which of the most promising functions can realistically be constructed, operated, and maintained by the community in Sisal. Its purpose is to determine which measures deliver visible environmental and social value while remaining manageable for a community-led cooperative. Although the MCDA already includes the economic dimension through the profit criterion, this represents the perceived economic value that stakeholders associate with each option, such as potential savings or additional income. The attainability assessment, in contrast, considers practical financial and technical feasibility. Whether the cooperative can actually finance, build and sustain these measures under local conditions. In this way, both analyses complement each other rather than overlap: the MCDA captures perceived community value, whereas the attainability analysis tests real-world implementability.

From the ten multifunctional options evaluated in the MCDA, the top five were selected for detailed assessment. These represent the most feasible balance between ecological benefit, social participation, and technical simplicity. The lower-ranked options, such as IMTA, desalination, or solar integration, are not essential for achieving social acceptance at this stage, as the MCDA results indicate that they are viewed as too technical, costly, or complex for the cooperative's current capacity. Nevertheless, these advanced measures could become relevant in the future once local experience, financial resources, and external partnerships expand.

1. Artificial reefs
2. Fish health and environmental monitoring
3. Snorkelling and eco-tourism
4. Educational and research visits
5. Safe harbour features

The remaining options including Integrated Multi Trophic Aquaculture, solar energy integration, fish aggregation through cage structures, small scale desalination units, and connectivity systems are ex-

cluded from the current attainability analysis because they exceed the practical and methodological scope of this study. These functions also ranked lowest in the MCDA, confirming that they are perceived by stakeholders as less valuable or relevant under current local conditions. Implementing them would require advanced technical knowledge, specialised equipment, and sustained financial investment that are not attainable within the capacity of a community led cooperative or within the timeframe of this project. Beyond their technical and financial complexity, these measures also offer limited additional utility in terms of community participation and short term feasibility, making them less effective for achieving immediate social acceptance or operational resilience. For these reasons, they are considered beyond the scope of the present report. Nevertheless, as they hold long term potential to enhance sustainability and multifunctionality once technical capacity, partnerships, and funding improve, they are identified as promising directions for future research and pilot implementation.

Each of the five selected functions is evaluated using verified interview data, literature evidence, and engineering judgement. The analysis focuses on realistic implementation rather than theoretical potential, translating stakeholder preferences from the MCDA into socially grounded and technically achievable design choices suited to Sisal's environmental and socioeconomic context.

4.5.2. Methodology

The attainability assessment applies a structured, semi-quantitative scoring system. Each function and its variants are evaluated on a five-point scale across five criteria representing financial, technical, and social feasibility. The scoring integrates local cost data, exposure conditions, and community participation potential, with weighting factors assigned according to their relative importance under Sisal's conditions. Investment requirement and robustness each carry a weight of 0.25, community engagement 0.20, and required skills and operational simplicity 0.15 each.

These unequal weights reflect the specific feasibility constraints faced by a community-led offshore initiative. Investment and robustness receive the highest weights because financial capacity and structural durability are essential prerequisites: if an option is unaffordable or cannot withstand waves and corrosion, it cannot be implemented regardless of its ecological or social benefits. Community engagement is weighted slightly lower but remains decisive for long-term acceptance and cooperative ownership. Required skills and operational simplicity have the smallest weights, as both can improve gradually through training and experience once financially and structurally viable systems are in place. Together, this weighting scheme captures that in Sisal, affordability and reliability determine what can be built, while engagement, skills, and simplicity influence how well it can be sustained.

Evaluation Criteria and Weights

1. **Investment requirement (weight: 0.25)**
   This criterion measures the relative financial effort needed to implement each option. Since cost varies substantially between functions, investment is compared within each category rather than across all options. Scores range from 1 (highest relative cost, dependent on major external funding) to 5 (lowest relative cost, feasible within cooperative means).
2. **Robustness in local conditions (weight: 0.25)**
   Reflects how well the system can operate under Sisal's marine exposure. A score of 5 indicates proven performance in comparable offshore environments with minimal maintenance needs; a 1 represents designs unlikely to withstand such exposure without damage or failure.
3. **Community engagement potential (weight: 0.20)**
   Evaluates how directly the option involves or benefits the local community, including fishers, students, and NGOs. A score of 5 denotes active local participation in construction, maintenance, or operation, while 1 indicates minimal or no direct engagement.
4. **Required skills (weight: 0.15)**
   Considers the level of technical knowledge, training, or external expertise needed to build, operate, and maintain the system. A score of 5 means the cooperative can manage the activity after basic instruction, whereas 1 represents full dependency on specialized external support.
5. **Operational simplicity (weight: 0.15)**
   Captures the complexity and frequency of tasks needed for daily operation and upkeep. High-

scoring options (4–5) can be maintained through simple, low-frequency routines; low scores (1–2) require intensive or technically demanding work.

Calculation Method
Each option j receives a score $a_{j,k}$ on criterion k. Weighted aggregation yields the composite attainability score:

$$S_{\text{att},j} = \sum_{k=1}^{5} w_k \, a_{j,k} \tag{4.2}$$

where w_k represents the criterion weight. Attainability scores $5.0 \geq S_{\text{att},j} \geq 4.0$ indicate solutions can be implemented immediately or with small grants. Scores $4.0 > S_{\text{att},j} \geq 3.0$ suggest partial external support is needed. $S_{\text{att},j} > 3.0$ Indicates that the option is not feasible for community-led implementation under current conditions.

Structure of Results
Each function is presented using the same structure for clarity and comparison:

- Context and relevance
- Variants considered
- Cost and feasibility overview
- Scoring by criterion and composite results
- Interpretation and recommendation

This consistent format ensures that differences between options can be traced transparently to their underlying criteria.

4.5.3. Artificial Reefs

Context and Relevance
Artificial reefs are among the most direct and attainable measures to enhance the ecological performance of the fish farm in Sisal. They provide structural habitat for marine organisms, increase biodiversity, and can also serve as anchoring structures for cages or platforms. Their durability and limited maintenance demands make them well suited for a community-based initiative operating in exposed conditions with limited technical resources. Considering Sisal's marine environment, concrete structures are preferred over lightweight or mechanically complex designs (Interview Reefy, 2025 Appendix A).

Variants Considered
Two viable artificial reef configurations were identified through interviews with 'Reefy' and the 'Reef Ball Foundation' and supported by published references. These represent contrasting approaches in scale, logistics, and community involvement:

Reef Balls
Reef Balls are hollow, dome-shaped modules made from pH-balanced, marine-grade concrete without steel reinforcement, which prevents corrosion and ensures a long service life . Their perforated geometry enhances hydrodynamic stability and provides complex habitat niches for colonization. Over 500,000 units have been deployed worldwide for ecological restoration and habitat enhancement. A typical group of deployed Reef Balls can be seen in Figure 4.4, where their rounded forms and openings promote current flow and diverse colonization patterns.(Interview Reef Ball Foundation, 2025 Appendix A)

According to the Reef Ball Foundation's representative for Mexico, one-tonne units can be fabricated locally using transportable moulds provided by the organization. Sub-tonne modules can be deployed from small boats with lift bags and basic handling equipment, while larger ones require contractor vessels. Fabrication costs are approximately USD 500 per tonne assuming moulds are locally available. Additional vessel or labour costs depend on sea conditions but remain moderate compared to fabrication. Reef Balls can also be fitted with stainless inserts for mounting light equipment. Multiple units

can be combined to create reef patches or to function as anchors. Field experience shows rapid colonization by algae and sponges within weeks, followed by fish presence within months and mature reef development after two to three years (Interview Reef Ball Foundation, 2025; Appendix A).

Figure 4.4: Example of deployed Reef Balls used for marine habitat restoration. The hollow, perforated design enhances hydrodynamic stability and provides complex habitats for colonization [Reef Ball Foundation, 2025].

Reefy Modular Blocks

Reefy designs interlocking concrete modules for ecological enhancement and, when needed, hydrodynamic attenuation. The standard block discussed for Sisal measures approximately $1\,\text{m} \times 1\,\text{m} \times 3\,\text{m}$, weighs 5.3–6 t depending on mix design, and is cast without reinforcement. Calcium carbonate surface treatments can be applied to promote colonization (Interview Reefy, 2025 Appendix A). Reefy confirmed that these modules could act as reef elements and potential anchoring points, subject to stability checks under local loading. However, installation would require specialist lifting or contractor vessels due to their weight. Indicative production cost is around USD 1,200 per block excluding logistics. The company indicated that molds could be transported to Mexico for local casting, but this would still require organizing heavy-lift capacity and trained personnel. Permitting, mold shipping, and professional supervision increase logistical complexity and cost. Arrays designed for hydrodynamic attenuation would require several layers of blocks, further increasing total investment (Interview Reefy, 2025 Appendix A).

For reference, plain cast concrete blocks fabricated locally in Yucatán cost approximately 13,500–27,000 MXN for 1 t, 21,000–42,000 MXN (1,000–2,050 USD) for 4 t, and 24,750–42,500 MXN (1,200–2,100 USD) for 5.5 t units [José López Gonzalez, Personal communication, 2025]. These figures provide a local benchmark for material and fabrication costs.

Cost and Feasibility Overview

Table 4.6 summarizes the verified cost ranges and qualitative feasibility characteristics for both systems, normalized per tonne for comparability.

Table 4.6: Indicative unit costs and feasibility for artificial reef options (2025 values; normalized to approximate USD per tonne)

Option	Approx. cost (USD/t)	Evidence and feasibility summary
Plain cast concrete (reference)	250–430	Based on UNAM data (2025), converted from 13,500–42,500 MXN per 5.5 t unit using 17 MXN = 1 USD. Locally fabricated using simple molds, deployable from small fishing boats.
Reef Balls	≈ 500 (fabrication only)	Locally cast with reusable molds. Deployment possible from small vessels using lift bags. Moderate additional costs for handling and vessel time.
Reefy modular blocks	≈ 240 (fabrication only)	Indicative production cost per block ($1,200 for 5 t). Local feasibility depends on mold transport, heavy-lift access, and supervised installation.

Note: Costs exclude mold transport and installation logistics.

Scoring by Criterion

The attainability scores for each reef option were determined using the weighted criteria defined in Section 4.5.2. The justification for each score is summarized in Table 4.7.

Table 4.7: Attainability scores and rationale for artificial reef options.

Criterion (weight)	Reef Balls	Reefy blocks	Justification
Investment requirement (0.25)	3	4	Reef Balls are moderately priced and feasible with cooperative resources. Reefy blocks appear cheaper per tonne but require imported molds and heavy-lift installation, which increases total investment.
Robustness in local conditions (0.25)	5	5	Both options are massive, unreinforced concrete structures proven in similar offshore environments.
Required skills (0.15)	4	3	Reef Balls can be produced locally with basic training; Reefy blocks require engineering supervision and specialized handling.
Operational simplicity (0.15)	5	4	Reef Balls require minimal post-installation maintenance. Reefy blocks are passive but involve more demanding logistics.
Community engagement potential (0.20)	5	2	Reef Balls enable direct local participation in casting, placement, and monitoring. Reefy blocks rely on external support, limiting local involvement.

Weighted scoring results

Each criterion was multiplied by its weight according to the methodology described earlier. The resulting composite attainability scores are summarized in Table 4.8. Note that in this table the full calculation is shown for clarification. For further calculations only the final score is shown.

Table 4.8: Weighted attainability scoring for artificial reef options in Sisal.

Criterion weight summary	Reef Balls	Reefy modules
Investment requirement (0.25)	0.75	1.00
Robustness in local conditions (0.25)	1.25	1.25
Required skills (0.15)	0.60	0.45
Operational simplicity (0.15)	0.75	0.60
Community engagement (0.20)	1.00	0.40
Composite attainability score	**4.35**	**3.70**

Interpretation and Recommendation

Reef Balls achieve a composite score of 4.35, representing high attainability under Sisal's local condi-

tions. Their moderate cost, simple fabrication, and potential for community involvement make them the preferred reef configuration. Because molds can be shared regionally, fabrication can be organized locally with basic training and low logistical dependency. Reefy modular blocks score 3.70, reflecting strong technical durability but lower local feasibility due to lifting and installation constraints. Therefore Reef Balls are recommended as artificial reef and anchor solution.

4.5.4. Fish Health and Environmental Monitoring

Context and Relevance

Environmental and fish health monitoring are essential for responsible aquaculture management. Monitoring systems enable early detection of water-quality deterioration, support transparent reporting, and provide data for regulatory or scientific collaboration [Food and Agriculture Organization of the United Nations, 2010]. In Sisal's offshore environment, maintenance capacity is limited, and exposure to waves, corrosion, and biofouling increases the risk of equipment failure. Monitoring technologies must therefore be robust, autonomous, and simple to maintain under these conditions [Delauney et al., 2010].

Variants Considered

Two realistic monitoring configurations were identified: a commercial Sofar Ocean Spotter buoy and a low-cost Do-It-Yourself (DIY) sensor kit. Both can collect basic water-quality data but differ strongly in durability, investment level, and maintenance requirements.

Sofar Ocean Spotter Platform

The Spotter is a compact, solar-powered surface buoy that measures waves, temperature, and barometric pressure and can integrate current and water-quality sensors through a Smart Mooring system [Sofar Ocean, 2025]. It weighs 7.5 kg, can be deployed from a small boat, and transmits data via satellite or cellular link. Vendor information indicates a cost between USD 7,000 and 15,000 depending on configuration [Sofar Ocean, 2025]. Maintenance consists of periodic cleaning and sensor calibration. The buoy has been widely used for coastal monitoring, demonstrating long-term robustness under marine exposure. A Spotter buoy is shown in Figure 4.5, illustrating its compact form and integrated solar panel design. It can provide reliable environmental data for both the cooperative and research institutions such as UNAM.

Figure 4.5: The Sofar Ocean Spotter buoy used for marine environmental monitoring. The buoy is solar-powered, transmits data via satellite or cellular networks, and supports additional Smart Mooring sensors for current and water-quality measurement (Source: Sofar Ocean, 2025).

DIY Sensor Kit

Open-hardware projects for aquaculture monitoring offer documented designs for buoys that measure temperature, pH, and dissolved oxygen using low-cost sensors and microcontrollers. Examples include

the systems described by Medina et al. (2022) and Lu et al. (2022), which cost between USD 660 and 2,015 including solar power and flotation housing [Medina, Monroy, et al., 2022; Lu et al., 2022]. These prototypes functioned in sheltered waters but suffered from condensation, sensor drift, and biofouling. Regular recalibration and component replacement are required, limiting their practicality for continuous offshore operation.

Cost and Feasibility Overview
Table 4.9 summarizes indicative costs and operational characteristics for both systems.

Table 4.9: Indicative costs and operational feasibility for monitoring system options.

Option	Approx. cost (USD)	Operational characteristics and feasibility
Spotter buoy (Sofar Ocean)	7,000–15,000	Fully autonomous, solar-powered buoy with real-time telemetry. Proven long-term performance in open-sea conditions. Requires only basic deployment and periodic cleaning.
DIY sensor kit	660–2,015	Open-source buoy using low-cost sensors. Functional in sheltered waters but vulnerable to biofouling and humidity. Requires frequent recalibration and technical supervision.

Note: Costs exclude anchoring and data subscription fees.

Scoring by Criterion
Scores were assigned according to the evaluation criteria defined in Section 4.5.2. Justifications are summarized in Table 4.10.

Table 4.10: Attainability scores and rationale for monitoring options.

Criterion (weight)	Spotter buoy	DIY kit	Justification
Investment requirement (0.25)	2	4	The Spotter requires significant upfront investment, whereas the DIY kit is inexpensive but short-lived.
Robustness in local conditions (0.25)	5	2	The Spotter is engineered for marine exposure; the DIY design is unsuitable for continuous offshore use.
Required skills (0.15)	4	3	The Spotter requires minimal training; the DIY kit demands technical assembly and troubleshooting.
Operational simplicity (0.15)	5	2	The Spotter operates autonomously; the DIY kit needs frequent maintenance and recalibration.
Community engagement potential (0.20)	3	4	The DIY kit encourages participation in construction and learning. The Spotter involves less direct handling but can support joint data analysis with UNAM.

Composite Results
Weighted aggregation of the criteria yields the composite attainability scores in Table 4.11.

Table 4.11: Weighted attainability scoring for monitoring options in Sisal.

Option	Composite score
Spotter buoy (Sofar Ocean)	3.70
DIY sensor kit	3.05

Interpretation and Recommendation
The Spotter buoy achieves a composite attainability score of 3.70, making it the only viable option for reliable environmental monitoring in Sisal. It offers high robustness, minimal maintenance, and integration potential with UNAM research programs. Although the investment is substantial, partial funding through academic or environmental grants would make implementation feasible. The DIY kit, despite its educational value, is unsuitable for continuous offshore use due to durability limitations. Therefore, the Spotter buoy is recommended as the sole attainable monitoring solution when protection against theft and external funding is available.

4.5.5. Snorkelling and Eco-Tourism

Context and Relevance

Marine tourism around the fish farm can provide social value and supplementary income when designed for safety and minimal ecological disturbance. In Sisal, community participation through nature-based tourism is already increasing, and such activities can complement existing cooperative operations [Meza-Osorio et al., 2024]. In this study, the focus is on simple, small-scale configurations that combine education, recreation, and environmental tours rather than commercial mass tourism.

Variants Considered

Three practical tourism configurations were identified: guided surface snorkelling, small-scale dive tourism, and a hybrid community operator model. Each represents a different balance between investment, training needs, and operational complexity.

Guided Surface Snorkelling

Supervised snorkelling around the fish farm is the most accessible tourism function. It relies on small groups accompanied by trained local guides and requires only basic infrastructure such as life vests, fins, and safety markers. The activity can be managed within existing cooperative operations and combined with environmental education briefings before entry. Group control, route planning, and no-touch rules minimize ecological disturbance to reefs and cages. Evidence from comparable shallow-water programs shows that well-supervised snorkelling significantly reduces habitat impact while improving visitor awareness [Hannak et al., 2011]. This variant can be launched with limited funding and provides immediate opportunities for local employment and environmental outreach.

Small-Scale Dive Tourism

Diving attracts a different visitor segment seeking closer underwater experiences but introduces higher safety and cost demands. Operations require certified instructors, liability insurance, and reliable equipment such as tanks, compressors, and oxygen systems. Diving sessions are restricted to calm sea conditions due to wind and current exposure typical of the Sisal coast. Although environmental disturbance can be controlled through strict dive codes and active supervision [Giglio et al., 2020], the necessary infrastructure and certification make this option unrealistic without external partners or sustained demand. Its relevance lies mainly in longer-term development once the cooperative acquires operational experience.

Hybrid Community Operator Model

The hybrid configuration combines community-based snorkelling and education with professionally managed diving. Local cooperatives conduct snorkelling tours, environmental interpretation, and logistics, while certified dive operators organize limited diving sessions on favourable weather days. The model distributes responsibilities and investment, provides training opportunities for local guides, and ensures that diving activities meet professional safety standards. This cooperative–commercial structure has proven successful in Latin American coastal tourism, promoting equitable benefit-sharing and conflict reduction between resource users [Cárdenas-Torres et al., 2007]. In Sisal, it offers a gradual and low-risk path toward diversified marine ecotourism.

Cost and Feasibility Overview

Table 4.12 summarizes indicative costs and operational characteristics for the three options.

Table 4.12: Operational prerequisites and feasibility for tourism configurations.

Option	Indicative investment level	Key feasibility characteristics
Guided surface snorkelling	Low	Requires trained guides, safety equipment, and clear procedures. Easily integrated with existing cooperative activities.
Small-scale dive tourism	High	Requires certified instructors, insurance, compressors, and safety infrastructure. Strongly weather-dependent.
Hybrid community operator model	Medium	Combines local snorkelling and externally managed diving. Shared investment in gear and insurance. Enables skill transfer and equitable benefit sharing.

Scoring by Criterion

Scores were assigned according to the evaluation criteria defined in Section 4.5.2. Justifications are summarized in Table 4.13.

Table 4.13: Attainability scores and rationale for tourism configurations.

Criterion (weight)	Snorkelling	Dive tourism	Hybrid	Justification
Investment requirement (0.25)	5	2	3	Snorkelling needs minimal equipment. Diving is capital- and insurance-intensive. The hybrid model reduces the cooperative's investment burden through shared responsibilities.
Robustness and environmental suitability (0.25)	4	3	4	Snorkelling can operate safely under calm conditions. Diving is limited by exposure. The hybrid model applies conservative scheduling and professional supervision.
Required skills (0.15)	4	2	4	Snorkelling requires guide training; diving demands certified instructors. The hybrid model combines both capacities.
Operational simplicity (0.15)	5	3	4	Snorkelling logistics are straightforward. Diving involves more complex maintenance and safety routines. The hybrid setup maintains simplicity in daily operations.
Community engagement potential (0.20)	5	3	5	Snorkelling and the hybrid model promote local employment and environmental education. Dive tourism relies on external professionals.

Composite Results
Weighted aggregation of the criteria yields the composite attainability scores in Table 4.14.

Table 4.14: Weighted attainability scores for tourism configurations.

Option	Composite score
Guided surface snorkeling	4.60
Hybrid community operator model	3.95
Small-scale dive tourism	2.60

Interpretation and Recommendation
Guided surface snorkeling achieves the highest attainability score of 4.60 and should be implemented as the first tourism function. It combines low cost, simple logistics and social engagement. The activity strengthens environmental awareness among visitors and creates direct community income without requiring new infrastructure. The hybrid community operator model, with a score of 3.95, can follow after the snorkeling phase. It offers a way to expand activities safely through collaboration with certified dive operators while slowly increasing local skills. Small-scale dive tourism, scoring 2.60, is not recommended under current conditions and should be deferred until sufficient technical capacity, insurance, and demand exist. Overall, tourism development in Sisal should begin with guided snorkeling and progress toward the hybrid model once experience and partnerships are established.

4.5.6. Educational and Research Visits

Context and Relevance
Educational and research activities can be integrated into the multifunctional fish farm to strengthen community engagement, environmental awareness, and transparency. Unlike other functions, there are no distinct technical variants to compare. These activities either occur or they do not. The analysis therefore focuses on one integrated program that combines environmental education, citizen participation, and academic collaboration.

Program Description
In Sisal, the proximity of the UNAM campus offers a direct opportunity for cooperation between re-

searchers, students, and the local cooperative. This collaboration can support field courses, joint monitoring projects, and data exchange without requiring new infrastructure. The fish farm can thus act as a living laboratory for applied studies, training, and demonstrations [Falk and Dierking, 1997]. School visits and community workshops can expose students to marine ecosystems and sustainable aquaculture practices. Citizen science initiatives, such as basic water-quality logging or biodiversity observations, can involve fishers, students, and residents in data collection and interpretation [Bonney et al., 2009]. Together, these activities strengthen environmental literacy and reinforce the farm's social legitimacy [Ardoin et al., 2020].

Cost and Feasibility Overview

Table 4.15 summarizes the operational characteristics and feasibility aspects of the integrated educational and research program.

Table 4.15: Feasibility characteristics of the educational and research program.

Aspect	Description
Main partners	Collaboration with UNAM Sisal for supervision, data collection, and safety oversight, supported by local schools and the cooperative.
Infrastructure	Uses existing boats, safety kits, and teaching materials. No new facilities or specialized equipment required.
Activities	Guided visits, ecological interpretation, and simple monitoring tasks linked to UNAM projects.
Operational needs	Coordination with academic and school calendars, flexible scheduling under suitable sea and weather conditions.
Community benefit	Builds trust, promotes learning, and strengthens the visibility of sustainable aquaculture.

Attainability Scoring

The program was evaluated using the same five weighted criteria described in Section 4.5.2. The scores and rationale are summarized in Table 4.16.

Table 4.16: Attainability scores for the educational and research program.

Criterion (weight)	Score	Justification
Investment requirement (0.25)	5	Relies entirely on existing resources and infrastructure. Costs are limited to fuel and coordination.
Robustness in local conditions (0.25)	5	Can be rescheduled depending on weather. No permanent installations exposed to marine conditions.
Required skills (0.15)	4	Requires basic guiding and safety training, which can be provided locally through UNAM.
Operational simplicity (0.15)	4	Straightforward to organize and integrate into cooperative routines. No special permits needed.
Community engagement potential (0.20)	5	Directly involves students, fishers, and researchers in collaborative learning and monitoring.

Composite Results

Weighted aggregation of the criteria yields the composite attainability scores in Table 4.17.

Table 4.17: Composite attainability score for the educational and research program.

Option	Composite score
Integrated educational and research program	4.70

Interpretation and Recommendation

The integrated educational and research program achieves a composite attainability score of 4.70, confirming that it is among the most feasible and socially valuable functions for the fish farm in Sisal. It can

be implemented immediately through coordination with UNAM and local schools, using existing vessels and safety infrastructure. The program promotes environmental education, strengthens collaboration between science and the cooperative, and reinforces transparency in aquaculture practices. It should be prioritized alongside early-stage measures such as the basic safety kit, guided snorkeling, and Reef Ball deployment. Together, these functions create an attainable foundation for a multifunctional fish farm that delivers tangible ecological, educational, and community benefits.

4.5.7. Safe Harbor Features

Context and Relevance

Safe harbor features increase the safety and social acceptance of offshore fish farms by enabling immediate aid, reliable communication, and temporary refuge during short weather events. A stepwise implementation allows safety to improve in parallel with operational experience and cooperative growth. Authoritative guidance for small vessels and aquaculture platforms in exposed conditions emphasizes simplicity, corrosion resistance, high visibility, and routine inspection of equipment [Food and Agriculture Organization of the United Nations et al., 2012].

Variants Considered

Three attainable configurations were evaluated: a Basic Safety Kit, an Emergency Communication Link, and a Reinforced Safe Platform. These options represent progressively higher investment and technical complexity and can be introduced sequentially as capacity grows.

Basic Safety Kit

The foundation of any safety setup is a fixed emergency kit on the cage or service platform, following standard recommendations for small vessels. Essential components include a marine first aid kit, throwable flotation device with a line, whistle or sound signal, waterproof torch, and approved distress signals. Items should be clearly labeled, stored above the splash zone, and made from corrosion-resistant materials with reflective markings. Regular inspection ensures that all components remain functional and perishable items are replaced [Food and Agriculture Organization of the United Nations et al., 2012].

Emergency Communication Link

Once basic equipment is in place, an independent communication capacity provides emergency contact and coordination. Guidance for small craft highlights the importance of VHF radio or equivalent means, standardized distress procedures, and operator familiarization. Where coverage gaps exist, satellite messengers or registered distress beacons can provide redundancy. Clear instructions and periodic drills are essential for readiness without advanced systems [Food and Agriculture Organization of the United Nations et al., 2012].

Reinforced Safe Platform

At a later development stage, a reinforced section of the service platform can provide temporary refuge and workspace during short weather events. The structure typically includes non-slip decking, guardrails, secure cleats, and bollards for fastening lines or equipment. High-visibility markings, fenders, and corrosion-resistant materials improve safety and durability. Reinforcement through cross-bracing or load-spreading joints enables the structure to withstand dynamic forces transmitted through the mooring system. Regular inspection of joints, surfaces, and safety fittings ensures continued operability and compliance with offshore maintenance practices [Fredriksson and Beck-Stimpert, 2019; Buck and Langan, 2017].

Cost and Feasibility Overview

Table 4.18 summarizes the indicative investment level and main feasibility considerations.

Table 4.18: Relative investment level and feasibility for safe harbor configurations.

Option	Relative investment level	Key feasibility characteristics
Basic safety kit	Low	Uses standard marine components. Easily assembled and maintained by the cooperative. Provides immediate safety improvement.
Emergency communication link	Moderate	Requires purchase and installation of a VHF radio or satellite device. Needs short training and periodic testing.
Reinforced safe platform	High	Involves structural upgrades such as cleats, fenders, guardrails, and reinforcement. Requires hardware, materials, and technical oversight during installation.

Attainability Scoring Inputs

Table 4.19 shows the criterion-by-criterion ratings using the five weighted criteria from Section 4.5.2.

Table 4.19: Explanation of attainability scores for safe harbor configurations.

Criterion (weight)	Basic safety kit	Communication link	Safety platform	Justification
Investment requirement (0.25)	5	4	2	The basic safety kit uses inexpensive and widely available components. The communication link adds moderate cost and training needs, while the mooring platform requires higher investment in hardware and installation.
Robustness and environmental suitability (0.25)	5	4	3	The safety kit and communication systems are durable when properly protected. Mooring components such as chains and fittings are prone to corrosion and wear, reducing long term robustness under Sisal's saline and high energy conditions.
Required skills (0.15)	5	3	4	The safety kit requires no special training. Communication systems require familiarity with radio operation, while mooring installations require some mechanical skills and inspection routines.
Operational simplicity (0.15)	5	4	4	The safety kit is easily maintained. Communication systems need periodic testing, and mooring systems involve simple visual inspections and occasional replacement of worn parts.
Community engagement potential (0.20)	4	4	4	Safety kits and communication systems strengthen community trust and safety awareness. Mooring platforms visibly enhance cooperative safety culture and offer opportunities for hands on maintenance.

Table 4.20: Weighted attainability scores for safe harbor configurations.

Option	Composite attainability score
Basic safety kit	4.80
Emergency communication link	3.85
Reinforced safe platform	3.25

Interpretation and Recommendation

The basic safety kit achieves the highest attainability score (4.80) and is the only configuration recommended for immediate implementation. It offers clear and direct safety benefits at minimal cost, can be assembled entirely from locally available materials, and requires no external support. The emergency

communication link, with a score of 3.85, may be added later if the basic kits prove durable and reliable in daily use. The reinforced safe platform, at 3.25, is not recommended under current conditions and at the scale of the current fish farms. Priority should therefore be placed on equipping fish farms with a standardized safety kit and ensuring its proper maintenance and periodic inspection.

4.5.8. Conclusion Attainability of Solutions

The attainability analysis complements the MCDA by translating stakeholder preferences into practical feasibility under current community and environmental conditions in Sisal.

The composite scores differentiate clearly between options. For artificial reefs, Reef Balls score 4.35 and Reefy modules score 3.70. For environmental monitoring, the Spotter buoy scores 3.70 and the DIY kit scores 3.05. Within tourism, guided snorkelling scores 4.60, the hybrid model scores 3.95, and dive tourism scores 2.60. The integrated educational and research program scores 4.70. Safe harbour features are led by the basic safety kit at 4.80, followed by the communication link at 3.85, and the reinforced platform at 3.25.

Across functions, three factors explain high attainability: low investment, limited technical complexity, and strong community engagement. Options with minimal maintenance and direct local participation score highest, while systems that require specialist equipment, high capital cost, or continuous maintenance score lower.

Key sensitivities are maintenance frequency under bio fouling, sea state limitations for tourism and diving, lifting logistics for reef deployment, and the risk of theft or loss of safety equipment.

4.6. Conclusion

The chapter shows that social acceptance in Sisal is most likely when multifunctional measures are simple, visible, attainable and directly involve the community. Both the TBL analysis and the MCDA highlight options that combine ecological value with social benefits, while the attainability assessment finds measures that can actually be built and maintained with existing capacity. The standardized safety kit, guided snorkelling, educational and research visits with UNAM, locally fabricated Reef Balls, and the Spotter buoy with partial funding all meet these conditions. Each measure appears near the top of the rankings because it links technical performance to participation, learning, or safety that community members can observe and take part in.

Responses collected through the community questionnaire also provided valuable qualitative insight into why these measures are socially accepted. Among students, multifunctionality was seen as a way to “help local families” and “not harm the sea.” Many described fish farms as opportunities for learning and school visits, emphasizing curiosity, education, and future employment. For them, acceptance grows when the project visibly protects the environment and creates new spaces for youth involvement and education.

Fishers, in contrast, approached multifunctionality through practicality. Their open-ended responses emphasized “clean water,” “safety at sea,” and “cooperation among fishers,” showing that acceptance depends as much on reliability and shared responsibility as on ecological gain. They value operational simplicity, equipment that works, routines they can manage, and solutions that do not add technical burden. In their view, multifunctional elements gain legitimacy when they enhance daily safety and reduce risks rather than complicate operations.

The near-term path is therefore clear. Implement safety kits on all cages, organize regular educational and research visits, start guided snorkelling at small scale, and deploy Reef Balls as early ecological and anchoring measures. A Spotter buoy should follow when funding allows, supported by UNAM for data interpretation. Communication links and other advanced features can be considered once these foundations prove reliable.

By prioritizing attainable, transparent, and participatory measures, the fish farm can strengthen its credibility and build durable social acceptance. These first steps, focused on safety, education, and environmental care, align with both the aspirations expressed by students and the pragmatic expectations of fishers in the questionnaire. Together, they provide a shared foundation for sustainable and community-supported aquaculture development in Sisal.

5

Environmental Conditions Assessment

5.1. Introduction

Offshore aquaculture near Sisal is exposed to energetic and directionally consistent waves combined with cross-shore currents, conditions that challenge conventional circular cages typically designed for sheltered bays and fjords [Zhuo et al., 2024]. This chapter establishes the environmental basis and analytical framework for comparing a traditional round cage with a vessel-shaped alternative designed to reduce hydrodynamic loads in exposed offshore locations. The following sections present the data sources, analysis methods, and resulting input parameters used to define five representative environmental scenarios for subsequent simulation and design evaluation.

5.2. Data Analysis

This section summarises the datasets and processing steps used to define the environmental conditions for the offshore aquaculture site near Sisal, Yucatán. Complete methods, diagnostic plots and sensitivity checks are documented in the Appendix (F.2.2, F.3.4, F.2.3, and F.2.4).

Three complementary datasets were used to ensure both local accuracy and long-term statistical consistency. The first dataset consists of in-site measurements obtained from the ADCP, providing a twelve-year record of waves and currents at the offshore site. The second dataset is the reference study by Bakker et al., 2024, which combined ERA5 offshore reanalysis data with an earlier ten-year ADCP record to derive preliminary design conditions. The third dataset is the forty-seven-year Radial Basis Function (RBF) downscaled ERA5 series, representing long-term reconstructed nearshore wave conditions at the ADCP location. The methodology used for this downscaling process is described in Section F.3.2.

For the wave component, statistical analyses were conducted to describe both normal and extreme sea states. The applied approach and results are detailed in Appendix F.2.2 for the ADCP dataset and in Appendix F.3.4 for the RBF dataset. These analyses establish representative and design wave parameters that reflect both the local site measurements and the broader long-term variability.

Current velocities were analysed using the 12 year ADCP record to determine representative and near-extreme flow values. The processing and cleaning procedures applied to the velocity components are described in Appendix F.2.3. The resulting vertical profiles provide insight into how current speeds vary with depth, which is essential for estimating forces on the aquaculture.

The interaction between waves and currents was examined to identify how directional alignment and concurrent values influence hydrodynamic loads on aquaculture structures. Directional statistics and joint-occurrence analyses were performed to isolate rare but critical events that produce the largest combined flow stresses. The associated directional joint-extreme results are presented in Appendix F.2–

F.4.

Based on the analyses, five representative environmental scenarios were defined to support the subsequent design and simulation work:

1. Most frequent sea state
2. 20-year return storm
3. 5-year return storm (no current)
4. 5-year return storm
5. Towing operation

Each scenario represents a distinct combination of wave and current conditions that together define the operational and structural boundaries for offshore aquaculture. The full set of environmental input parameters adopted for the simulations are significant wave height (H_s), spectral peak period (T_p), wave direction, current velocity (U) and current direction.

This towing scenario differs slightly from the other simulations, as it represents a towing operation rather than a stationary offshore condition. The setup is nevertheless based on the most frequent sea-state scenario, ensuring that realistic and locally representative conditions are used as input.

Fishermen emphasized during interviews that being self-sustaining is essential for their operations, particularly for maintenance and logistics. Consequently, the size and weight of the fish farm must remain limited so that it can be towed inshore or offshore using their own vessels [Bakker et al., 2024]. This capability is important both for routine maintenance and as an emergency measure when severe storms or hurricanes approach the Yucatán coast.

In this towing scenario, both the circular and vessel-shaped designs are assumed to be moved offshore by two to three small boats under calm conditions. The structures are towed northward at a constant velocity of approximately 6 km/h, consistent with the safe towing speed of small fishing boats. To reduce hydrodynamic resistance, fishermen indicated that the net can be partially raised and therefore only about 40% of its designed depth is assumed to remain submerged during towing.

5.2.1. Wave Height and Period

The H_s and corresponding T_p used in this study were derived from three complementary datasets analysed using the Extreme Value Analysis (EVA) procedures detailed in Appendix F.2.2 and Appendix F.3.4. These datasets capture different spatial and temporal scales: (1) the regional reanalysis by Bakker et al., 2024, (2) a locally measured twelve-year ADCP record and (3) a forty-seven-year statistically downscaled RBF series. All datasets were modelled to represent wave conditions at the same nearshore location of the ADCP site, ensuring spatial consistency across analyses and allowing direct comparison of results.

Table 5.1: Threshold values and 20-year return wave parameters obtained from the three datasets.

Wave height data	**Threshold (m)**	H_s **(m)**	T_p **(s)**
Bakker et al. (2024)	2.70	3.40	8.50
12-year ADCP dataset	2.55	2.96	7.85
Extended RBF (1979–2025)	2.35	3.06	8.42

The ADCP- and RBF-based results show close agreement, both yielding 20-year return heights near 3.0 m with corresponding peak periods of approximately 7.8 s. In contrast, Bakker et al., 2024 reported a slightly higher 20-year estimate ($H_s = 3.4$ m, $T_p = 8.5$ s).

The ADCP analysis (F.2.2) provides the most direct representation of local conditions but is statistically limited by its shorter time span. The RBF dataset (F.3.4) extends this record to 47 years while maintaining calibration to the ADCP data, improving the stability of extreme value estimates without sacrificing local accuracy. For that reason, the RBF dataset was adopted as the basis for defining the design and operational scenarios used in this research.

Consistency between ADCP and RBF datasets.

The RBF record successfully reproduces the magnitude and temporal variability of the locally measured ADCP waves. Figure 5.1 compares the full RBF series with the overlapping ADCP measurements (2014–2025), while Figure 5.2 shows a strong one-to-one correlation between concurrent H_s observations. The calculated correlation coefficient ($r = 0.88$) confirms excellent agreement between both datasets.

The directional comparison in Appendix F.3.3 further confirms consistency, with a mean absolute directional error (MAE) of $32.5°$ and a 90th-percentile difference (P90) of $75.1°$. In simple terms, the MAE indicates that, on average, the RBF and ADCP wave directions differ by about $32°$, while the P90 value means that 90% of all directional differences are smaller than $75°$. This shows that the majority of the wave directions align well between both datasets, with only a few larger deviations during more variable sea conditions.

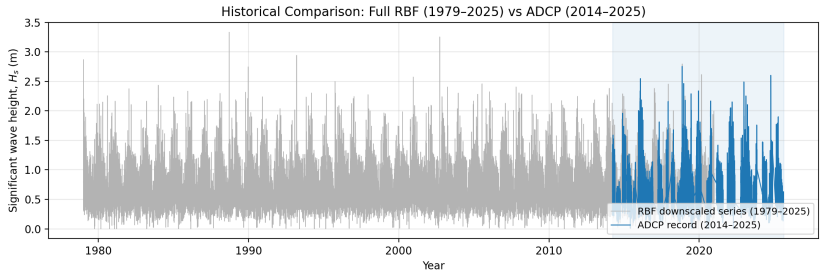

Figure 5.1: Historical comparison of H_s: full RBF versus ADCP. The shaded region indicates the overlap period.

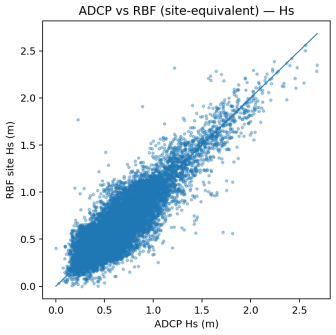

Figure 5.2: Scatter comparison of H_s between ADCP and RBF datasets. Data align closely along the 1:1 line, with a correlation of $r = 0.88$, confirming strong consistency.

Selection of H_s for scenario definition

The long-term RBF dataset provides the statistical foundation for defining the representative and extreme sea states used in the five simulation scenarios. Two analyses were applied: (1) a frequency analysis to identify the most common (modal) conditions and (2) a Peaks-Over-Threshold extreme value analysis to determine 5- and 20-year return heights.

Normal sea states

Figure 5.3 shows the frequency distribution of H_s for the full RBF record. The distribution is skewed to the right, with the most occurrences between 0.4 m and 0.8 m. The mode ($H_s = 0.61$ m) represents the most frequent sea state and was selected as the representative value for Scenario 1. This height characterises the average operational conditions at the site based on the long term RBF dataset.

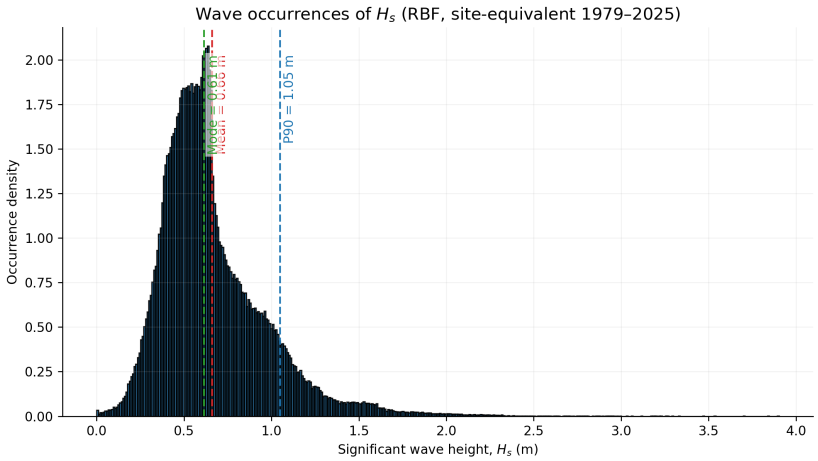

Figure 5.3: Distribution of H_s in the RBF dataset. The green dashed line indicates the modal value (0.61 m).

Extreme sea states

The 5-year and 20-year design wave heights were derived from the RBF-based Peaks-Over-Threshold analysis described in Appendix F.3.4. Figure 5.4 shows the fitted return-level curve, based on a threshold of $u = 2.35$ m. The fitted GPD parameters ($\sigma_u = 0.217$ m, $\xi = 0.216$) indicate a moderately heavy-tailed distribution. The corresponding return levels are $H_s = 2.62$ m for the 5-year event and $H_s = 3.06$ m for the 20-year event.

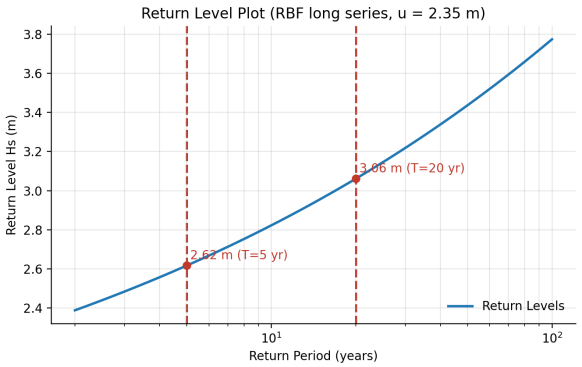

Figure 5.4: Return-level plot of H_s derived from the RBF dataset. The 5-year and 20-year return levels correspond to 2.62 m and 3.06 m, respectively.

These values form the basis for the three storm-related scenarios:

- **Scenario 2: 20-year return storm** – representing the extreme design condition.
- **Scenario 3: 5-year return storm (no current)** – used to compare with the analytical calculations in Section 6.3, which neglect current effects with the Aquasim.
- **Scenario 4: 5-year return storm** – representing severe but more frequently occurring conditions.

The use of the RBF dataset ensures that both representative and extreme sea states are statistically stable and physically realistic, as it merges the local accuracy of the ADCP record with the long-term variability of the regional climate.

Wave period

The T_p associated with each scenario was derived using the RBF downscaled dataset. Because this dataset provides the longest continuous record and shows a stronger correlation between H_s and T_p ($R^2 = 0.21$ compared to $R^2 = 0.13$ for the ADCP data), it was adopted as the leading source

for determining representative and design wave periods. The regression follows the same power-law relation applied in Appendix F.2.2, linking H_s and T_p.

Extreme sea states For the 5-year and 20-year return storms, the regression yielded peak periods of $T_p = 7.82$ s and $T_p = 8.42$ s, corresponding to wave heights of $H_s = 2.62$ m and $H_s = 3.06$ m, respectively. These values are in alignment with those obtained from the twelve-year ADCP record, which produced a design period of $T_p = 7.85$ s at $H_s = 2.96$ m. This consistency confirms that the downscaled RBF record reproduces local wave behaviour while providing improved long-term stability. Figure 5.5 shows the fitted H_s–T_p relationship with the 5- and 20-year design conditions highlighted.

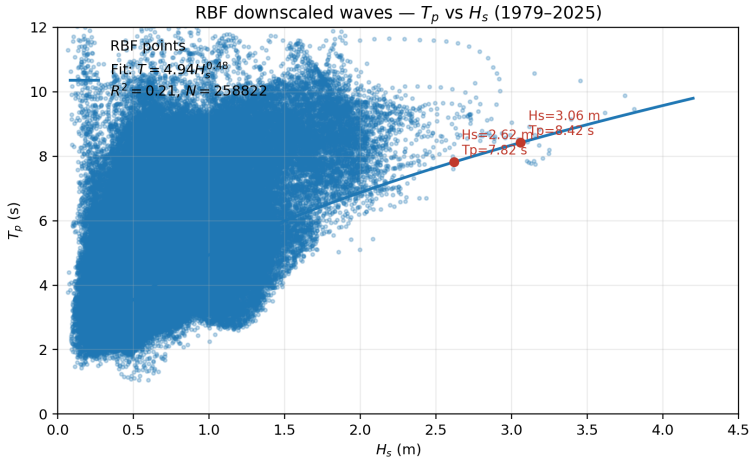

Figure 5.5: Relationship between H_s and spectral peak period T_p for the RBF downscaled dataset. The red markers indicate the 5-year and 20-year design conditions ($H_s = 2.62$ m, $T_p = 7.82$ s and $H_s = 3.06$ m, $T_p = 8.42$ s).

Normal sea state For the most frequent sea state (Scenario 1), the mean wave period (T_m) was used instead of the spectral peak period. This better represents the continuous lower-energy conditions at the site. Figure 5.6 shows the relationship between H_s and T_m derived from the RBF dataset. The modal wave height ($H_s = 0.66$ m) corresponds to a mean period of $T_m = 3.14$ s, which characterises the typical operational environment under calm conditions.

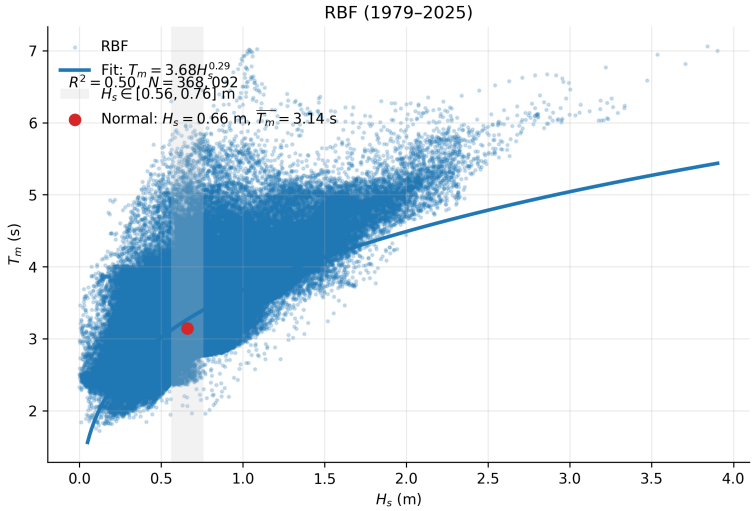

Figure 5.6: Relationship between H_s and T_m in the RBF dataset. The red marker indicates the most frequent sea state ($H_s = 0.66$ m, $T_m = 3.14$ s).

Towing Operation

During towing, the fish farm moves northward (360°) at a velocity of 6 km/h, while waves bears toward 220° as in scenario 1. This relative motion increases the encountered wave frequency. Applying the Doppler relation $\omega_e = \omega - kU\cos\theta$, with $T = 3.14$ s, $U = 1.67$ m/s, and $\theta = 140°$, yields an encounter period of approximately $T_e = 2.50$ s. The significant wave height remains unchanged at $H_s = 0.66$ m, but the effective period experienced by the structure decreases due to the forward motion during towing.

Scenario Summary

The final environmental parameters used for the simulations are summarised in Table 5.2, show the scenario's that will be used the structural analysis. Each scenario represents a distinct combination of wave and current conditions corresponding to either operational or design states.

Table 5.2: Simulation scenarios used for the structural analysis

Scenario	H_s [m]	T_p [s]
1. Most frequent sea state	0.66	3.14
2. 20-year return storm	3.06	8.42
3. 5-year return storm (no current)	2.62	7.82
4. 5-year return storm	2.62	7.82
5. Towing operation	0.66	2.50

5.2.2. Currents

Currents are a key hydrodynamic forcing on offshore aquaculture systems, influencing mooring loads, cage deformation and water exchange. The present analysis is based on the twelve-year ADCP dataset collected offshore of Sisal between 2014 and 2025 (Appendix F.2.3). Compared to the earlier ten-year record analysed by Bakker et al., 2024, the extended dataset provides improved statistical confidence and captures a wider range of seasonal and interannual variability.

General characteristics

The ADCP provides horizontal velocity components (u, v) across depth bins from approximately -9.6 m to -1.1 m, from which the resultant current speed U was computed. After two-pass outlier filtering, the near-surface regime shows steady but moderate currents that weaken with depth.

The distribution of raw speeds at -1.1 m depth (Figure 5.7) highlights the modal behaviour of the flow. The most frequently observed speed is 0.17 m/s, while most observations fall between 0.1 and 0.4 m/s. Maximum values remain below 0.7 m/s, indicating that previously reported 1 m/s currents likely stemmed from methodological or calibration differences. Therefore, this year's extended twelve-year dataset was used as the basis for the final design values.

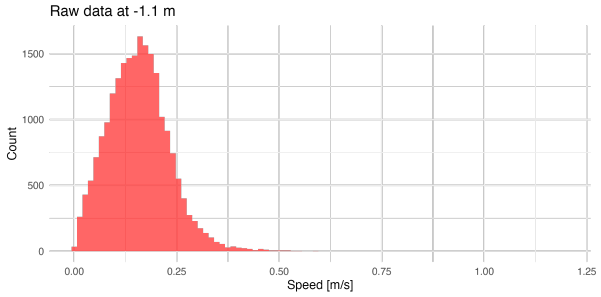

Figure 5.7: Histogram of raw current speeds at -1.1 m depth. The modal current speed is approximately 0.17 m/s.

Design current speed

Representative design conditions were defined using the 95th percentile of current speed at each measured depth (Appendix F.2.3). This percentile represents regularly occurring upper-end events, consistent with aquaculture design guidance.

The vertical profile in Figure 5.8 shows that currents are strongest near the surface ($U_{95} = 0.43$ m/s) and decrease to about 0.2 m/s below -6 m. This trend reflects the influence of surface winds and tidal mixing, with reduced shear at depth.

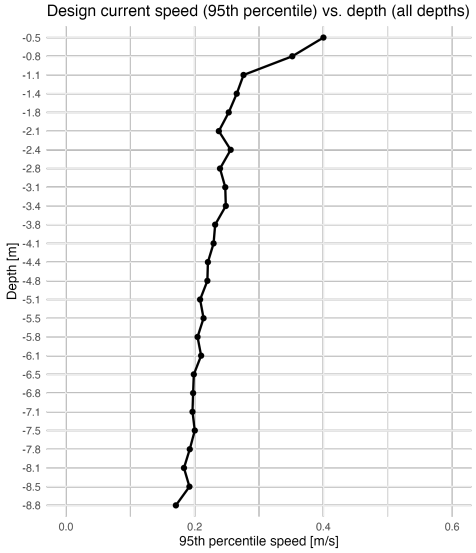

Figure 5.8: Design current speed profile based on the 95th percentile of measured current speed (2014–2025 dataset).

The 20-year design current speed was therefore defined as $U = 0.43$ m/s. The 5-year value was derived proportionally from the ratio of the 5-year to 20-year return wave heights (Section 5.2.1). Since $H_{s,5yr}/H_{s,20yr} = 2.62/3.06 = 0.86$, the 5-year current was taken as $U = 0.37$ m/s. This maintains physical consistency between storm intensities for waves and currents.

Towing operation

During towing operations, the aquaculture structure is transported northward from the port of Sisal at a speed of approximately 6 km/h (1.67 m/s). The local current field remains the same as during normal operation (mode = 0.17 m/s at $245°$), but the towing motion introduces an additional velocity vector oriented towards $0°$ (north).

Using standard oceanographic notation (angles measured clockwise from north), the resultant flow speed U_{tow} can be obtained by vector addition:

$$U_{\text{tow}} = \sqrt{v_1^2 + v_2^2 + 2v_1 v_2 \cos(\theta)}, \tag{5.1}$$

where $v_1 = 1.66$ m/s at $180°$ (towing direction), $v_2 = 0.17$ m/s at $245°$ and θ is the angle between the two vectors ($65°$). The resulting combined velocity is approximately:

$$U_{\text{tow}} = 1.74 \text{ m/s}. \tag{5.2}$$

This represents the effective flow acting on the structure during offshore towing operations and forms the basis for Scenario 5 in Table 5.3.

Scenario summary

The final current speeds adopted for all simulation scenarios are summarised in Table 5.3. These values represent the typical and design conditions derived from the extended ADCP record and the towing velocity calculation.

Table 5.3: Representative U adopted for the simulation scenarios.

Scenario	U [m/s]
1. Most frequent sea state	0.17
2. 20-year return storm	0.43
3. 5-year return storm (no current)	0.00
4. 5-year return storm	0.37
5. Towing operation	1.74

5.2.3. Wave–Current Interaction

The interaction between waves and currents determines the combined hydrodynamic loading on aquaculture systems. When the two are aligned, drag forces increase; when they are cross, large transverse stresses develop on the moorings and cage frame. This analysis uses the twelve-year ADCP dataset to identify dominant alignments and the most critical joint extreme events. Supporting figures and tables are provided in Appendix F.2.4.

Wave direction

Wave directions for the simulation scenarios were derived from the twelve-year ADCP wave statistics. Both the full dataset and the extreme-event subset confirm that waves predominantly approach from the northeast, consistent with Bakker et al., 2024.

For the 5-year and 20-year storm scenarios, a common wave heading of 350° was selected. As shown in Table F.4, the three highest-stress events at -1.1 m depth occur within 350–355°, indicating directional stability of storm-driven waves. The same trend is observed at greater depths (variations below 10°), justifying a single representative storm direction for both cases.

For normal operational conditions (Scenario 1), the dominant wave direction is 40°, representing typical conditions during calm to moderate seas.

Current direction

Current headings were extracted from the ADCP velocity components and evaluated under joint 95th-percentile conditions (Table F.3). All critical events fall within the “cross” category, confirming that strong waves and currents generally act at cross angles. Near the surface (-1.1 m), the dominant current direction ranges from 59° to 68°, producing an average wave–current misalignment of about 70°. This pattern persists across the water column, showing a consistent east–west current orientation characteristic of the Yucatán shelf.

The representative current directions used in the design scenarios are 241° for storm conditions and 245° for the most frequent sea state, corresponding to the mean headings observed during joint extremes.

Towing direction

The towing scenario represents deployment or retrieval of the aquaculture system along a northward route from the port of Sisal. Two current components were combined to determine the resulting flow direction. The first current of 1.66 m/s was directed southward (180°), resulting from towing the aquastructure northwards. The second, smaller component of 0.17 m/s was directed toward 245°, representing the prevailing current direction of the most common sea-state scenario. By resolving both currents into their east–west and north–south components and summing them, a resultant vector with a magnitude of 1.74 m/s and a direction of 185.1° was obtained, indicating a flow approximately 5° west of due south.

Scenario Summary

The final wave and current directions used in the five simulation scenarios are summarised in Table 5.4. These values reflect the dominant and statistically consistent orientations derived from the twelve-year ADCP dataset and the joint wave–current interaction analysis.

Table 5.4: Wave and current directions adopted for the five simulation scenarios.

Scenario	Wave dir [°]	Curr. dir [°]
1. Most frequent sea state	40	245
2. 20-year return storm	350	241
3. 5-year return storm (no current)	350	–
4. 5-year return storm	350	241
5. Towing operation	40	185.1

5.2.4. Conclusion and Final Scenario Matrix

The combined analysis of the twelve year ADCP record, RBF based wave statistics and joint wave–current interaction provides a consistent and locally accurate set of environmental input values. Normal conditions are defined by the most frequent sea state and the modal near surface current. The design storms use the RBF five and twenty year return heights with their corresponding periods from the H_s–T_p relation. Current speeds for the storm cases are based on the ADCP ninety fifth percentile scaling. The towing condition represents the vector sum of the towing speed and the prevailing current from the most frequent sea state.

Table 5.5 presents the final environmental parameters used in the further calculations. These values describe the typical operational, design and towing conditions for the offshore aquaculture site near Sisal.

Table 5.5: Final scenario matrix used for MWDF validation and AquaSim runs.

Scenario	H_s [m]	T_p [s]	Wave dir [°]	U [m/s]	Curr. dir [°]
1. Most frequent sea state	0.66	3.14	40	0.17	245
2. 20 year return storm	3.06	8.42	350	0.43	241
3. 5 year return storm (no current)	2.62	7.82	350	0.00	–
4. 5 year return storm	2.62	7.82	350	0.368	241
5. Towing operation	0.66	2.50	40	1.74	185.1

These scenarios cover the full range from normal operation to extreme design conditions and towing. They reflect the observed wave directions from trade wind and storm conditions, the perpendicular current directions from the ADCP data and the consistent current speeds derived from the extended analysis.

6

Design Optimization

6.1. Introduction

Hydrodynamic performance of both cage geometries is evaluated with AquaSim, and a simplified analytical estimate of the second-order mean wave drift force (MWDF) is used as an order-of-magnitude check. Together, these elements provide a consistent foundation for the comparison of mooring loads and for assessing whether a vessel-shape configuration offers a meaningful reduction in forces under Sisal's offshore conditions.

6.2. Methodology

This section outlines the methodology used to evaluate the hydrodynamic performance of a round and a vessel-shape aquaculture system under realistic local wave conditions near Sisal. The analysis combines numerical simulations in AquaSim with a simplified analytical MWDF estimation. The MWDF calculation serves solely as a consistency check to verify the order of magnitude and physical plausibility of the AquaSim simulation results.

6.2.1. Objective and Approach

The objective of this study is to quantify the (mean) hydrodynamic forces acting on both aquaculture systems and to assess whether the vessel-shape configuration leads to reduced loads compared to the conventional round cage. The primary focus lies on the numerical simulations performed in AquaSim, which model the full fluid–structure interaction of the cages under five different environmental scenarios.

The procedure consists of five main steps:

1. Defining geometric parameters of both structures and specifying environmental conditions
2. Setting up and running AquaSim simulations for five representative sea states
3. Measuring mean hydrodynamic loads from AquaSim outputs as mooring line tensions
4. Computing MWDF analytically for identical conditions using linear wave theory
5. Comparing analytical MWDF and AquaSim results to confirm physical consistency.

6.2.2. Geometric and Material Design Parameters

To ensure a fair comparison between both cage configurations, each system was designed to enclose an equivalent volume and surface area. This approach allows the influence of geometry on hydrodynamic behaviour and mooring line forces to be evaluated independently from differences in size or production capacity. The vessel-shape design features a streamlined half-circular bow intended to reduce flow resistance, while the circular configuration consists of a conventional floating ring. Both share equal draft, total projected height, and tube diameter, ensuring comparable hydrostatic and buoyancy characteristics.

Since Sisal does not yet have an operational fish farm, all design parameters (ranging from materials and structural dimensions to the overall cage shapes) can still be adapted to local conditions. As this study focuses on evaluating design performance rather than conducting a full structural optimisation, the principal parameters had to be defined prior to performing calculations and simulations.

The design process was based on three main sources of information: (1) literature on large-scale commercial aquaculture systems, (2) design parameters of the Celestún aquaculture described by Bakker et al. Bakker et al., 2024, p. 33, and (3) the most recent insights into local needs and opportunities for improvement compared to the Celestún case. Literature on industrial aquaculture provided an overview of common (industrial) design standards, including material selection, component ratios, and general cage shapes. The Celestún design served as a valuable local reference, while interviews with fishermen and local engineers helped identify practical requirements and existing challenges.

The cages in Celestún were developed by engineers from Ingenieria de Jaulas Marinas De México [Bakker et al., 2024], but their current design appears suboptimal, as two of the three cages have failed within the past year. Fishermen reported that nets frequently tear and that the structure lacks stability, occasionally submerging when weight is applied to the outer ring. The Celestún system uses High-Density Polyethylene (HDPE) floating pipes with a diameter of 160 mm, which has proven insufficient to maintain rigidity under load [Pipe, 2023]. In contrast, industrial-scale aquaculture systems, which typically cover an area up to eight times larger, use HDPE pipes of approximately 315 mm diameter [Zhuo et al., 2024]. To address the observed structural weaknesses while maintaining practical feasibility, a pipe diameter of 200 mm was selected as a balance between increased buoyancy and material handling capacity. This dimension also corresponds to one of the most readily available HDPE pipe sizes on the market [Industry, 2025].

For dimensional consistency, both cages were designed to maintain an equivalent net depth of 4.7 m. Based on Bakker et al., 2024, p. 34, a circular cage with a radius of 6 m and a depth of 4.7 m resulted in the lowest mooring line tension among three comparable designs. Using the same depth and projected surface area (approximately 113 m^2), a vessel-shape configuration was modelled with a length of 19.5 m and a width of 6 m, ensuring similar enclosed volume, leading to vessel-shape design depicted in figure 6.1

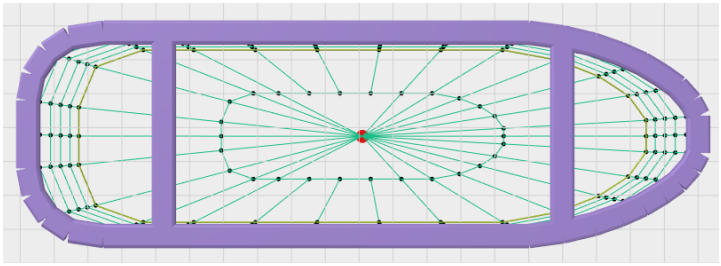

Figure 6.1: Vessel-shaped aquaculture design of a birds-eye view.

When design parameters derived from literature and local expertise conflicted, practical feasibility and local material availability were prioritised over industrial scaling factors. This choice ensures that the proposed design could realistically be built and maintained in Sisal, including being pulled ashore by two to three small fishing vessels for maintenance and inspection.

The mooring configuration was designed considering a local water depth of approximately 10 m. Each cage was connected using mooring lines of 30 m attached to a 20 m anchor chain. The additional chain segment acts as a mechanical damper, reducing peak tension by allowing gradual load transfer during wave motion. Since hardly any scientific literature is available on small-scale, single mooring-line offshore structures, optimal parameters should be further investigated in future research.

All resulting design parameters are summarised in Table 6.1. These dimensions were used as fixed input for subsequent hydrodynamic analysis, of the 5 scenarios from chapter 5.5, in the MWDF formulation and in AquaSim. Further design refinements and parameter sensitivity analyses are recommended for future work once field data from the Sisal site become available.

Table 6.1: Aquaculture design properties and dimensions.

Cage properties	**Amount**	**Unit**
Floating tube diameters (HDPE)	200	mm
Floating tube wall thickness	20	mm
Distance between floats	320	mm
Sinker tube diameter (stainless steel)	50	mm
Sinker tube wall thickness	10	mm
Net thread thickness	2	mm
Net depth	4.7	m
Net grid width	25	mm
Circular cage diameter	6	m
Vessel shaped length	19.76	m
Vessel shaped width	6	m
Length width ratio [Zhuo et al., 2024]	3.2-3.8	[-]
Surface area single cage	113.1	m^2
Anchor system		
Bridle line thickness	48	mm
Mooring line thickness	64	mm
Anchor chain thickness	30	mm
Bridle line length	5.4	m
Mooring line length	30	m
Anchor line length	20	m

6.2.3. Analytical MWDF Formulation as a Limit Check

The Mean Wave Drift Force (MWDF) represents the steady, second-order component of the wave-induced load on a structure. This analytical formulation was derived to provide a necessary order-of-magnitude reference for the line forces calculated by AquaSim, specifically focusing on the structure's response in the shallow-water limit.

The wave angular frequency ω and wavenumber k are rigorously coupled through the linear dispersion relation:

$$\omega^2 = gk \tanh(kh), \tag{6.1}$$

where $\omega = 2\pi/T_p$. This equation was solved iteratively for the wavenumber k for each specified wave period.

The mean wave drift force per unit draft is generally expressed as:

$$F_x^{(2)} = \frac{1}{2}\rho g A^2 Q(\omega, h, R), \tag{6.2}$$

where $A = H/2$ is the wave amplitude, R is the characteristic radius of the cage geometry, and $Q(\omega, h, R)$ is a dimensionless hydrodynamic coefficient. For slender geometries ($R \ll L$) in the shallow-water limit ($kh \ll 1$), this formulation simplifies to the following expression:

$$F_x^{(2)} \approx \rho g \frac{H^2}{4}(2R)\left(\frac{1}{(kh)^2}\right). \tag{6.3}$$

While this specific closed-form expression is an approximation primarily valid for $kh \ll 1$ (very shallow water), it effectively demonstrates the principle that the steady load must increase drastically as the depth decreases due to the body's proximity to the seabed, which is captured by the $(kh)^{-2}$ term. This limit provides a critical boundary check for the numerical model.

Geometric Porosity Correction

Since the structural surface is predominantly netting, a correction for geometric solidity was introduced to account for the reduction in the solid surface area exposed to the waves. The total mean wave drift

force on the structure was then estimated as the sum of the solid frame force and the geometrically corrected net force:

$$F_{\text{tot}} = F_{\text{tube}} + \phi F_{\text{net}}, \tag{6.4}$$

where F_{tube} is the force on the solid buoyant frame and F_{net} is the force calculated assuming a fully solid net surface. The applied factor ϕ is explicitly a geometric reduction factor derived from the netting's physical characteristics, as seen in equation 6.5.

$$\phi = \frac{(l+t)t}{l^2}. \tag{6.5}$$

This geometrically defined ϕ is used as a simple, linear multiplier to the net force, acknowledging that it only represents the exposed solid area and does not capture the complex hydrodynamic transmission effects.

Assumptions and Simplifications

To ensure that any observed differences are primarily attributable to the hydrodynamic shape effects, several simplifying assumptions were made for both the analytical and numerical models:

- The cage structures were modelled as rigid, vertical, and impermeable bodies, neglecting flexibility and structural coupling;
- The netting was treated as a rigid, porous vertical surface with the geometrically derived porosity ϕ;
- Linear wave theory was applied, assuming the absence of wave breaking or strong nonlinear effects;
- Waves were incident head-on to the cage;
- A constant water depth of $h = 10$ m was used.
- Effects from fish/biomass, viscous damping, and current–structure coupling were neglected.

Validation and Interpretation

Scenario 3, which represents a 5-year return storm without ambient currents (as detailed in table 5.5), was selected as the benchmark condition. The goal was to establish that the mean line forces obtained from AquaSim were consistent in order of magnitude with the analytical MWDF estimates.

6.2.4. Aquasim simulation

AquaSim is a hydrodynamic analysis software developed by Aquastructures AS in Norway and is widely used in the design and certification of commercial aquaculture structures such as floating cages, nets and mooring systems. The program has become an salmon industry standard for simulating how fish farms behave under combined wave and current loads and is routinely applied in the Norwegian aquaculture sector for both engineering design and regulatory verification [AS, 2024b; AS, 2024a]. Its established use in exposed-site aquaculture makes it a suitable and validated tool for our study, which investigates how alternative cage shapes would perform under similar environmental conditions to those near Sisal.

AquaSim uses the Finite Element Method to calculate the structural and hydrodynamic response of marine systems. In this approach, each structural component such as, floating pipes, mooring lines and net panels, is divided into a series of small connected elements. For each element, the governing equations of motion are solved to determine forces, deformations and interactions with surrounding water. By assembling all elements into one model, AquaSim can simulate how the entire aquaculture structure responds to environmental loading from waves, currents and gravity in a physically consistent way. The program combines Morison-type hydrodynamic formulations for drag and inertia with non-linear dynamic equations for structural motion [AS, 2024a, p 5–12]

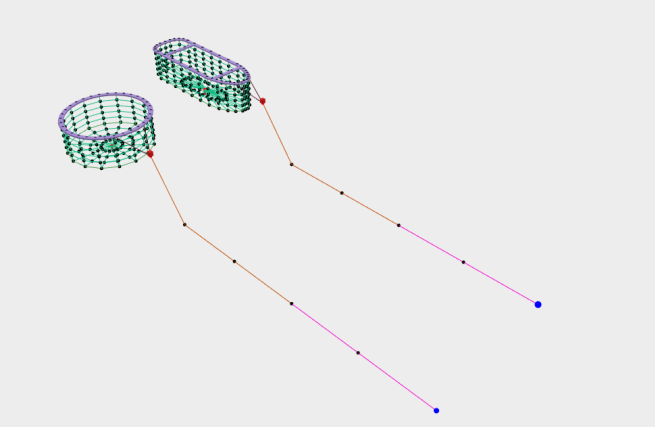

Figure 6.2: Round and vessel-shape design in AquaEdit.

The detailed model-building process resulted in the setup shown in Figure 6.2. Further explanation of AquaSim's theoretical basis, the full configuration and boundary conditions of the simulations and the model setup are described in Appendix D.

Assumptions and Simplifications

Several simplifying assumptions were introduced during the AquaSim model setup to ensure computational efficiency and to focus the analysis on comparing the hydrodynamic forces acting on the different cage shapes under typical offshore conditions.

- Linear wave theory was applied to represent the sea states. This assumes regular waves and neglects non-linear and breaking effects, which are expected to be limited under typical offshore conditions near Sisal. Wind forces on the structure not taken into account by themself.
- Steady state current conditions were used with uniform velocity and direction through the water column. This avoids the need to model vertical current profiles or transient flow variations.
- Mooring lines were represented as linearly elastic elements. Seabed friction, catenary effects and anchor–soil interaction were not included to keep the model focused on relative force differences between cage shapes. The end of the anchor chain was fixed to the seabed, which made it impossible to displace.
- Fatigue and wear effects of the mooring components were not considered. These long-term processes require extended time-domain simulations that fall outside the project scope.
- Numerical simplifications were applied to ensure feasible computation times. Fixed time steps, simplified convergence criteria and optimized mesh resolution were used for efficiency. Additionally the cage design was simplified to decrease the interaction effects between component to decrease numerical errors.

Limitations of the AquaSim Model

The AquaSim simulations provide valuable insight into the hydrodynamic behaviour of different cage shapes. However, several limitations should be acknowledged as they may influence the accuracy and reliability of the results. These limitations are primarily related to the numerical characteristics of the Finite Element Method, the representation of physical processes, and the available input data.

- Element length, mass, and stiffness idealization have a strong influence on the dynamic behaviour of the model. The chosen discretization determines the system's natural frequencies, and small variations in element size or stiffness distribution can lead to unrealistic vibration modes or altered tension responses in the mooring lines.
- The stability and accuracy of the time integration depend on the chosen time step. When the time step is too large, numerical errors may accumulate and cause energy drift or unrealistic oscillations over time. In addition, short simulation periods may still include start-up transients, which can bias the initial force results.

- The use of linear wave kinematics simplifies the environmental forcing by assuming small, regular waves and neglecting nonlinear and breaking effects. This may lead to an underestimation of low-frequency drift loads and extreme wave-induced forces.
- Uncertainty in the environmental input data, particularly from hindcast and reanalysis sources such as ERA5, introduces potential deviations in wave height, period, and current velocity. Climate change brings uncertain weather events and input differences harsh conditions can have a significant influence on the calculated forces and mooring tensions.
- The model does not account for fatigue, wear, or degradation of materials, and no explicit failure modes such as line rupture or net tearing were included. As a result, the simulations cannot represent long-term structural performance or predict behaviour during extreme events.
- The model setup was not calibrated or validated with experimental or field data. This limits confidence in the absolute magnitude of the predicted forces, although the comparative trends between the round and vessel-shape designs remain useful for design evaluation. Additionally, the absence of knowledge about fish mass and internal damping in the model means that the total inertia and energy dissipation of the system are lower than in reality.

These limitations should be taken into account when interpreting the simulation outcomes, as they may explain potential deviations between simulated and real-world behaviour.

6.3. Results

The analytical validation of the AquaSim setup using the MWDF method is presented first, followed by the simulation results for the four main environmental scenarios. This order allows the analytical results to serve as a reference for interpreting the numerical simulations.

6.3.1. Analytical validation (MWDF)

Figures 6.3 and 6.4 show the outcomes of the analytical mean wave drift force calculations for a full reference cylinder and a porous fish net cylinder for the complete dataset, respectively. The solid-cylinder case (Figure 6.3) represents the theoretical upper limit of wave loading, while the porous configuration (Figure 6.4) accounts for hydrodynamic permeability. As expected, the porous geometry yields substantially lower MWDF values, consistent with the partial transmission of wave energy through the net. These analytical estimates serve as a benchmark for evaluating the AquaSim simulations.

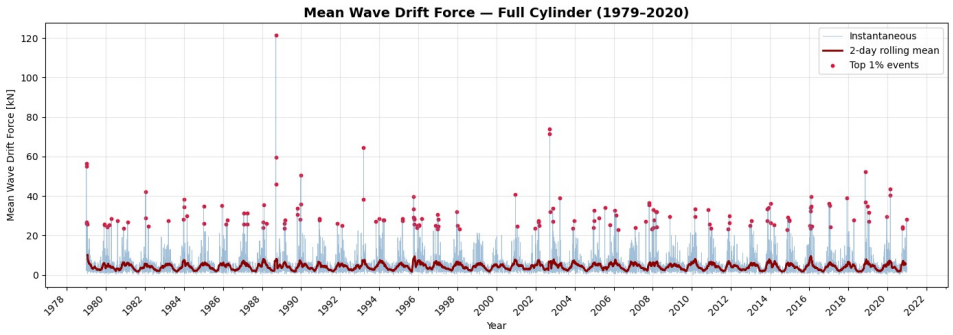

Figure 6.3: Calculation of the MWDF for a full cylinder.

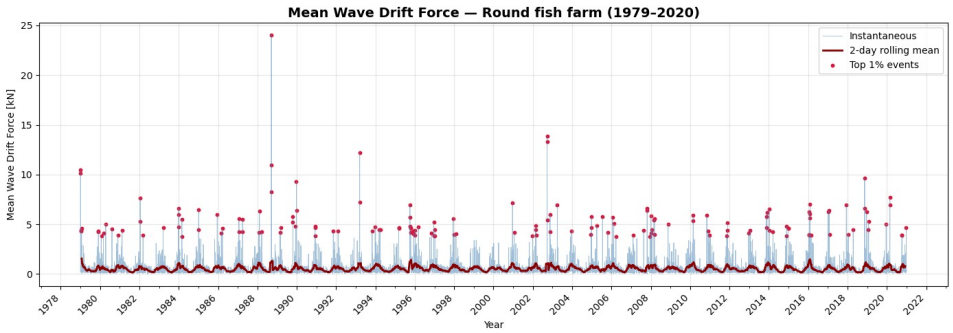

Figure 6.4: Calculation of the MWDF of a round fish farm with porous fishnet.

6.3.2. AquaSim Simulation Results

The AquaSim data results were obtained and visualized using the AquaView module of the AquaSim software. Within this environment, different environmental scenarios and structural parameters can be selected and analysed. The software allows users to extract numerical data from multiple sources while simultaneously generating a visual animation output. This visual representation is valuable for validating the realism and stability of the simulated fish farm behaviour under varying sea states. Two examples of such visualizations, under different environmental conditions, are shown in Figures 6.5a and 6.5b.

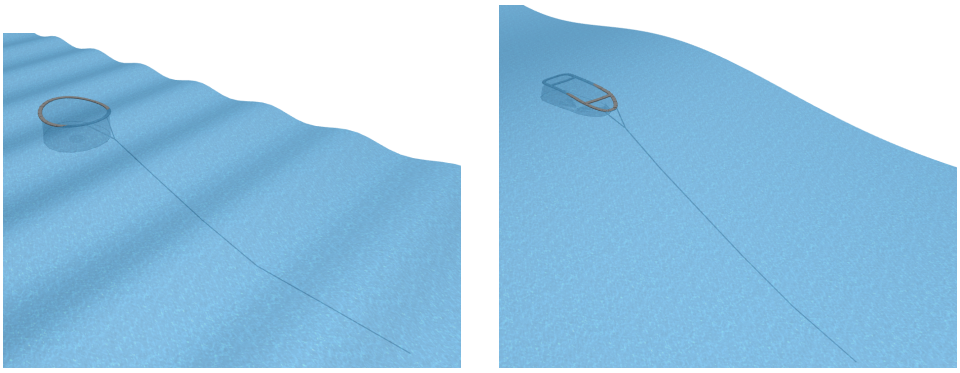

(a) AquaView circular aquaculture visualization under most frequent sea state conditions.

(b) AquaView vessel-shape aquaculture visualization under most 20-year storm conditions.

Figure 6.5: Example outputs from AquaView illustrating the hydrodynamic simulation environment used for analysis. The visualizations assist in verifying model behaviour and data integrity across different scenarios.

The results of the AquaSim simulations for the four main environmental scenarios are presented in Figures 6.6–6.9. For each case, the steady-state mooring line forces were obtained for both the round and vessel-shape aquaculture systems. The results illustrate how mooring line tension varies with environmental severity and allow direct comparison between the two geometries.

In Figure 6.6, corresponding to the most frequent sea state, the mooring line forces remain relatively low for both configurations. The vessel-shape cage shows slightly higher mean and peak tensions than the round cage, indicating greater hydrodynamic loading under mild combined wave and current conditions.

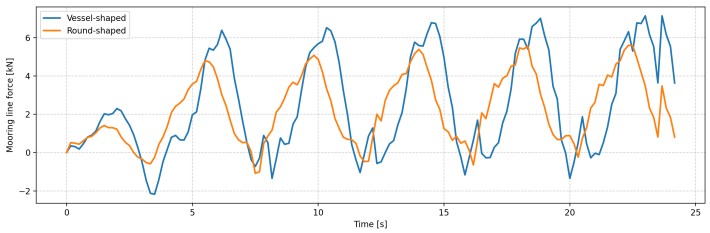

Figure 6.6: Scenario 1. Mooring line forces (kN) for the vessel-shape and round-shaped configurations under the most frequent sea state.

Under the 20-year return storm (Figure 6.7), a substantial increase in mooring line forces is observed for both configurations. The vessel-shape cage again experiences slightly lower overall tension.

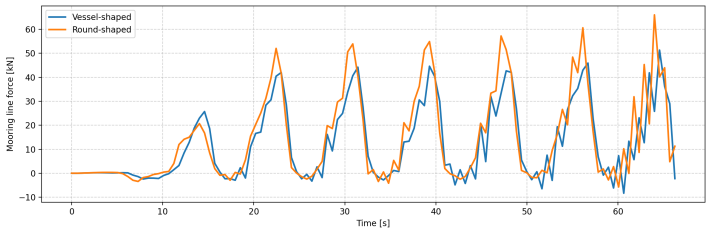

Figure 6.7: Scenario 2. Mooring line forces (kN) for the vessel-shape and round-shaped configurations during the 20-year return storm.

Figure 6.8 presents the results for the 5-year return storm without current. In this case, the absence of current isolates the wave-induced response. The mean line forces obtained from AquaSim align closely with the magnitude predicted by the analytical MWDF estimates, confirming the internal consistency of the model. The vessel-shape configuration again shows a lower mean load compared to the round cage.

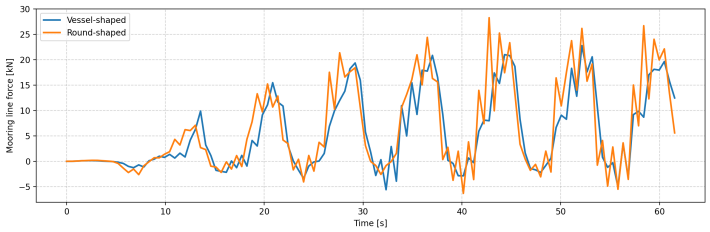

Figure 6.8: Scenario 3. Mooring line forces (kN) for the vessel-shape and round-shaped configurations during the 5-year return storm without current.

Figure 6.9 shows the 5-year return storm including current. The presence of current increases total line forces, particularly for the vessel-shaped configuration, which experiences higher peak loads when wave and current directions are misaligned. This effect highlights the sensitivity of the vessel-shaped geometry to combined wave–current interaction.

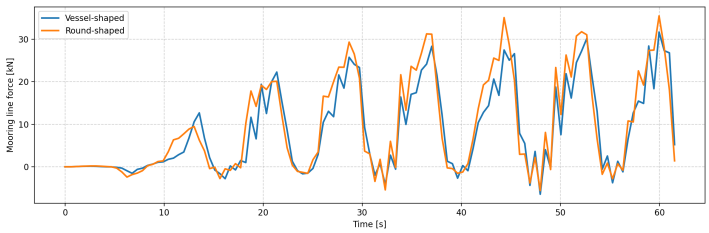

Figure 6.9: Scenario 4. Mooring line forces (kN) for the vessel-shape and round-shape configurations during the 5-year return storm.

Then, figure 6.10 presents the results for Scenario 5, representing the towing operation. This scenario differs from the environmental load cases, as the hydrodynamic forces are mainly generated by the towing velocity and flow direction rather than by waves. The results indicate that the vessel-shaped configuration experiences markedly reduced mooring line forces compared to the round-shaped system throughout the towing sequence. This reduction can be attributed to the streamlined geometry of the vessel-shaped cage, which leads to lower drag and more favorable flow separation during translational motion. The round configuration, by contrast, exhibits higher resistance and consequently greater line tension under identical towing conditions. These findings suggest that the vessel-shaped design offers significant hydrodynamic advantages when subjected to steady current or towing-related loads.

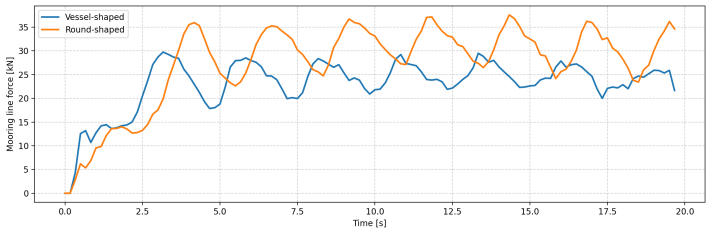

Figure 6.10: Scenario 5. Mooring line forces (kN) for the vessel-shaped and round-shaped configurations during the towing operation.

Table 6.2 shows the difference per scenario of the vessel shaped cage when compared to the round shaped fish cage. The mean of the 90th percentile highest values are taken for comparison. To eliminate jerking forces obscuring the highest forces.

Scenario	Difference
1. Most frequent sea state	128%
2. 20 year return storm	77%
3. 5 year return storm (no current)	95%
4. 5 year return storm	93%
5. Towing operation	69%

Table 6.2: Vessel compared to round, mean difference of the 90th percentile highest forces per scenario.

Finally, for scenario 3, the difference between the Analytical model and the AquaSim simulation can be found in table 6.3. For the AquaSim simulation the mean force of the 90th percentile was used for the comparison.

Model	Force [kN]
Analytical	13.381
Simulation	24.478

Table 6.3: Analytical model compared to the simulation of the round shaped fish farm in scenario 3, using the mean of the 90th percentile forces for the AquaSim simulation.

6.4. Discussion

The comparison between the round and vessel-shaped fish cages under different environmental conditions shows that the vessel-shaped configuration performs well and in most scenarios better than the round cage.

In Scenario 1, the vessel-shaped cage experiences slightly higher mooring forces compared to the round cage. However, as the absolute loads in this condition are approximately one order of magnitude lower than in the storm cases, this difference is not considered critical. It may, however, contribute to a reduction in fatigue life over long-term operation.

In Scenario 2, representing the 20-year return storm with the largest wave heights, the vessel-shaped cage shows a clear reduction in mooring loads. This demonstrates that the streamlined shape can reduce wave-induced forces under extreme sea states.

Scenario 3, representing the 5-year return storm without current, is primarily used for verification purposes. The numerical results show good agreement with the simplified analytical estimate in table 6.3, the simulation is a factor 1.83 higher, which is to be expected, considering that additional first order forces are incorporated into the simulation.

When both waves and currents are present, as in Scenario 4, the vessel-shaped cage continues to perform well. The comparison between Scenarios 3 and 4 shows that the vessel-shaped configuration handles combined loading more effectively than the round cage. This suggests that the streamlined geometry reduces current-induced drag forces while maintaining stability in waves.

Scenario 5 represents a towing operation. In this condition, the vessel-shaped design shows a large reduction in hydrodynamic resistance compared to the round cage. This implies that significantly less energy, or fuel, is required when towing the fish farm between sites, resulting in clear operational and economic benefits.

Overall, the results indicate that the vessel-shaped fish farm performs better than the round cage in most tested conditions. The only exception occurs in the lowest loading condition, where 25% higher mooring forces are observed. Despite this, the advantages in all other scenarios make the vessel-shaped design a promising alternative for fish farming in Sisal.

6.5. Design Recommendation

This chapter integrated long-term wave statistics with locally measured currents to construct a site-specific, internally consistent set of environmental inputs for hydrodynamic assessment near Sisal. The RBF-based extremes, calibrated to the ADCP record, yielded stable 5- and 20-year return heights and periods, while the twelve-year ADCP series defined realistic current magnitudes, vertical structure, and headings. Combined with directional joint analysis, these informed five scenarios representing normal operation, design storms, and towing. Using these scenarios, AquaSim simulations, benchmarked against analytical MWDF estimates, indicated that the vessel-shaped cage generally experiences lower mean and peak mooring tensions than the round cage under storm and towing conditions, with a modest penalty under the mild, most-frequent sea state. The findings support the premise that streamlined geometry reduces wave- and current-induced loads in exposed environments, while underscoring sensitivities to wave–current misalignment and the importance of appropriate mooring design. Given the simplifying assumptions, the results should be interpreted comparatively rather than as absolute design values.

The design recommendation, using AI rendering, shown in figure 6.11 brings together these environmental and social findings into a coherent concept for a multifunctional fish farm suited to the coastal conditions and community context of Sisal. The goal is to define a configuration that performs reliably at sea, aligns with local capacity, and visibly reflects environmental care and community participation.

The environmental assessment shows that the vessel-shaped cage performs better than the traditional circular cage in nearly all tested conditions. It reduces mooring loads during storms and lowers towing resistance by approximately 23% which directly translates to lower fuel use and easier handling during relocation. The social assessment further revealed that ease of handling and low operational cost were repeatedly emphasized as key priorities. Under high wave conditions, the streamlined geometry

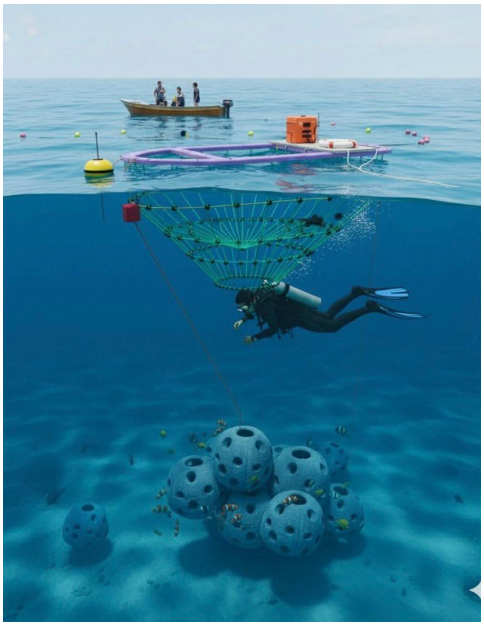

Figure 6.11: AI rendered visualisation of possible fish farm with multi-functionality.

reduces hydrodynamic forces, limiting fatigue on nets and mooring lines. This makes the structure more stable, less maintenance-intensive, and safer to operate. The improved storm performance also means the fish farm does not need to be towed into port as frequently, reducing the risk of premature fish harvests. Together, these characteristics align closely with the community's stated preference for reliability, simplicity, and safety.

The social assessment highlights that local acceptance depends on practicality, visibility, and shared benefit. Fishers emphasized "healthy water," "safety at sea," and "cooperation among fishers," showing that acceptance is grounded in daily experience rather than abstract ideals. Students, meanwhile, associated multifunctional projects with "helping local families," "not harming the sea," and opportunities for education and curiosity-driven engagement. The measures that gained most support, such as safety kits, guided snorkelling, and educational collaboration with UNAM, were those that are tangible, understandable, and participatory.

Combining these insights leads to a design concept centred on a vessel-shaped cage anchored through artificial reef modules that double as ecological enhancement structures . This combination addresses a key technical and ecological challenge: integrating a damping mooring chain system that partially rests on the seabed while preserving the biological function of a reef. Embedding the mooring bases within reef-like concrete modules allows the system to gain both structural and ecological benefits. The reef modules help distribute tension more evenly along the seabed, reducing peak loads, while simultaneously providing habitat for marine species. Over time, this dual function strengthens the ecological foundation of the farm and creates visible proof of environmental responsibility, a trait valued by both fishers and students.

At the operational level, the vessel-shaped cage reduces technical burden and simplifies maintenance. Lower towing resistance and balanced mooring forces make relocation and maintenance less demanding, while reduced mechanical stress extends the lifetime of nets and lines. These effects lower long-term costs and the need for external technical assistance, directly matching the fishers' preference for affordable, manageable systems. In practice, this results in a farm that is easier to operate, more predictable in maintenance, and resilient during storms.

Multifunctional elements are included where they enhance operations without adding complexity. A compact environmental monitoring kit, recording temperature, salinity, and oxygen, documents local conditions and makes data available to both the cooperative and researchers at UNAM. A standardized safety kit is placed on the cage and service float, improving preparedness and reinforcing a visible

culture of safety. Guided snorkelling and educational visits take place under calm conditions, allowing students and visitors to observe the reef modules and learn about sustainable aquaculture. These activities turn the farm into a local learning platform and source of community pride while maintaining focus on the core aquaculture tasks.

In conclusion, the vessel-shaped multifunctional fish farm anchored through artificial reef bases represents a practical synthesis of technical performance and social acceptance. Its streamlined geometry reduces hydrodynamic resistance, lowering energy use, mooring loads, and maintenance requirements, while the reef modules transform structural foundations into living habitats that visibly enrich the marine environment. Together, these features create a system that is efficient to operate, resilient in storms, and grounded in ecological care. By integrating safety, monitoring, and educational components without complicating daily work, the design makes sustainability both visible and attainable for the community. The result is not just a durable fish farm, but a locally grounded model of aquaculture, one that strengthens trust, supports learning, and aligns environmental responsibility with the everyday realities of life and work in Sisal.

7

Further research

7.1. Further optimizing design for local conditions

The present analysis provides a first indication of the hydrodynamic advantages of vessel-shaped fish cages compared to traditional circular systems. However, several aspects of the design and modelling can be optimized further to enhance operational performance and reliability in offshore environments. The following subsections outline the most relevant directions for future research.

7.1.1. Anchoring Options

Future studies should explore different anchoring concepts and configurations. Key parameters include anchor length, weight, and the connection mechanism between the anchor and the fish farm. The anchoring system must provide sufficient holding capacity while allowing for easy release during relocation or maintenance. One potential improvement is the implementation of detachable or quick-release connectors, which would enable the cage to be towed efficiently without diver intervention. Additionally, redundancy should be built into the mooring layout to avoid a single point of failure. Using multiple load paths or distributed mooring points could ensure that local damage or line failure does not compromise the strength of the entire structure. An analysis should be made of the effects of multiple lines on the motions of the structure.

7.1.2. Dimensions

The overall geometry of the fish cage, particularly its length to width ratio, strongly affects both the hydrodynamic performance and the swimming behaviour of the fish. The optimal ratio should balance structural stability, fish welfare, and anchoring forces. Further simulations could identify the range of dimensions where the anchoring loads remain minimal while maintaining sufficient volume and internal flow for healthy fish activity.

Natural Frequency

Another aspect of the geometric design involves the dynamic response of the fish farm and mooring system. The natural frequency of the structure should not coincide with the dominant wave frequencies at the deployment site, as this may lead to resonance and extreme mooring loads. Future work should therefore include an analysis to determine the natural frequencies of the combined cage and mooring system and adjust its stiffness and geometry accordingly. Small changes in cable length, pretension, or buoyancy distribution could shift the natural frequency away from the excitation range of local wave spectra, reducing fatigue and dynamic loading.

7.1.3. Materials

Material fatigue is another important consideration for long-term offshore deployment. Mooring lines, connectors, and cage joints are subjected to cyclic loading from waves and currents, which can lead to wear and failure over time. Future research should investigate fatigue life predictions for the materials used, incorporating realistic load spectra derived from field data. A study can be made to determine

the best material for different parts of the fish farm based on fatigue life, cost and local availability.

7.1.4. Biomass

The effect of fish and fouling biomass on hydrodynamic forces remains uncertain and is often neglected in preliminary simulations. However, the presence of biomass alters the internal flow through the cage and increases overall drag. As the fish stock density and fouling increases, the effective resistance of the system may rise, resulting in higher anchor loads and reduced water exchange. Incorporating biomass as a distributed damping or porous zone in future numerical models would improve the accuracy of predicted loads and better represent realistic operating conditions.

7.1.5. Verifying Findings through Future Wave Testing

The numerical results obtained in AquaSim should ultimately be verified through physical wave testing. A flume experiment was originally planned at the UNAM campus in Sisal to compare the hydrodynamic behaviour and mooring line tension of the circular and vessel-shaped cages under controlled conditions. However, the experiment could not be carried out due to the absence of a critical data acquisition component required for the load cell system.

Despite this limitation, substantial preparatory work was completed, including the experimental design, scaling framework, and model specifications, which are documented in Appendix E. This groundwork provides a ready foundation for future teams to conduct the physical validation once the required equipment becomes available. Executing these flume tests would enable direct observation of mooring loads, cage deformation, and orientation stability, thereby strengthening confidence in the numerical findings and refining design optimization for the environmental conditions near Sisal.

7.2. Social Acceptance and Multifunctionality

The analysis identified multifunctional measures that are both valued and attainable within the community of Sisal. The highest-ranked functions demonstrate that multifunctionality is conceptually accepted and technically feasible. However, whether these measures can operate effectively, remain socially supported, and deliver the expected ecological and economic outcomes has not yet been verified.

7.2.1. Operational Responsibilities and Long-Term Functioning

While the attainability assessment clarified which measures are realistic to implement, it remains uncertain how they will be organized and maintained once operational. Future research should examine how responsibilities evolve over time, how maintenance and monitoring tasks are divided among actors, and whether these arrangements remain stable. This includes studying the management of technical components such as the Spotter buoy and artificial reef units, as well as the continuity of essential yet simple features like safety equipment. Understanding how local ownership and accountability develop over time will be key to ensuring long-term functioning and resilience.

7.2.2. Governance, Inclusion, and Institutional Support

The collaboration between UNAM, fishers, and municipal actors proved essential during this study but has yet to be formalized. Future research should therefore examine how multifunctional aquaculture can be embedded within existing governance frameworks, ensuring continuity beyond individual initiatives. This includes identifying how decision-making, funding, and regulatory mechanisms can support cooperative management structures. In parallel, it is necessary to understand how participation and acceptance vary among social groups and how these dynamics evolve once operations begin. Ensuring equitable inclusion and transparent governance will determine whether multifunctional aquaculture can maintain long-term legitimacy and community support.

7.2.3. Evaluating Real Outcomes and Social–Ecological Linkages

The current analysis assessed potential benefits through community perception and theoretical evaluation. Whether multifunctional measures will deliver the intended ecological, social, and economic outcomes remains uncertain. Future research should therefore monitor actual performance, measuring environmental indicators such as biodiversity and water quality alongside social indicators like participation, trust, and income diversification. These measurements should also investigate how tangible

ecological improvements, such as cleaner water or higher fish abundance, influence local motivation and support. Understanding this feedback between ecological results and social acceptance is essential to determine the durability of multifunctional aquaculture as a genuinely integrated social–ecological system.

7.2.4. Emerging Opportunities

The multifunctional measures assessed in this study represent only a subset of possible applications. Future exploration should remain focused on attainable, low-complexity extensions that reinforce ecological and social value, such as small-scale educational or monitoring facilities. Once experience and resources grow, further opportunities could include renewable energy integration or onshore processing initiatives. Identifying such realistic developments will help broaden multifunctional potential without exceeding local capacity or compromising simplicity.

8

Conclusion

This project establishes a locally grounded model for sustainable aquaculture in Sisal, designed around technical resilience and social simplicity. The outcome is a single, coherent concept that links hydrodynamic performance with community acceptance and ecological value.

The environmental adaptation of the fish farm began with a detailed assessment of local sea conditions. Using a twelve-year ADCP record and a forty-seven-year downscaled wave dataset, the study defined realistic environmental scenarios to test structural performance. Storm resilience emerged as the decisive technical factor for long-term operation. Across all energetic sea states, the vessel-shaped cage demonstrated clear advantages over the conventional round cage, particularly under cross-flow conditions typical of the North Yucatan shelf.

In the most severe design case ($H_s = 3.06$ m, $T_p = 8.42$ s, the vessel geometry reduced mean mooring line forces by 23% compared to the round cage, indicating greater stability and lower risk of failure. While it produced 128% higher loads in calm conditions, this trade-off favours operational safety: efficiency in mild weather is sacrificed for durability in extreme events. Towing simulations at 1.74 m s^{-1} confirmed lower hydrodynamic resistance, supporting its practicality for relocation before storms. Together, these results show that the vessel-shaped cage offers a robust, low-maintenance solution suited to Sisal's energetic coastal environment.

Alongside technical adaptation, the project explored how the fish farm could deliver wider ecological and social benefits. Guided by the Triple Bottom Line framework and evaluated through Multi-Criteria Decision Analysis, the social research identified community preferences for measures that are visible, participatory, and manageable with local skills. Fishers, students, and other stakeholders prioritised the addition of artificial reefs, educational and research visits, and snorkelling or eco-tourism activities.

These options proved achievable within the community's technical and financial capacities. Combined with a basic safety kit and local environmental monitoring through a Spotter buoy, they form a practical, cooperative-scale system. The findings reject high-complexity, capital-intensive solutions such as integrated multi-trophic aquaculture or desalination, in favour of attainable interventions that strengthen environmental transparency and community trust.

The technical and social strands of the study converge in one configuration: a vessel-shaped cage anchored through locally fabricated artificial reef modules (Reef Balls). This arrangement integrates structural resilience with habitat enhancement and visible community benefit. The result is a mutually reinforcing system where hydrodynamic stability supports ecological restoration and public engagement, linking engineering performance directly to social legitimacy.

The study's limitations stem from data coverage, modelling simplifications, and evolving social dynamics. Wave and current extremes depend on statistical downscaling and interpolation, while AquaSim modelling excludes fatigue, biomass, wind, and fouling effects. Social findings reflect the preferences of current stakeholders, and governance structures for long-term operation are still developing. These

uncertainties are recognised, and “Further research” already outlines the necessary steps; flume testing, anchoring trials under misalignment, fatigue and material studies, and long-term monitoring of ecological and social outcomes to confirm or refine the present conclusions.

A conservative baseline suggests that a cooperative-scale vessel-shaped cage with modest multifunctionality can operate effectively under Sisal’s conditions when designed within the studied parameters. Its success depends on maintaining local operational independence, stable water quality, and effective governance. Risks increase if maintenance capacity declines, monitoring lapses, or security problems lead to equipment losses.

Overall, the project provides a strong foundation for sustainable aquaculture in Sisal. It demonstrates how a design grounded in the local environmental and community priorities can unite resilience with simplicity. While not yet a full implementation plan, the concept offers a clear and evidence-based path toward a technically sound and socially accepted aquaculture system on the Yucatan coast.

References

Anderson, James L. et al. [2015]. “The Fishery Performance Indicators: A management tool for triple bottom line outcomes”. In: *Proceedings of the National Academy of Sciences* 112.34, pp. 10717–10722. DOI: 10.1073/pnas.1504429112.

Antolínez, José Antonio A. et al. [2018]. “Downscaling Changing Coastlines in a Changing Climate: The Hybrid Approach”. In: *Journal of Geophysical Research: Earth Surface* 123.10, pp. 2298–2319. DOI: 10.1029/2018JF004790.

Ardoin, Nicole M., Alison W. Bowers, and Estelle Gaillard [2020]. “Environmental education outcomes for conservation: A systematic review”. In: *Biological Conservation* 241, p. 108224. DOI: 10.1016/j.biocon.2019.108224.

AS, Aquastructures [Oct. 2024a]. *The Aquasim package theory user manual*. Tech. rep. TR-20000-2049-1. URL: https://aquasim.no/files/validation/Theory_User_Manual_2_20.pdf.

— [Dec. 2024b]. *User manual AquaEdit*. Tech. rep. TR-20000-583-1. URL: https://aquasim.no/files/documentation/User_manual_AquaView.pdf.

Bakker, C. et al. [Dec. 2024]. “Developing Sustainable Fish Farms”. In: MP374. URL: https://resolver.tudelft.nl/uuid:df6e179c-4579-4fe7-884d-efa6149cc22f.

Bañuelos-García, M. et al. [2021]. “Assessment of social acceptance of caged fish culture for improvement and sustainability: A study on Volta Lake, Ghana”. In: *International Journal of Multidisciplinary Research and Growth Evaluation* 6.4, pp. 52–61. DOI: 10.54660/anfo.2022.3.2.9.

Belausteguigoitia, J. et al. [2019]. “Strengthening policy action to tackle social acceptability”. In: *ICES Journal of Marine Science* 76.5, pp. 983–993. DOI: 10.1093/icesjms/fsy059.

Bergan, P.I., D. Gausen, and L.P. Hansen [Oct. 1991]. “Attempts to reduce the impact of reared Atlantic salmon on wild in Norway”. In: *Aquaculture* 98.1-3, pp. 319–324. DOI: 10.1016/0044-8486(91)90396-o. URL: https://doi.org/10.1016/0044-8486(91)90396-o.

Beverly, Steve, Don Griffiths, and Robert Lee [2012]. *Anchored Fish Aggregating Devices for Artisanal Fisheries in South and Southeast Asia: Benefits and Risks*. Tech. rep. Bangkok: Food, Agriculture Organization of the United Nations Regional Office for Asia, and the Pacific. URL: https://www.fao.org/fileadmin/templates/rap/files/NRE/Fisheries/rap_pub2012_20_anchored_fish_aggregating_devices_report.pdf.

Bi, Changwei et al. [2018]. “Hydrodynamic performance of square and circular fish cages in steady current”. In: *Aquaculture* 484, pp. 76–83. DOI: 10.1016/j.aquaculture.2017.11.025. URL: https://doi.org/10.1016/j.aquaculture.2017.11.025.

Bøhn, Thomas et al. [Feb. 2024]. “Ecological interactions between farmed Atlantic salmon and wild Atlantic cod populations in Norway: A review of risk sources and knowledge gaps”. In: *Reviews in Aquaculture* 16.3, pp. 1333–1350. DOI: 10.1111/raq.12899. URL: https://doi.org/10.1111/raq.12899.

Bonney, Rick et al. [2009]. “Citizen Science: A Developing Tool for Expanding Science Knowledge and Scientific Literacy”. In: *BioScience* 59.11, pp. 977–984. DOI: 10.1525/bio.2009.59.11.9.

Boudouresque, Charles-François et al. [Apr. 2020]. “Impacts of marine and lagoon aquaculture on macrophytes in Mediterranean benthic ecosystems”. In: *Frontiers in Marine Science* 7. DOI: 10.3389/fmars.2020.00218. URL: https://doi.org/10.3389/fmars.2020.00218.

Bouwman, Lex et al. [Nov. 2013]. “Mariculture: significant and expanding cause of coastal nutrient enrichment”. In: *Environmental Research Letters* 8.4, p. 044026. DOI: 10.1088/1748-9326/8/4/044026. URL: https://doi.org/10.1088/1748-9326/8/4/044026.

Bracho-Villavicencio, C., H. Matthews-Cascon, and S. Rossi [2023]. “Artificial reefs around the world: A review of the state of the art and a meta-analysis of its effectiveness for the restoration of marine ecosystems”. In: *Environments* 10.7, p. 121.

Braña, Carlos Brais Carballeira et al. [Apr. 2021]. “Towards environmental sustainability in marine FinFish aquaculture”. In: *Frontiers in Marine Science* 8. DOI: 10.3389/fmars.2021.666662. URL: https://doi.org/10.3389/fmars.2021.666662.

Brumley, Bruce H. et al. [1991]. “Performance of a Broad-Band Acoustic Doppler Current Profiler”. In: *IEEE Journal of Oceanic Engineering* 16.4, pp. 402–407. DOI: 10.1109/48.97293.

Buck, Bela H. and Richard Langan, eds. [2017]. *Aquaculture Perspective of Multi-Use Sites in the Open Ocean: The Untapped Potential for Marine Resources in the Anthropocene*. Cham: Springer. ISBN: 978-3-319-51157-3. DOI: 10.1007/978-3-319-51159-7. URL: https://library.oapen.org/handle/20.500.12657/27776.

Cahuich-López, Miguel A. et al. [2020]. “Spatial and temporal variability of sea breezes and synoptic influences over the surface wind field of the Yucatán Peninsula”. In: *Atmósfera* 33.2, pp. 123–142. DOI: 10.20937/ATM.52713.

Camus, Pablo, Fernando J. Mendez, and Raul Medina [2011]. “A hybrid model for estimating nearshore wave conditions”. In: *Coastal Engineering* 58.11, pp. 851–862. DOI: 10.1016/j.coastaleng.2011.05.007.

Cárdenas-Torres, Nirari, Roberto Enríquez-Andrade, and Natalie Rodríguez-Dowdell [2007]. “Community-Based Management through Ecotourism in Bahía de los Ángeles, Mexico”. In: *Fisheries Research* 84.1, pp. 114–118. DOI: 10.1016/j.fishres.2006.11.019.

Carral, Luis et al. [Nov. 2017]. “Social interest in developing a green modular artificial reef structure in concrete for the ecosystems of the Galician rías”. In: *Journal of Cleaner Production* 172, pp. 1881–1898. DOI: 10.1016/j.jclepro.2017.11.252. URL: https://doi.org/10.1016/j.jclepro.2017.11.252.

Cheng, Hui et al. [2020]. “Typical hydrodynamic models for aquaculture nets: A comparative study under pure current conditions”. In: *Aquacultural Engineering* 90, p. 102070. DOI: doi.org/10.1016/j.aquaeng.2020.102070.

City of Fort Bragg [2025]. *Oneka Seawater Desalination Buoy Pilot Study*. Municipal Public Works Project Webpage. URL: https://www.city.fortbragg.com/departments/public-works/current-public-works-projects/oneka-seawater-desalination-buoy-pilot-study.

Dagorn, L. et al. [2013]. “Is it good or bad to fish with FADs? What are the real impacts of the use of drifting fish aggregating devices on pelagic marine ecosystems?” In: *Fish and Fisheries* 14.3, pp. 391–415.

Delauney, L., C. Compère, and M. Lehaitre [2010]. “Biofouling protection for marine environmental sensors”. In: *Ocean Science* 6, pp. 503–511. DOI: 10.5194/os-6-503-2010. URL: https://os.copernicus.org/articles/6/503/2010/os-6-503-2010.pdf.

Dempster, T et al. [Apr. 2009]. “Coastal salmon farms attract large and persistent aggregations of wild fish: an ecosystem effect”. In: *Marine Ecology Progress Series* 385, pp. 1–14. DOI: 10.3354/meps08050. URL: https://doi.org/10.3354/meps08050.

Det Norske Veritas [2014]. *DNV-RP-C205: Environmental Conditions and Environmental Loads*. Oslo, Norway: Det Norske Veritas AS.

Elkington, John [1997]. *Cannibals with Forks: The Triple Bottom Line of 21st Century Business*. Oxford: Capstone.

Elvines, Dm et al. [Dec. 2023]. “Assimilation of fish farm wastes by the ecosystem engineering bivalve Atrina zelandica”. In: *Aquaculture Environment Interactions* 16, pp. 115–131. DOI: 10.3354/aei00475. URL: https://doi.org/10.3354/aei00475.

Eriksen, Katrine and Eirik Mikkelsen [2024]. “What affects the level of local social acceptance of salmon farming in Norway?” In: *Aquaculture* 588, p. 740926. DOI: doi.org/10.1016/j.aquaculture.2024.740926.

Estévez, Rodrigo A. and Stefan Gelcich [2015]. “Participative multi-criteria decision analysis in marine management and conservation: Research progress and the challenge of integrating value judgments and uncertainty”. In: *Marine Policy* 61, pp. 1–7.

Falk, John H. and Lynn D. Dierking [1997]. “School Field Trips: Assessing Their Long-Term Impact”. In: *Curator: The Museum Journal* 40.3, pp. 211–218. DOI: 10.1111/j.2151-6952.1997.tb01304.x.

Fang, J et al. [Apr. 2016]. “Integrated multi-trophic aquaculture (IMTA) in Sanggou Bay, China”. In: *Aquaculture Environment Interactions* 8, pp. 201–205. DOI: 10.3354/aei00179. URL: https://doi.org/10.3354/aei00179.

Fernández, Pamela [2024]. *The History of Henequén, Yucatán’s Green Gold*. Accessed: 2025-10-28. URL: https://yucatantoday.com/en/blog/history-of-henequen-yucatans-green-gold.

Fletcher, W. J. et al. [2010]. “Ecosystem-based fisheries management case study: Western Rock Lobster Fishery”. In: *ICES Journal of Marine Science* 67.5, pp. 981–992. DOI: 10.1093/icesjms/fsp277.

Flores-Iwasaki, M. et al. [2025]. “Internet of Things (IoT) sensors for water quality monitoring in aquaculture systems: A systematic review and bibliometric analysis”. In: *AgriEngineering* 7.3, p. 78.

Food and Agriculture Organization of the United Nations [2010]. *Environmental Impact Assessment and Monitoring in Aquaculture*. Tech. rep. FAO Fisheries and Aquaculture Department. URL: https://www.fao.org/4/i0970e/i0970e.pdf.

Food and Agriculture Organization of the United Nations, International Labour Organization (ILO), and International Maritime Organization (IMO) [2012]. *Safety Recommendations for Decked Fishing Vessels of Less than 12 metres in Length and Undecked Fishing Vessels*. Rome: FAO/ILO/IMO. ISBN: 978-92-5-107397-1. URL: https://www.ilo.org/sites/default/files/wcmsp5/groups/public/%40ed_dialogue/%40sector/documents/publication/wcms_216664.pdf.

Fredriksson, David W. and Jessica Beck-Stimpert [2019]. *Basis-of-Design Technical Guidance for Offshore Aquaculture Installations in the Gulf of Mexico*. NOAA Technical Memorandum NMFS-SER-9. U.S. Department of Commerce, NOAA Fisheries. DOI: 10.25923/r496-e668. URL: https://www.fisheries.noaa.gov/s3/dam-migration/technical_guidance_for_offshore_aquaculture_installations.pdf.

Gansel, Lars C. et al. [2015]. “Drag forces on, and deformation of, circular fish cages in uniform flow”. In: *Journal of Fluids and Structures* 54, pp. 235–249. DOI: 10.1016/j.jfluidstructs.2015.01.004. URL: https://doi.org/10.1016/j.jfluidstructs.2015.01.004.

Giglio, Vinicius J., Osmar J. Luiz, and Carlos E. L. Ferreira [2020]. “Ecological Impacts and Management Strategies for Recreational Diving: A Review”. In: *Journal of Environmental Management* 256, p. 109949. DOI: 10.1016/j.jenvman.2019.109949.

Goda, Yoshimi [2010]. *Random Seas and Design of Maritime Structures*. 3rd. Singapore: World Scientific. DOI: 10.1142/7425.

Han, Y., Y. Choi, and J. Lee [2022]. “Floating solar photovoltaics: Assessing global potential and techno-economic prospects”. In: *Renewable and Sustainable Energy Reviews* 156, p. 112014.

Hannak, Judith S. et al. [2011]. “Snorkelling and Trampling in Shallow-Water Fringing Reefs: Risk Assessment and Proposed Management Strategy”. In: *Journal of Environmental Management* 92.11, pp. 2723–2733. DOI: 10.1016/j.jenvman.2011.06.012.

Herbers, Thomas H. C. and Steven J. Lentz [2010]. “Observing Directional Properties of Ocean Swell with an Acoustic Doppler Current Profiler (ADCP)”. In: *Journal of Atmospheric and Oceanic Technology* 27.1, pp. 210–225. DOI: 10.1175/2009JTECHO707.1.

Hishamunda, N. et al. [2014]. *Policy and governance in aquaculture: Lessons learned and way forward*. FAO Fisheries and Aquaculture Technical Paper 577. Rome: FAO.

Hutchison, G. et al. [2020]. “Offshore wind farm artificial reefs affect ecosystem structure and functioning: a synthesis”. In: *Oceanography* 33.4, pp. 54–64. DOI: 10.5670/oceanog.2020.405.

Industry, PUHUI [Mar. 2025]. *HDPE Pipe Specification Size Table - Commercial available configurations*. URL: https://www.phhdpepipe.com/hdpe-pipe-specification-size-table.html.

Jamroen, Chaowanan et al. [2023]. “A standalone photovoltaic/battery energy-powered water quality monitoring system based on narrowband internet of things for aquaculture: Design and implementation”. In: *Smart Agricultural Technology* 3, p. 100072.

Kingma, Enzo M et al. [2024]. “Guardians of the seabed: Nature-inclusive design of scour protection in offshore wind farms enhances benthic diversity”. In: *Journal of Sea Research* 199, p. 102502. DOI: doi.org/10.1016/j.seares.2024.102502.

Klebert, Pascal et al. [2013]. “Hydrodynamic interactions on net panel and aquaculture fish cages: A review”. In: *Ocean engineering* 58, pp. 260–274. DOI: doi.org/10.1016/j.oceaneng.2012.11.006.

Lader, Pål F. and Birger Enerhaug [2013]. “Experimental investigation of forces and deformations on a net cage in uniform flow”. In: *Aquacultural Engineering* 52, pp. 35–44. DOI: 10.1016/j.aquaeng.2012.09.003. URL: https://doi.org/10.1016/j.aquaeng.2012.09.003.

Leith, P., E. Ogier, and M. Haward [2014]. “Science and Social License: Defining Environmental Sustainability of Atlantic Salmon Aquaculture in South-Eastern Tasmania, Australia”. In: *Social Epistemology* 28.3-4, pp. 277–296. DOI: 10.1080/02691728.2014.922641.

Li, Jing et al. [2023]. “A multi-dimensional comprehensive assessment of water pollution treatment technologies”. In: *Water* 15.4, p. 751.

Liu, Y. et al. [2022]. “Effects of shellfish and macro-algae IMTA in North China: Carbon sequestration and mitigation of ocean acidification”. In: *Frontiers in Marine Science* 9, p. 864306.

Lu, Hoang-Yang, Chih-Yung Cheng, Shyi-Chyi Cheng, et al. [2022]. “A Low-Cost AI Buoy System for Monitoring Water Quality at Offshore Aquaculture Cages”. In: *Sensors* 22.11, p. 4078. DOI: 10.3390/s22114078. URL: https://www.mdpi.com/1424-8220/22/11/4078.

Margeson, Matthew J. et al. [2024]. “Refractory plasmonic material based floating solar still for simultaneous desalination and electricity generation”. In: *iScience* 27.11, p. 111225. DOI: 10.1016/j.isci.2024.111225.

Medina, Juan Camilo, José Camilo Monroy, et al. [2022]. “Open-source low-cost design of a buoy for remote water quality monitoring in fish farming”. In: *PLOS ONE* 17.7, e0270202. DOI: 10.1371/journal.pone.0270202. URL: https://journals.plos.org/plosone/article?id=10.1371/journal.pone.0270202.

Mendez, Fernando J., Inigo J. Losada, and Raul Medina [2004]. “Transformation model of wave height distribution on planar beaches”. In: *Coastal Engineering* 50.3, pp. 97–115. DOI: 10.1016/j.coastaleng.2003.09.005.

Meza-Osorio, Yari Tatiana, Gabriela Mendoza-González, and M. Luisa Martínez [2024]. “Sun and Sand Ecotourism Management for Sustainable Development in Sisal, Yucatán, Mexico”. In: *Sustainability* 16.20, p. 8807. DOI: 10.3390/su16208807. URL: https://www.mdpi.com/2071-1050/16/20/8807.

Mi, J. et al. [2023]. “Experimental investigation of a reverse osmosis system powered by wave energy for seawater desalination”. In: *Desalination* 564, p. 115851. DOI: 10.1016/j.desal.2023.115851.

Miche, A. [1944]. *Mouvements ondulatoires de la mer en profondeur constante ou décroissante*. Translated title: Wave motion in constant or decreasing depth. Original in French. Paris: Annales des Ponts et Chaussées.

Michler-Cieluch, T., G. Krause, and B. H. Buck [2009]. “Reflections on integrating operation and maintenance activities of offshore wind farms and mariculture”. In: *Ocean & Coastal Management* 52.1, pp. 57–68.

Miller, M. W. [2002]. “Using ecological processes to advance artificial reef goals”. In: *ICES Journal of Marine Science* 59.Supplement S1, S27–S31. DOI: 10.1006/jmsc.2002.6756.

Murata, Hiroki et al. [2021]. “Monitoring oyster culture rafts and seagrass meadows in Nagatsura-ura Lagoon, Sanriku Coast, Japan before and after the 2011 tsunami by remote sensing: their recoveries implying the sustainable development of coastal waters”. In: *PeerJ* 9, e10727. DOI: 10.7717/peerj.10727.

Nasyrlayev, Nazhmiddin et al. [2023]. “Modelling the response of offshore aquaculture fish pens to environmental loads in high-energy regions”. In: *Applied Ocean Research* 135, p. 103541. DOI: 10.1016/j.apor.2023.103541. URL: https://doi.org/10.1016/j.apor.2023.103541.

National Oceanographic and Atmospheric Administration (NOAA), NESDIS [2019]. *World Ocean Atlas 2018: Volume 5 – Density*. Calculated from climatological temperature and salinity data to derive seawater density fields. Washington, D.C.: U.S. Government Printing Office.

Olsen, Marit Schei et al. [2024]. “Social license to operate for aquaculture: A cross country comparison”. In: *Aquaculture* 584, p. 740662. DOI: 10.1016/j.aquaculture.2024.740662.

Pipe, Valor [Mar. 2023]. *4 Characteristics of HDPE pipes*. URL: https://www.pedredgepipe.com/resources/4-characteristics-of-hdpe-pipes.html.

Puspito, Gondo et al. [2015]. “Utilization of light-emitting diode lamp on lift net fishery”. In: *Aquaculture, Aquarium, Conservation & Legislation* 8.2, pp. 159–167. URL: https://bioflux.com.ro/docs/2015.159-167.pdf.

Quijano Quiñones, Daniel R. et al. [2021]. “Spatial Dynamics Modeling of Small-Scale Fishing Fleets With a Random Walk Approach”. In: *researchgate*. URL: https://www.researchgate.net/publication/351841684_Spatial_Dynamics_Modeling_of_Small-Scale_Fishing_Fleets_With_a_Random_Walk_Approach.

Santos, Beatriz [2023]. “Floating solar tech for aquaculture”. In: *pv magazine*. Online article. URL: https://www.pv-magazine.com/2023/01/04/floating-solar-tech-for-aquaculture/.

Sauvé, Pierre et al. [2022]. “Multicriteria Decision Analysis to Assist in the Selection of Coastal Defence Measures”. In: *Frontiers in Marine Science* 9, Article 871845.

Schirmann, Matthew L., Matthew D. Collette, and James W. Gose [2020]. “Significance of wave data source selection for vessel response prediction and fatigue damage estimation”. In: *Ocean Engineering* 216, p. 107610. DOI: 10.1016/j.oceaneng.2020.107610.

Schupp, Maximilian Felix et al. [2019]. “Toward a common understanding of ocean multi-use”. In: *Frontiers in Marine Science* 6, p. 165. DOI: doi.org/10.3389/fmars.2019.00165.

Sofar Ocean [2025]. *Spotter Platform Specification Sheet*. Accessed: 2025-10-02. URL: https://www.xylem.com/siteassets/brand/xylem/sofar-spotter/sofar-spotter-data-sheet.pdf.

Stevenson, J. R. and A. Irwin [2018]. “Social license to operate and aquaculture: An insight into community acceptance of aquaculture in Europe”. In: *Marine Policy* 94, pp. 128–137.

Team, Fish Farming Expert Editorial [2022]. “Floating solar power plant now on the market”. In: *Fish Farming Expert*. Online article. URL: https://www.fishfarmingexpert.com/inseaenergy-salmon-farming-solar-power/floating-solar-power-plant-now-on-the-market/.

Torres-Freyermuth, A. et al. [2017]. “Nearshore circulation on a sea breeze dominated beach during intense wind events”. In: *Continental Shelf Research* 151, pp. 40–52. DOI: 10.1016/j.csr.2017.10.008.

U.S. Department of Energy [2021]. *Waves to Water Prize: Advancing small, modular, wave-powered desalination systems*. Tech. rep. Washington, D.C.: U.S. Department of Energy, Water Power Technologies Office.

— [2023]. *Open Water Tests of US Department of Energy–Funded Desalination Devices*. Tech. rep. Office of Energy Efficiency & Renewable Energy. URL: https://www.energy.gov/eere/water/open-water-tests-us-department-energy-funding.

Vo, Thi Thu Em et al. [2021]. “Overview of solar energy for aquaculture: The potential and future trends”. In: *Energies* 14.21, p. 6923.

Wang, Zhi et al. [2024]. “Dynamic response analysis of vessel-shaped aquaculture cages considering wave diffraction and radiation effects”. In: *Journal of Shanghai Jiao Tong University (Science)* 29.2, pp. 145–154. DOI: 10.1007/s12204-024-1234-5. URL: https://xuebao.sjtu.edu.cn/EN/volumn/volumn_2992.shtml.

Whitmore, Emily H., Matthew J. Cutler, and Eric M. Thunberg [2022]. *Social License to Operate in the Aquaculture Industry: A Community Focused Framework*. Tech. rep. NOAA Technical Memorandum NMFS-NE 287. NOAA Northeast Fisheries Science Center. DOI: 10.25923/htvb-s306.

Wilson, Matthew W. et al. [2020]. “Status and trends of moored fish aggregating device (MFAD) fisheries in the Caribbean and Bermuda”. In: *Marine Policy* 121, p. 104148. DOI: 10.1016/j.marpol.2020.104148.

Zhuo, Yue et al. [2024]. “A Study on the Hydrodynamic Response Characteristics of Vessel-Shaped Cages Based on the Smoothed Particle Hydrodynamics Method”. In: *Journal of Marine Science and Engineering* 12.12, p. 2199. DOI: 10.3390/jmse12122199. URL: https://doi.org/10.3390/jmse12122199.

A

Interviews

In this appendix, a summary of the key takeaways from each interview is presented. Throughout this research, valuable information has been gathered from meetings and interviews with various stakeholders and experts involved in the project. Given the large volume of conversations, we have chosen to present concise summaries highlighting the most important conclusions, insights, and discussions.

As additional interviews will take place over the course of the project, this appendix will be updated and refined to include the outcomes of those future meetings.

Table A.1: Chronological overview of all conducted interviews and discussions.

Date	Type	Participants
02/09/2025	Interview professors UNAM	Dr. Alec Torres Freyermuth, Dr. Carlos Rosas, Dr. Alex Robledo
08/09/2025	Interview coastal engineer	Dr. Alec Torres Freyermuth
10/09/2025	Dicussion marine biology	Dr. Carlos Rosas, Daisy Pineda-Suazo
19/09/2025	Interview Artificial Reefy	Daniel Dacomba
24/09/2025	Interview Reef Ball Foundation	Javier Dajer

Interview Professors UNAM – 2 September 2025

Participants: Prof. Carlos Rosas (Marine Biology), Dr. Alex Robledo (Oceanography), Dr. Alec Torres Freyermuth (Coastal Engineering)

Purpose and Context

On September 2nd, we met with three professors who have been closely involved in aquaculture research in Yucatán. The meeting gave us the opportunity to discuss the findings of last year's MDP project, reflect on our analysis of their report, and test the feasibility of our new research ideas for this year. We also used the session to better understand current developments in the region and to identify local challenges that could inform our approach.

Key Insights from Last Year's Research

The professors confirmed that last year's project provided a useful foundation, particularly with regard to anchoring systems for offshore cages. Prof. Rosas had been working with the fishing community in Celestún to evaluate whether the anchoring system proposed by MP374 could be applied there. However, it was emphasized that further development of the farms is necessary, especially to make them more robust against stormy seasons. Strong winds, currents, and waves demand a careful redesign of both the underwater structure and the mooring systems.

A key limitation is the lack of scientific data for the offshore zone identified in the previous study at around 8 km from the coast. Installing monitoring equipment is difficult because instruments that protrude above the water are often stolen. The experts stressed the importance of determining the optimal offshore location, ideally within 40 km from shore. Beyond that distance, fuel and operational costs become prohibitive.

Current Status of Aquaculture in Sisal and Celestún

At present, no aquaculture farms operate in Sisal itself. The nearest example is in Celestún, where development is already several years ahead. However, even there, adoption by local fishermen has been limited. One major reason is that fishermen cannot carry out the maintenance themselves and depend on external contractors, which undermines their sense of ownership.

For Sisal, the intended model is small scale and community based aquaculture aimed at providing fishermen with an additional source of income. The objective is not industrial production, but rather a system that creates local benefits with minimal ecological disruption, ideally having a neutral or even positive effect on the ecosystem.

Environmental Concerns: Red Tide Events

A pressing environmental challenge discussed was the increasing frequency and severity of red tide events, harmful algal blooms that release toxins and deplete oxygen in the water. The professors explained that these events are exacerbated by untreated wastewater discharges and nutrient run-off from inland agriculture.

The 2022 red tide created dead zones along Yucatán's coast, leading to fishing bans and raising public health concerns. The current bloom appears to follow a similar trajectory, with dead fish washing ashore in recent weeks. Typically, such events last around 15 days, but due to warming waters and climate change, the risk of longer lasting episodes extending for months is increasing.

For aquaculture, this poses a serious threat. If a red tide persists near a fish farm, oxygen depletion could wipe out the entire stock. This factor must therefore be explicitly accounted for when determining farm location, design, and contingency planning.

Roles and Expertise of the Professors

- **Dr. Alex Robledo**: Expertise in oceanography, currents, hydrodynamics, and the use of submarine equipment.
- **Prof. Carlos Rosas**: Works closely with fishermen's groups, specializes in squid biology, and links marine biology with agriculture and fisheries. He also manages the hatchery at UNAM.
- **Dr. Alec Torres Freyermuth**: Coastal and offshore engineer, advising on cage robustness and mooring design for local sea conditions.

Visit to the UNAM Hatchery

During the meeting, Prof. Rosas gave us a tour of the hatchery facilities on campus. Here, mature broodstock of several species are kept in approximately ten aquaria of around 3 m^3 each. Eggs are harvested from these broodfish and, once hatched, the larvae are transferred to three additional tanks for grow out. After about two months, the juveniles reach a size suitable for transfer to community farms along the coast.

The cycle is designed to ensure a continuous supply. While some cohorts are being raised, new eggs are incubated so that the tanks are never left empty. Periodically, batches of juveniles are donated to fishermen's cooperatives, lowering entry barriers and strengthening community involvement in aquaculture.

Implications for This Year's Research

From the discussion, several implications for our own project became clear:

1. Robust design is essential to cope with stormy conditions. This requires exploring alternative cage structures and anchoring systems.

2. Location must balance feasibility and resilience. It should be far enough offshore to ensure water quality, but close enough to remain economically viable.
3. Community ownership and maintenance capacity are key to long term adoption. Designs must allow for independent upkeep by fishermen.
4. Red tide risk must be factored into siting and operations, with consideration of mitigation and contingency measures.

Interview Coastal Engineer – 8 September 2025

Participants: Dr. Alec Torres Freyermuth (Coastal Engineering), Dr. Alex Robledo (Oceanography)

Purpose and Context

On September 8th we met with Dr. Alec Torres Freyermuth and Dr. Alex Robledo. The main focus of this meeting was to refine our research direction, particularly in preparation for the upcoming interviews with fishermen later in September. We also discussed the challenges of offshore design in Sisal, limitations in available data, and practical considerations for ensuring resilience against extreme weather events.

Developing the Fishermen Interviews

Alec and Alex emphasized that, in the absence of reliable long-term datasets on offshore conditions, direct knowledge from fishermen can provide valuable insights. For example, questions about feasible distances from shore or traditional practices during storms could be integrated into our interview guidelines. This practical knowledge is critical to evaluate community acceptance and to ground our research in local experience.

Design Requirements and Environmental Conditions

The professors noted that the design must withstand winter storms, where waves can reach 2.5 to 3 meters. In many locations, thirty years of time series data are needed to establish robust design criteria. In Sisal, however, only about ten years of data are available. To overcome this, they suggested simulating longer time series by comparing local data with external datasets and applying correction factors.

For this purpose, the ERA5 reanalysis dataset from the Copernicus Climate Data Store was recommended as a valuable tool for wave and climate analysis. Local adaptation of models is necessary, especially because coastal morphology and shallow water depth around Sisal increase friction, which significantly influences local hydrodynamics. The coastline in this area is highly dynamic, further complicating model calibration.

Currents were described as generally persistent and of similar strength in both Sisal and Celestún. However, limitations exist since many of the available measurements originate from Campeche, rather than directly from Sisal.

Seasonal and Extreme Weather Patterns

The experts outlined the seasonal cycles relevant to offshore aquaculture:

- **Storm season:** October to March, with peaks in December and January.
- **Cold front season:** Occurs during the same period and requires further study. Cold fronts can interact with hurricanes when they are pushed back while traveling north.
- **Hurricane season:** June to November. Hurricanes are more common in the Caribbean, but can still affect the Yucatán coast.

If a hurricane approaches, and the cage structures may not withstand the conditions, one option is to temporarily remove them from the water once the fish are harvested. This would also create opportunities for fishermen to carry out their own maintenance, ensuring independence from external contractors.

Learning from Celestún
Both professors encouraged us to visit the aquaculture initiatives in Celestún, which are considered several steps ahead of Sisal. The farm located approximately 10 km offshore has been operational since 2014. A key question is how the community there dealt with extreme events, such as hurricanes in recent years. Asking local operators whether cages were removed during storms could provide practical insights for the Sisal project.

Implications for Our Project
From this discussion, several implications stand out:

1. Fishermen's knowledge will be a critical data source in the absence of long-term scientific datasets.
2. Offshore design must be able to withstand waves of at least 3 meters and adapt to limited local data availability through reanalysis datasets and model adjustments.
3. Seasonal storm, cold front, and hurricane dynamics need to be integrated into the risk assessment and operational planning.
4. Maintenance independence is essential for community ownership and long-term sustainability of the farms.
5. Visiting Celestún to learn from ongoing practices will provide valuable lessons for implementation in Sisal.

Discussion with Prof. C. Rosas - 10 and 19 September 2025
Participants: Prof. Carlos Rosas (Marine Biology, UNAM), PhD Candidate Daisy Pineda-Suazo (Ecology)

Purpose and Context
On September 10th, we met with Prof. Carlos Rosas to discuss practical next steps for the design and community engagement aspects of the Sisal aquaculture project. In the follow-up meeting, Daisy Pineda-Suazo, one of Carlos' PhD students and an ecologist, joined the discussion. The meeting focused on technical considerations for farm design, strategies for effective communication with the fishing community, and plans for community outreach activities.

Technical and Regulatory Considerations
Carlos highlighted that installing concrete structures in the ocean requires government permits, which means project planning and timelines must be taken into account. He supported our proposal to use the flume (wave simulator) to test different fish farm cage designs under controlled conditions, exploring options such as foam, PVC, stones, and pipes. He emphasized that robust design is crucial, given the high frequency of small waves during the winter season in Sisal.

Carlos explained that in Celestún, an earlier fish farm was brought back to shore two years ago, underlining the importance of designing a farm that can withstand local wave and wind conditions. He considered the idea of a monitoring system for environmental and structural parameters highly valuable for ensuring farm safety and long-term viability.

Community Engagement and Communication
A major focus of the discussion was how to communicate effectively with the local fishing community. Carlos stressed that multi-functionality should be explored together with fishermen to build their trust and support. Because of language barriers and differences in technical understanding, he recommended creating a clear, visually engaging video to explain the concept of aquaculture and its benefits. This approach could help bridge the gap between scientific knowledge and fishermen's perceptions, making it easier for them to understand the potential consequences and benefits of aquaculture.

Input from Daisy Pineda-Suazo
Daisy joined the conversation and proposed not only engaging fishermen but also involving local high school students in the project, as they represent the future of Sisal's community. She emphasized the

importance of showing, through visuals, that the natural beauty of Sisal is not guaranteed to remain unchanged without ecological preservation. The video should create a contrast between degraded environments elsewhere and Sisal's current state, making the link between healthy ecosystems, tourism income, and community well-being explicit.

Daisy offered to collaborate on the production of this video, creating images and animations based on a script we provide. She noted that combining animations with real photographs would be most effective. The video could then be shown to both fishermen and students to compare their reactions and stimulate discussion.

Next Steps

Carlos mentioned that on September 16th, juvenile fish produced at the UNAM hatchery would be transported to Celestún, and he suggested the possibility of us joining this trip. Additionally, a visit will be arranged to meet fishermen in Sisal and to present the video at the local high school once it is ready. Daisy indicated that she could complete the video within three days once the script is finalized, making this an actionable short-term deliverable.

Interview Artificial Reefy – 19 September 2025

Participant: Daniel Dacomba (Reefy Employee)

Purpose and Context

We held an introductory meeting with Daniel Dacomba from Reefy to explore the potential of using Reefy's modular artificial reefs to enhance the ecological performance of the planned fish farm in Sisal. Our aim was to investigate whether Reefy's solution could serve both as an anchor system and as a habitat-enhancing feature, potentially providing additional ecosystem and community benefits.

Discussion Points

We introduced the context of Sisal, including water depth of approximately 10 m, wave heights of around 2.7 m, and currents ranging between 0.2 and 0.4 m/s. Previous research indicated that dead weight anchors were most feasible given the limestone seabed and the need to minimize dependence on external contractors.

Daniel explained Reefy's approach to eco-engineering and their patented Reef Enhancing Breakwater technology, designed to provide coastal protection while creating habitat complexity to boost marine biodiversity. Unlike traditional reefs that are simply dropped into the water, Reefy's blocks are engineered for stability, stacking modularly like large Lego bricks with holes and textured surfaces to promote marine life attachment.

Technical and Ecological Considerations

Daniel confirmed that Reefy could carry out stability calculations for their blocks under Sisal's local conditions. The blocks are made from unreinforced concrete to avoid corrosion issues and use alternative surface materials such as calcium carbonate to attract marine life. A typical block measures 1 × 1 × 3 m and weighs approximately 5.3–6 tons, depending on aggregate density. Stacking multiple layers increases ecological performance but also raises cost.

He highlighted that the success of artificial reefs relies on long-term monitoring and leaving the structure undisturbed to allow natural colonization, which can take several years. Education and engagement of local fishermen are crucial to ensure compliance and protection of the developing reef. He also noted that organic waste from nearby aquaculture must be carefully managed, as it could lead to excessive algal growth if uncontrolled.

Anchoring Potential and Attachment Methods

When asked about the feasibility of using Reefy blocks as anchoring points, Daniel confirmed that this could be technically feasible provided stability calculations confirm that the blocks will remain in place. Possible attachment methods include stainless steel in-locks, though these significantly increase cost, or wrapping mooring lines directly around the blocks.

Regarding hydrodynamic effects, Daniel explained that at Sisal's depth the waves would have little impact on underwater structures, meaning multiple layers of blocks would be required for significant wave dissipation, which may be economically challenging.

Permitting and Financial Feasibility

Daniel noted that starting projects in Mexico can be challenging due to strict permitting requirements, and projects are expected to be near carbon neutral. The cost of Reefy blocks depends heavily on whether local production is set up, for example through their project in Quintana Roo. Current estimates suggest production costs of roughly €1,000 per block, with transportation adding around €3,500 per block. Installation costs remain uncertain and would need to be carefully assessed. Ultimately, feasibility will depend on aligning the ecological ambition with the project budget and business case.

Outcomes

The meeting provided valuable insights into how artificial reefs could complement the fish farm, both ecologically and structurally. Key takeaways include the importance of careful budgeting, community education, and long-term monitoring. Further steps involve assessing stability, economic feasibility, and stakeholder acceptance before considering implementation.

Interview Reef Ball Foundation - 24 September 2025

Participant: Javier Dajer (Reef Ball Foundation; México)

Purpose and Context

On September 24th, we met with Javier Dajer, an authorized contractor for the Reef Ball Foundation in Mexico. The Reef Ball Foundation is an international non-profit organization active in over 80 countries, focused on rehabilitating and protecting ocean ecosystems through the use of ecologically sound artificial reef systems. Their mission emphasizes research, public education, community involvement, and the creation of reefs that promote natural species diversity and population density. Our objective was to understand whether Reef Balls could complement the Sisal aquaculture project as both a habitat-enhancing measure and a potential anchoring solution.

Foundation Approach and Activities

Javier explained that the Reef Ball Foundation collaborates with governments, NGOs, and private companies to finance and deploy artificial reefs. In many cases, companies donate Reef Balls as part of their environmental compensation strategies. The selection of projects follows an annual cycle, with decisions made a year in advance. Globally, over 500,000 Reef Balls have been deployed, making the design one of the most widely used artificial reef solutions and a standard reference in scientific studies of reef restoration.

Most projects (80–85%) are focused on marine ecosystem restoration, while a smaller share involves collaborations with universities for specific research or endangered species projects. Reef Balls have also been adapted for species-specific applications, such as lobster and octopus habitats, and have been used in memorial reefs, breakwaters, and anti-trawling installations.

Design and Technical Details

The standard Reef Ball design is a hollow dome-like concrete unit with a textured surface and strategically placed openings that deflect currents and ensure stability on the seabed. The form factor minimizes the amount of concrete required while maximizing stability and surface area for marine colonization.

Key technical details include:

- **Material:** A specially formulated pH-balanced concrete (pH 8.2–8.5) that mimics seawater chemistry and contains no metal reinforcement. This ensures a lifespan of over 400 years.
- **Sizes:** The standard unit weighs approximately one metric ton, though larger models such as the "Goliath" (around four tons) exist for deeper water applications.

- **Deployment:** Standard Reef Balls can be floated using internal bladders and transported with the small boats typically used by fishing communities, making them logistically accessible. Larger models increases complexity since bigger boats and cranes need to be rented. In Mexico there are insufficient of these offshore vessels causing it to be expensive.
- **Modularity:** Multiple smaller units are generally preferred over a single large unit for cost efficiency, resilience, and redundancy.

When used for coastal protection, Reef Balls are submerged approximately 30 cm below the water surface with a spacing of no more than 10 cm between units, allowing them to dissipate wave energy effectively.

Anchoring Potential and Structural Strength

Reef Balls can be equipped with stainless steel inserts or anchor systems to secure buoys or marine platforms. Javier confirmed that such configurations, in small scale, are already in use. The expected durability of the anchoring components is 10–20 years without maintenance. For extreme events, such as Category 4 or 5 hurricanes, removal of attached structures is recommended since conditions can be hard to predict. Drilling into the seabed can further increase holding capacity where required.

Ecological Impact

Each deployment is preceded by a baseline ecological study and followed by monitoring six to twelve months after installation. Data typically show substantial increases in biomass and biodiversity. When designed for specific species such as lobsters or octopus, biomass increases can reach 300–400%. Colonization begins quickly, with algae and sponges appearing within weeks and fish populations establishing within the first month. A complete ecological transformation generally occurs within two to three years.

Production and Financial Feasibility

Reef Ball production can be carried out locally using transportable molds provided by the foundation. The cost per one-ton unit is approximately USD 500, with local production helping reduce transport costs. Installation costs vary depending on the size of the units and the equipment needed. Deploying larger units can be significantly more expensive, as it requires bigger vessels and cranes, making multiple smaller units more economical in most cases.

Implications for the Sisal Project

The conversation highlighted that Reef Balls could potentially serve as both habitat enhancement structures and anchoring points for the Sisal fish farm, provided that structural calculations confirm their holding capacity. Javier emphasized that it would be valuable to research not only the technical feasibility of using Reef Balls as anchors but also to compare different anchoring configurations. This includes assessing the performance of a single heavy anchor versus multiple smaller anchors with the same combined weight. Such a comparison would allow for evaluating which configuration offers the best balance between stability, cost, and ease of maintenance under Sisal's environmental conditions.

In addition to technical stability, Javier underlined the importance of aligning the anchoring solution with economic feasibility and local operational capacity. The solution must be practical for fishermen to manage and maintain independently over the long term. Together, these considerations provide a clear direction for further research into optimizing the fish farm design for durability, cost-effectiveness, and community involvement.

B

Explanation of Utility Scores

This appendix presents the reasoning behind the utility scores assigned to each multifunctional option in Table 4.1. Each design measure is evaluated according to the three dimensions of the Triple Bottom Line (TBL): Planet, People, and Profit, to explain how their environmental, social, and economic effects were interpreted within the context of Sisal [Elkington, 1997]. The analysis combines published evidence, interview insights, and engineering judgement to provide a transparent account of why specific scores were chosen.

For every option, the discussion describes how the measure performs ecologically, socially, and economically under local conditions. Where relevant, potential limitations, externalities, and uncertainties are noted to clarify how these factors could influence implementation or long-term outcomes. The explanations aim to provide sufficient detail for replication and to demonstrate how technical feasibility, community relevance, and sustainability considerations were balanced in the scoring process.

B.1. Interpreting the Scoring Dimensions

- **Planet** refers to the expected ecological contribution of the measure, ranging from 1 (no or negative impact) to 5 (clear ecological restoration or enhancement).
- **People** captures the social value and perceived benefit for local stakeholders, ranging from 1 (no value or reduced acceptance) to 5 (essential for safety, legitimacy, or trust).
- **Profit** reflects *perceived affordability and cost–benefit* from the community's perspective, consistent with the TBL framing in Section 4.2. As operationalized in Section 4.4.3, a score of 1 indicates a high relative investment or maintenance burden, and 5 represents a low-cost or cost-saving solution. This perception-based economic score in the MCDA is later *complemented* by the attainability assessment, which tests practical financial and technical feasibility.

The scores should be read as *relative within the set of ten options* rather than as absolute measures of sustainability. Each assessment considers both short-term feasibility and longer-term potential under community-led management in Sisal.

B.2. Artificial Reefs around Cages

Assigned scores: Planet = 5, People = 3, Profit = 2.

Artificial reef modules placed near the cages are among the most ecologically effective measures considered in this study. Their textured, porous geometry increases habitat complexity and provides refuge and settlement surfaces for algae, invertebrates, and juvenile fish. In the shallow and moderately exposed waters off Sisal, clusters of small reef units can act as stepping stones that strengthen local biodiversity without obstructing navigation or cage operations. The use of pH-balanced, unreinforced marine-grade concrete prevents corrosion and supports a long service life, ensuring stable ecological benefits. Evidence from regional and international projects reports measurable gains in local biodiver-

sity and fish abundance through modular reef deployment Bracho-Villavicencio et al., 2023. Interviews with the Reef Ball Foundation confirm rapid colonisation within months and long-term durability when locally fabricated (Interview Reef Ball Foundation, 2025). Reefy further verified the ecological functionality of similar unreinforced concrete blocks and their suitability for local hydrodynamic conditions (Interview Reefy, 2025). Considering these factors, the reefs clearly deliver a strong restorative effect that can be observed in the short term, which corresponds to a score of 5 for Planet.

The social value of artificial reefs is positive but indirect. Reef fabrication and placement can involve fishers, students, and volunteers in practical construction activities, creating learning opportunities and a sense of shared environmental responsibility. The structures can also serve as visible symbols of ecological commitment, supporting environmental education and community pride when integrated into school visits or guided snorkeling tours. However, the benefits are less immediate than those from direct safety improvements or new income-generating activities. Without organised outreach, the value of the reefs may remain abstract to some residents. Overall, this represents a moderate but clearly recognisable social benefit, supporting a score of 3 for People.

From an economic perspective (as perceived by stakeholders), artificial reefs require moderate investment. Costs arise from molds, concrete, aggregates, and vessel time for deployment, but local fabrication using reusable molds can keep expenses manageable. Interviews indicate that sub-tonne Reef Balls can be produced with basic tools and deployed using small cooperative vessels, making this measure feasible for a community-scale initiative. The reefs do not reduce operational costs directly and only provide indirect economic returns when combined with educational or tourism activities. When designed as dual-purpose anchors, some savings can be achieved, although this depends on mooring layout and sea conditions. Taken together, these factors indicate a modest but non-negligible cost burden, which corresponds to a score of 2 for Profit.

B.3. Integrated Multi-Trophic Aquaculture

Assigned scores: Planet = 4, People = 2, Profit = 1.

Integrated Multi-Trophic Aquaculture (IMTA) combines species from different trophic levels, typically finfish, shellfish, and seaweed, so that waste products from one species serve as nutrients for another. This creates a more balanced and ecologically efficient system that reduces nutrient discharge and improves water quality. Under Sisal's conditions, IMTA could help mitigate eutrophication in nearshore waters and promote ecological resilience by diversifying production and nutrient pathways. Studies demonstrate that multi-species systems can reduce dissolved nitrogen and phosphorus levels and contribute to the recovery of surrounding ecosystems [Liu et al., 2022]. However, the local context presents constraints: offshore exposure, high wave energy, and limited technical maintenance capacity pose challenges for the delicate infrastructure needed to sustain multiple species. Ecologically, the principle is sound and widely validated, but implementation risks are higher in the Gulf of Mexico than in sheltered bays or fjords. Considering these factors, IMTA offers a strong ecological contribution, corresponding to a score of 4 for Planet.

From a social perspective, IMTA provides limited immediate benefits to the community. While it represents an environmentally responsible innovation, it requires specialised aquaculture knowledge and careful coordination among operators. In Sisal, where most cooperative members have limited experience with complex multi-species systems, participation would initially depend on external technical support. The benefits are therefore less visible and tangible to the wider community compared to more accessible functions such as education or tourism. Over time, training programs or partnerships with academic institutions could build capacity, but these processes require sustained involvement. Overall, IMTA presents modest direct engagement opportunities and limited visibility to non-specialists, representing a moderate to low social benefit and supporting a score of 2 for People.

Economically, IMTA is perceived as the most demanding of all multifunctional options considered. Additional species require separate seed stocks, infrastructure for cultivation, continuous water-quality monitoring, and trained personnel for maintenance. These demands significantly increase both investment and operational costs. The expected revenue gains from by-products such as shellfish or seaweed are uncertain and would depend on establishing new supply chains and local markets. Un-

der current cooperative conditions, the perceived economic risk outweighs short-term benefits. Taken together, these factors indicate a high financial burden, which corresponds to a score of 1 for Profit.

B.4. Fish Aggregation through Cage Structures

Assigned scores: Planet = 3, People = 2, Profit = 1.

Fish cages can act as artificial aggregation devices that attract wild species seeking shelter, shade, and feeding opportunities. This effect is well-documented in tropical and subtropical environments where submerged structures increase local fish density by providing refuge from predators and improved access to suspended organic material [Dagorn et al., 2013]. Around Sisal, this process could lead to higher fish abundance near the farm site, indirectly benefiting local fisheries through spillover effects. However, aggregation does not equate to habitat creation or ecological restoration, as the mechanism concentrates existing biomass rather than producing new growth. Without proper management, it may also increase local fishing pressure or alter predator–prey dynamics around the cages. Considering these mixed effects, fish aggregation provides a moderate ecological contribution that can support local biodiversity but requires oversight to avoid ecological imbalance, corresponding to a score of 3 for Planet.

The social dimension of fish aggregation is limited, as the benefits are diffuse and not immediately visible to the community. Fishers may perceive short-term gains from higher catch rates near the structures, but this can lead to competition or conflict if access is not clearly regulated. The process offers little opportunity for community participation or learning compared to educational or monitoring functions. Social value could improve if the aggregation zones are used for research or demonstration purposes, linking them to community education programs or controlled fishing trials. At present, however, the lack of visibility, regulation, and direct engagement makes this a relatively low social benefit, supporting a score of 2 for People.

From an economic perspective, fish aggregation does not require new investment because it occurs passively. Yet the absence of clear, stable returns for the cooperative limits perceived value. Potential short-term gains from higher local catch may not translate into sustained income, especially if overfishing reduces long-term stock levels. Management or monitoring to prevent exploitation could add cost without direct compensation. Taken together, these factors indicate a high relative burden in relation to tangible benefits, which corresponds to a score of 1 for Profit.

B.5. Fish Health and Environmental Monitoring

Assigned scores: Planet = 4, People = 3, Profit = 2.

Environmental and fish health monitoring supports the ecological integrity of aquaculture systems by enabling early detection of poor water quality, disease onset, or environmental stress. Under the exposed marine conditions of Sisal, variations in temperature, salinity, and dissolved oxygen can rapidly affect fish welfare and local water quality. Monitoring systems that track these parameters allow for timely management actions such as aeration or feeding adjustments, thereby reducing mortality and waste discharge. Evidence from the FAO and related environmental assessment studies indicates that monitoring contributes significantly to environmental performance and ecosystem protection when data are regularly collected and interpreted [Food and Agriculture Organization of the United Nations, 2010]. Field research also highlights that biofouling and sensor degradation can affect data reliability and maintenance frequency [Delauney et al., 2010]. Interviews with researchers from UNAM confirm that reliable data can strengthen accountability and guide adaptive management in coastal aquaculture projects. Considering these factors, fish health and environmental monitoring provides a strong and proactive ecological contribution, corresponding to a score of 4 for Planet.

The social benefits of monitoring are moderate and depend largely on how information is shared. When implemented collaboratively, data collection and interpretation can involve fishers, students, and technicians, fostering learning and a shared understanding of environmental conditions. The visibility of monitoring activities, such as the deployment of buoys or sensors, can reinforce community confidence that aquaculture is being managed responsibly. Partnerships with UNAM further enhance transparency

and encourage dialogue between science and the cooperative. However, if monitoring remains a purely technical exercise managed by external actors, its social impact diminishes. Overall, this represents a moderate social benefit that enhances trust and accountability, supporting a score of 3 for People.

Perceived economic feasibility depends on equipment type and scale. Commercial systems like the Sofar Ocean Spotter buoy cost between USD 7,000 and 15,000 and include satellite telemetry, robust housings, and low maintenance requirements. Such systems offer long-term reliability but exceed what the cooperative could finance independently. Lower-cost alternatives based on open-source sensors can be assembled for under USD 2,015 [Medina, Monroy, et al., 2022; Lu et al., 2022], but these prototypes are sensitive to humidity and biofouling and require frequent recalibration. Both approaches involve maintenance effort and replacement of parts exposed to seawater. Taken together, these factors indicate a moderate to high financial burden, which corresponds to a score of 2 for Profit.

B.6. Educational and Research Visits

Assigned scores: Planet = 3, People = 4, Profit = 3.

Educational and research visits contribute to the ecological sustainability of aquaculture indirectly by fostering awareness, environmental literacy, and stewardship among participants. When students, researchers, and fishers engage in activities such as biodiversity observation, water-quality logging, or habitat assessment, they generate data and knowledge that support responsible farm management. Although these activities do not directly restore ecosystems, they promote a culture of care and understanding of ecological limits. Similar field-based education programs have been shown to strengthen conservation attitudes and long-term environmental behaviour [Falk and Dierking, 1997; Bonney et al., 2009; Ardoin et al., 2020]. In the specific context of Sisal, such visits could reinforce collaboration between UNAM and the local cooperative, leading to shared monitoring of environmental parameters and adaptive practices that maintain ecosystem integrity. Considering these indirect but meaningful effects, educational and research visits provide a moderate ecological contribution, corresponding to a score of 3 for Planet.

The social dimension of this option is particularly strong. Regular visits by students and researchers create opportunities for dialogue between science and local knowledge, improving transparency and building trust in aquaculture activities. These interactions help demystify aquaculture for community members and demonstrate that the project aligns with collective environmental and social goals. The visibility of such collaboration enhances the legitimacy of offshore fish farming and encourages participation in joint initiatives. In addition, hosting visitors offers fishers a chance to present their work and share experiences, which can strengthen community identity and pride. Overall, this represents a high social benefit, supporting a score of 4 for People.

Financially, the initiative is perceived as relatively accessible. The infrastructure required like boats, safety gear and basic monitoring equipment already exists within the cooperative or can be provided through university partnerships. Operational costs are limited to fuel, maintenance, and coordination time, which can be offset by small stipends, research grants, or educational program support. The activity may also generate minor indirect income through collaboration with schools or NGOs interested in sustainable aquaculture. Taken together, these factors indicate a moderate burden, which corresponds to a score of 3 for Profit.

B.7. Solar Energy Integration

Assigned scores: Planet = 3, People = 3, Profit = 1.

Integrating solar photovoltaic systems into aquaculture operations can reduce dependence on fossil fuels and lower greenhouse gas emissions, contributing to cleaner and more resilient energy use. In Sisal's coastal setting, solar energy offers clear environmental benefits due to high solar irradiance and the potential to replace diesel generators that are commonly used for feeding systems, aeration, or lighting. By reducing fuel transport and consumption, solar integration lessens the risk of spills and localized pollution while improving energy efficiency. However, exposure to salt spray, humidity, and corrosion significantly reduces the longevity and reliability of solar photovoltaic components in marine environments. These technical challenges limit the consistent ecological performance of solar systems

offshore unless they are specially protected and maintained. Considering these factors, solar energy integration provides a moderate but tangible ecological contribution, corresponding to a score of 3 for Planet.

From a social perspective, solar energy systems can improve working conditions and perceptions of modernisation. Cleaner, quieter operations enhance comfort and safety for workers while signalling environmental responsibility to the wider community. The visible shift from fuel to renewable power aligns with global sustainability goals and may increase acceptance among residents who associate aquaculture with pollution risks. In Sisal, where sustainability is a central concern for local institutions such as UNAM, visible use of renewable energy could reinforce collaboration and public trust. Yet, the measure requires minimal direct participation from community members and offers few educational or recreational touchpoints compared to other options such as guided snorkeling or reef construction. Overall, this represents a moderate social benefit, supporting a score of 3 for People.

Economically, solar energy integration presents a substantial investment challenge for a community-led cooperative. Marine-rated solar panels, corrosion-resistant frames, batteries, and charge controllers entail high upfront costs and continuous maintenance under harsh conditions. Replacing degraded components or battery storage further increases long-term expenses. For a small cooperative in Sisal, such costs are difficult to recover through operational savings, as energy use on small farms is intermittent and modest. External grants or institutional partnerships would therefore be required for implementation. Taken together, these factors indicate a high financial burden, which corresponds to a score of 1 for Profit.

B.8. Snorkeling, Diving, and Eco-Tourism

Assigned scores: Planet = 2, People = 4, Profit = 4.

Integrating low-impact tourism, such as guided snorkeling or diving around the aquaculture site, can strengthen the visibility and social legitimacy of fish farms while promoting marine awareness among visitors. Ecologically, this measure has limited direct restorative value but can still contribute to broader conservation outcomes if implemented under clear guidelines. Controlled access and supervision reduce the risk of reef damage, littering, or disturbance to wildlife [Hishamunda et al., 2014]. When combined with educational messaging, ecotourism can foster appreciation of marine ecosystems and highlight the role of sustainable aquaculture in preserving biodiversity. In Sisal, the shallow and clear waters provide favourable conditions for guided snorkeling, but increased human activity must be balanced with carrying capacity and safety protocols. Considering these factors, the measure provides a weak to moderate ecological contribution, corresponding to a score of 2 for Planet.

The social dimension of eco-tourism is considerably stronger. Guided snorkeling creates a visible and participatory experience that directly connects the community and visitors to the marine environment. It can showcase the farm as a learning site and reinforce local identity through environmental education and hospitality. Involving local youth or fishers as guides offers an opportunity to diversify skills and develop a sense of ownership over sustainable marine practices. This visibility and interaction can transform perceptions of aquaculture from a purely productive activity to a shared community enterprise linked with education and conservation. When implemented collaboratively with UNAM or local tour operators, tourism activities also serve as a platform for outreach and awareness-building. Overall, this represents a high social benefit, supporting a score of 4 for People.

Economically, snorkeling and low-impact tourism have strong potential for supplementary income at a relatively low initial cost. Essential investments include safety gear, signage, and training for guides, all of which can be scaled with demand. Unlike infrastructure-heavy activities such as diving, snorkeling requires minimal equipment and can be operated from small boats already available within the cooperative. Revenues can be shared among participants or reinvested in maintenance and educational materials. However, the activity remains sensitive to weather conditions and seasonality, which limits its income stability. Taken together, these factors indicate a low to moderate financial burden and a realistic opportunity for local revenue generation, which corresponds to a score of 4 for Profit.

B.9. Small-Scale Desalination Units

Assigned scores: Planet = 2, People = 4, Profit = 1.

Small-scale desalination systems can provide freshwater directly at sea using compact reverse osmosis units powered by renewable energy. Ecologically, these systems have limited direct restorative impact and must be carefully managed to prevent adverse effects such as brine discharge or energy inefficiency. In marine environments like Sisal, high salinity and biofouling present additional operational challenges, requiring pre-filtration and periodic maintenance to maintain performance. While renewable-powered prototypes demonstrate promise for reducing land-based water transport, they remain experimental in small-scale offshore contexts and have yet to prove long-term durability under constant exposure [U.S. Department of Energy, 2021]. The potential environmental advantage lies mainly in reducing emissions from boat trips for water resupply rather than in direct ecosystem enhancement. Considering these factors, desalination provides a weak ecological contribution, corresponding to a score of 2 for Planet.

Socially, desalination at sea can offer meaningful benefits for fishers, technicians, and students involved in aquaculture operations. Access to freshwater increases comfort and safety during long working hours offshore, supporting hygiene, first-aid capacity, and daily maintenance activities. When integrated into educational or research visits, freshwater availability also enables longer sessions for sampling, monitoring, or training without reliance on shore-based support. In regions like Sisal, where water scarcity is a known constraint, the symbolic value of clean water generation aligns with community perceptions of self-sufficiency and innovation. These tangible and visible benefits, along with potential use in safety or education, make desalination a socially valuable measure. Overall, this represents a high social benefit, supporting a score of 4 for People.

Financially, small-scale desalination remains one of the least feasible multifunctional options for a cooperative-scale project. Systems require expensive membranes, pumps, pressure vessels, and filters, which deteriorate quickly in saline and high-humidity conditions. Maintenance and spare parts availability are ongoing concerns, as biofouling and membrane scaling can impair performance within months. Even with renewable energy integration, operational costs per litre remain high, and replacement cycles for filters and seals add further expense. Without subsidies or research-driven funding, the investment is beyond the means of a community initiative. Taken together, these factors indicate a high financial burden, which corresponds to a score of 1 for Profit.

B.10. Connectivity Systems (Wi-Fi or Radio Link)

Assigned scores: Planet = 2, People = 4, Profit = 1.

Establishing reliable communication links between offshore aquaculture platforms and the shore enhances coordination, safety, and operational oversight. From an ecological standpoint, connectivity has only an indirect contribution. Real-time monitoring of environmental parameters and farm status can prevent incidents such as fish escapes, equipment loss, or pollution by enabling faster response to emergencies. In the context of Sisal, where fish farms are expected to operate in moderately exposed waters, a communication link could help minimize environmental risks associated with delayed intervention or equipment failure. However, the system itself does not restore or protect marine ecosystems, and its environmental benefit depends on how the information is used for management. Considering these factors, connectivity provides a weak but supportive ecological contribution, corresponding to a score of 2 for Planet.

The social benefits of connectivity are significant and strongly linked to perceptions of safety and professionalism. For small-scale operators and families in Sisal, maintaining contact with offshore workers improves confidence and reduces anxiety about accidents or communication loss during bad weather. Reliable communication also facilitates coordination between fishers, students, and researchers, allowing for better scheduling of visits and joint monitoring activities. When combined with simple emergency procedures, connectivity can enhance preparedness and trust in aquaculture operations. In addition, visible communication equipment, such as antennas or small solar-powered transmitters, signals that the farm is organized and responsibly managed. These qualities strengthen local legitimacy and help integrate the fish farm within existing coastal networks. Overall, this represents a high social benefit, supporting a score of 4 for People.

Financially, connectivity systems present notable challenges. Marine-rated communication devices, repeaters, or satellite modules are relatively costly, and ongoing service or data subscription fees add to the operational budget. For small cooperatives, these recurring costs may outweigh the benefits unless shared with research institutions or integrated into broader monitoring programs. Low-cost alternatives, such as radio links or limited-range Wi-Fi, can reduce expenses but require technical expertise to install and maintain. Exposure to salt, humidity, and storm conditions also shortens component lifespan, increasing replacement frequency. Taken together, these factors indicate a high financial burden, which corresponds to a score of 1 for Profit.

B.11. Safe-Harbor Features on Platforms

Assigned scores: Planet = 2, People = 5, Profit = 2.

Safe-harbor features enhance the security and resilience of offshore fish farms by ensuring that workers can respond effectively to emergencies and seek temporary refuge during sudden weather changes. From an ecological perspective, these provisions have only indirect benefits. By improving the safety and reliability of operations, they reduce the risk of accidents that could lead to environmental damage, such as fuel spills, gear loss, or net failures. Well-equipped platforms also enable faster and safer maintenance, which supports consistent environmental performance and reduces the likelihood of equipment degradation in the marine environment. Although these advantages do not directly restore ecosystems, they help prevent negative impacts and contribute to the overall sustainability of the operation. Considering these factors, safe-harbor features provide a weak but supportive ecological contribution, corresponding to a score of 2 for Planet.

The social value of safety measures is exceptionally high. The availability of emergency equipment—such as first-aid kits, flotation devices, waterproof torches, and signaling gear—directly improves the wellbeing of workers and increases confidence in offshore activities. For small-scale operators and students involved in fish farm visits, clear safety procedures foster a sense of professionalism and care, strengthening community trust in the initiative. Visible safety improvements also demonstrate that the project prioritizes human welfare, which aligns closely with social expectations in Sisal regarding responsible marine work. This perception can be reinforced through regular training or drills, further embedding safety culture into daily practice. The presence of standardized equipment, in line with FAO–ILO–IMO recommendations for small vessels [Food and Agriculture Organization of the United Nations et al., 2012], can therefore serve as a tangible symbol of responsibility and reliability. Overall, this represents a high social benefit, supporting a score of 5 for People.

From an economic standpoint (as perceived by participants), the investment required for basic safety provisions is relatively modest. The initial cost of purchasing corrosion-resistant equipment and installing it securely above the splash zone is minor compared to other infrastructure needs. However, some recurring expenses arise from replacing consumables such as flares, batteries, and first-aid materials, and from regular inspection routines to ensure continued readiness. The labour associated with training and equipment checks also represents a small but ongoing commitment. While these costs are manageable for a cooperative, they do constitute a non-zero burden that must be planned for in maintenance budgets. Taken together, these factors indicate a low to moderate financial burden, which corresponds to a score of 2 for Profit.

C

Questionnaire

The questionnaire was given to the two groups translated to Spanish by a professor. Afterwards the results where translated back and put in an excel file.

The link to the explanatory video can be found here.

Questionnaire MDP Fish Farms

Age:

Profession:

Planet: About protecting nature by keeping ecosystems healthy, reducing pollution, and saving resources. In fish farming, this means using eco-friendly cages and reducing waste.

People: About the social impact, focusing on community involvement, fair pay, and equality. It also includes creating other jobs, offering education, and linking tourism opportunities to the fish farm.

Profit: About keeping the farm financially healthy by producing efficiently, cutting costs, and earning extra income through things like eco-tourism or selling seaweed.

---

1. ***How important do you think these subjects are?***
   Give 0-5 points per subject.

   Planet O O O O O

   People O O O O O

   Profit O O O O O

2. **Please circle how you feel about the following questions.**

- I am willing to diversify my job into tourism. *Never - Maybe - Neutral - Yes – Definitely*
- I want to keep fishing in a traditional way. *Never - Maybe - Neutral - Yes – Definitely*
- I want WIFI near the fish farms so I can be In contact with my family. *Never - Maybe - Neutral - Yes - Definitely*
- I want freshwater makers on the fish farm to drink water out at sea *Never - Maybe - Neutral - Yes - Definitely*
- I want to have sensors on the fish farm to tell me where the fish are at a certain time. *Never - Maybe - Neutral - Yes – Definitely*
- I am willing to change my behaviour to promote ecological improvement. *Never - Maybe - Neutral - Yes – Definitely*

3. **Is there anything else you want to say about a fish farm in Sisal?**

Figure C.1: English questionnaire administered to high-schoolers and fishery stakeholders.

D

AquaSim Model Build

This appendix provides a concise overview of the AquaSim model setup used to perform the hydrodynamic simulations described in Chapter 5. The purpose is to provide sufficient information for future researchers to understand the model configuration, reproduce the workflow, and continue the development of the numerical analysis. For comprehensive background information on the theoretical formulations and available modelling tools, readers are referred to the official AquaSim documentation available online.

D.1. Software Environment

The numerical simulations were conducted using the *AquaSim* software package developed by Aquastructures AS. The software is widely applied in the Norwegian aquaculture industry for the design and certification of fish farming systems, moorings, and other offshore installations. AquaSim uses the Finite Element Method, dividing structural components such as floating pipes, mooring lines, and nets into a network of interconnected elements. The governing equations of motion are solved for each element, enabling the simulation of dynamic responses under combined wave and current loading.

Two complementary interfaces were used throughout the study:

- **AquaEdit:** The model-building environment where all structural components, hydrodynamic parameters, and environmental conditions were defined.
- **AquaView:** The post-processing and visualization environment used to inspect numerical outputs and generate time-series animations for result verification.

D.2. Investigating the AquaSim Model

D.2.1. Obtaining an AquaSim License

To further investigate or reproduce the created models, a valid AquaSim license (commercial software) is required. Interested users can obtain access by contacting Aquastructures AS through the official contact form or by emailing a member of the AquaSim team. Once a license is obtained, users can recreate the model setup following the configuration steps described in this appendix and using the parameters presented in Table 6.1 and Table 5.5.

D.2.2. Data Access and File Repository

All AquaSim project files developed in this study are publicly available via the Zenodo repository. Without an AquaSim license, only a limited number of related files, such as text, HTML, and video documents, can be accessed. The repository contains all input (*AquaEdit*) and output (*AquaView*) files, each corresponding to the simulation setup for different environmental scenarios.

Two separate *AquaEdit* files are provided: one representing the general model, and another specifically configured for the towing scenario. The latter was developed separately since the design of this

scenario differs from the standard offshore setup, as described in Section 5.2. All other files include visualisation outputs and configuration details. Future users can replicate the simulations by loading these files into their licensed version of AquaSim.

D.3. Model Configuration in AquaEdit

The model setup in *AquaEdit* was developed to represent two fish farm configurations, the circular and vessel-shape designs, under realistic environmental conditions near Sisal. The key design and environmental parameters are listed in Table 6.1 and Table 5.5, which formed the input for the hydrodynamic analysis.

The main model components created in AquaEdit included:

- Floating HDPE pipes modelled as beam elements with linear elastic material properties.
- Mooring lines represented as cable elements with prescribed pre-tension and fixed anchor points.
- A simplified net structure modelled as porous panels defined by hydrodynamic drag coefficients.
- Buoyancy elements and connecting nodes ensuring realistic weight distribution and system stability.
- Environmental conditions, including wave height, period, direction, and current velocity, applied according to the scenario matrix.

Each simulation was configured as a separate project file. The model coordinate system was oriented such that the wave and current directions aligned with the x-axis, ensuring comparability between designs. The simulation time step and mesh density were adjusted to maintain numerical stability and manageable computation times.

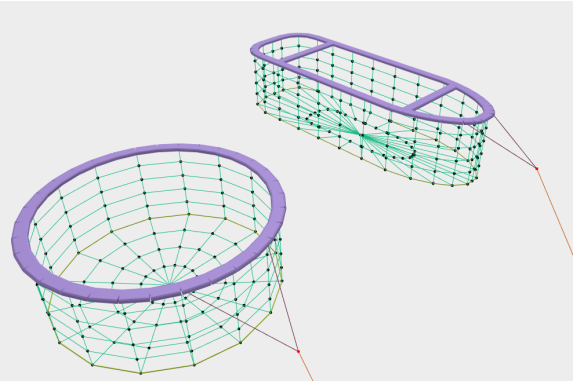

(a) General AquaEdit model setup, showing the vessel-shaped and circular fish farm geometries.

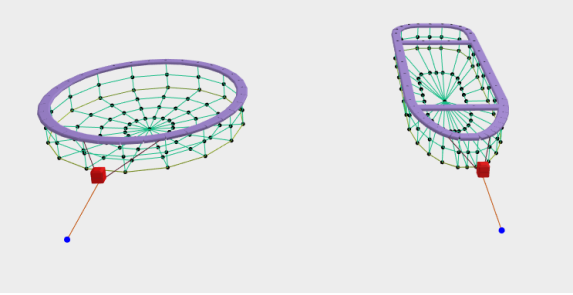

(b) Adapted AquaEdit setup for the towing scenario, with modified net depth and applied towing forces.

Figure D.1: Overview of the AquaEdit model configurations. (a) shows the general model setup, while (b) illustrates the modified towing scenario, which was developed as a separate model due to its different structural and hydrodynamic boundary conditions.

D.4. Post-Processing in AquaView

After each simulation, the output files were analysed using *AquaView*. This interface enables users to select specific scenarios and visualise variables such as mooring line tension, cage displacement, and net deformation over time. AquaView also supports exporting numerical data for further post-processing in external programs (e.g., MATLAB or Excel). The visualisation capabilities of AquaView, as illustrated in Figure D.2, were used to validate that the simulated motion and tension behaviour matched realistic physical responses under varying sea states.

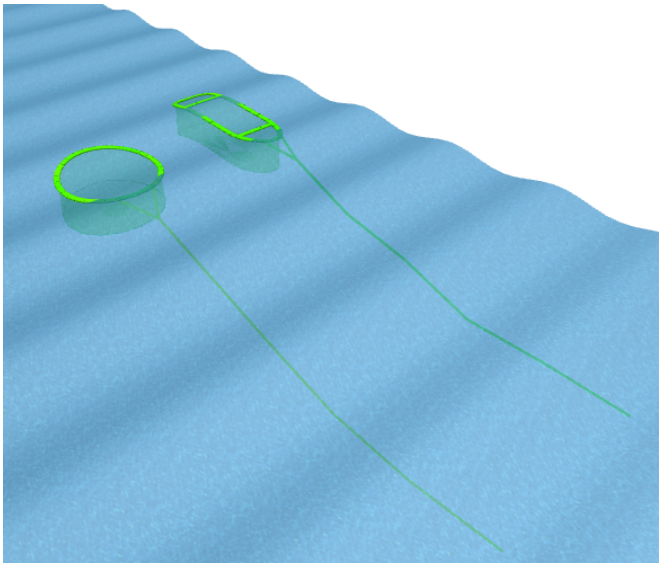

Figure D.2: Example of AquaView output showing hydrodynamic response visualisation during a moderate sea state. This visual inspection was used to verify the physical accuracy and consistency of the model behaviour.

E

Flume Research Design and Recommendations

In the early stages of this research, a flume experiment was planned at the UNAM Campus in Sisal to experimentally compare the maximum mooring line tension of circular and vessel-shape aquaculture designs. However, during the final stages of preparation a critical data acquisition component was found to be missing. Because of this, the experiment could not be executed within the project time frame.

This appendix presents a complete blueprint for the flume research setup that can be used for future validation of the vessel-shape aquaculture design in Sisal. It outlines the scientific background, objectives, and methodology for a physical experiment that builds on the numerical results from the current study. The main focus is a mooring line tension experiment, with an additional sub-experiment proposed for analysing the stability of the cage and anchoring system through optical recordings. Together, these experiments aim to bridge the gap between simulation and real hydrodynamic behaviour.

E.1. Background Information

The experiment was designed to complement and validate the outcomes of the numerical simulations performed with the MWDF and AquaSim software. These simulations partly justified the hypothesis that a vessel-shape aquaculture system performs better than a comparable circular design when using a single mooring line. They indicated that the vessel-shape experiences lower maximum mooring line tension and improved directional stability.

Physical validation remains essential to confirm these findings and to gain a deeper understanding of how cage geometry, mooring configuration, and hydrodynamic forces interact under realistic conditions. The design concept presented here was inspired by the flume study of Zhuo et al., 2024, who conducted a series of wave basin tests on vessel-shape aquaculture cages. Their results provide valuable theoretical and methodological insights relevant to this study:

- “The maximum force exerted on the mooring rope increases with wave height, while changes in the wave period have a less pronounced effect.”
- “When simulating the actual size of a vessel-shape fish cage, it is important to note that the simulation model is a rigid body model. As a result, the wave dynamics and the fish cage do not completely conform to the water surface. The flexible deformation of the floating tube causes the actual force data on the fish cage to be lower than the simulation data.”
- “When wind, wave, and current directions are inconsistent, the fish cage experiences increased torque, making it susceptible to localised damage and potential losses.”
- “In practice, the mooring line force can be alleviated by increasing the length of the anchor rope, thereby minimising the risk of anchor rope failure.”

- "In comparison to traditional circular fish cages, the unique triangular structure at the head of the fish cage reduces its wave facing surface area. This design minimises the impact of wave currents, thereby decreasing the forces acting on the fish cage and enhancing its hydrodynamic characteristics."

Zhuo et al., 2024 used a 1:108 scale for a 75.6 m by 23.8 m prototype cage and applied strict Froude scaling to reproduce realistic hydrostatic and dynamic behaviour. Their study emphasised the importance of matching displacement, stiffness, and mooring properties between the model and prototype. The experiment proposed in this appendix follows similar principles but with a focus on capturing the *flexible deformation* of the structure, which is particularly relevant for HDPE collars commonly used in aquaculture.

E.2. Objective

The primary objective of this flume experiment is to assess how the geometric design of offshore aquaculture structures influences their performance under environmental conditions representative of the Sisal region. Specifically, it aims to compare a traditional circular cage with a vessel-shape cage at model scale and to determine whether the vessel-shape, which has a smaller wave facing area, produces lower mooring line forces and improved hydrodynamic stability.

A secondary objective is to evaluate whether the flume setup can be used to visually assess the stability of the cage and anchoring system, allowing for a combined investigation of mooring load and frame deformation.

E.3. Pre-experiment Checklist for UNAM

The following preparations must be completed before the experiment can be conducted:

- Ensure that UNAM purchases and installs the **signal conditioning module**, which converts the analogue output of the load cell into readable data for computer analysis.
  - Item: FSH03944
  - Purchase directl possible here or inquiry possible on Futek's website
  - Estimated cost is approximately $2250 USD.
- Verify that the flume's current generation system and wave paddles are fully functional and calibrated.
- Confirm that all **sensor licences and calibration tools** (including the Futek data acquisition software) are active.
  - Currently two Futek S Beam Jr. (LSB210) Load Cell are present at UNAM campus. This submersible sensor is available for a wide range of capacities from 1N – 445N. It should be checked whether this sensor satisfies or if alternative sensors fit the experiment better.
- Ensure that **three high resolution cameras** and appropriate video analysis software are available if the stability sub-experiment will be performed.
- **Research team expertise:**
  - Include at least one researcher experienced in 3D printing or physical model building.
  - Include one researcher with knowledge of wave dynamics and flume operation.
  - Collaborate closely with **Camilo S. Rendon Valdez**, the Wave Channel Technician, to determine the appropriate model scale and to assist in the calibration of the flume.
- Begin flume preparations immediately at the start of the project to allow sufficient time for model construction, calibration, and testing.

E.4. Flume Safety and Risk Considerations

Standard laboratory safety procedures apply, including the use of closed footwear, restricted water access during operation, and supervision by qualified flume staff. Electrical equipment such as sensors

and conditioning modules must be water protected and tested for insulation before use. Researchers should be trained in emergency shutdown procedures and maintain a clear communication protocol during testing.

E.5. Experiment: Analysis of Mooring Line Forces

E.5.1. Hypothesis

The main hypothesis is that the vessel-shape fish farm design will experience lower maximum mooring line tension than the circular design under identical wave and current conditions. This is expected due to its more streamlined geometry, which reduces the wave facing area and distributes hydrodynamic loads more evenly.

A secondary hypothesis proposes that increasing mooring line length will further reduce dynamic loading and fatigue on the mooring system, in line with the findings of Zhuo et al., 2024.

E.5.2. Sub-experiment: Stability Observation

An additional sub-experiment can be conducted simultaneously to assess the structural stability and motion behaviour of the cages. The goal is to record the *x, y,* and *z* displacement of the cage and anchoring system under varying wave conditions. This visual analysis would provide valuable information about how the shape of the cage affects its movement, pitch, and roll stability.

To conduct this sub-experiment:

- Install three synchronised high-resolution cameras around the flume (front, side, and top view) to capture all movement directions.
- Apply small reflective markers to the structure at key points (e.g., cage corners, collar joints, and mooring attachment) to allow optical tracking.
- Place a stationary reference grid in the camera frame for motion calibration.
- Use video analysis software to extract movement data and compare displacements between cage types.

This experiment does not require additional sensors and can be performed simultaneously with the mooring tension test.

E.5.3. Materials and Equipment

The following equipment is required for the experiment:

- Two scaled physical models: one circular and one vessel-shape, constructed from lightweight, water resistant materials (PVC or 3D printed polymer).
- Adjustable internal ballast to match scaled displacement, draft, and metacentric height.
- Single mooring line setup with identical line stiffness and pretension for both models (e.g., using nylon fishing line or equivalent flexible material).
- In line load cell (Futek) for measuring mooring line tension.
- Signal conditioning module for data conversion and computer interface.
- Data acquisition computer with Futek software licence.
- Wave flume at the UNAM Campus Sisal, capable of generating regular and irregular wave conditions.
- 3D printer and modelling software for creating precise model geometries.

For the optional stability sub-experiment:

- Three high resolution cameras (minimum 60 frames per second).
- Video analysis software (e.g., Tracker or MATLAB-based optical tracking).
- Visual reference grid for motion calibration.

E.5.4. Variables

- **Independent variable:** Cage geometry (circular vs. vessel-shape).
- **Dependent variable:** Maximum mooring line tension.
- **Controlled variables:** Wave height, wave period, current velocity, water depth, model scale, and mooring stiffness.

E.5.5. Method and Procedure

The experiment will follow the principles of Froude similarity to ensure dynamic equivalence between the model and full scale structure. The model scale (expected to be between 1:20 and 1:25) will be determined in collaboration with the Wave Channel Technician, based on flume dimensions and target wave characteristics.

Step 1: Model preparation Both models will be constructed to identical displaced volume and draft. Internal ballast will be adjusted until the models reproduce the correct buoyancy and metacentric height, ensuring similar hydrostatic stability. Table 6.1 contains the design parameters that were used in the simulation experiment, these could be used as a basis for the dimensions of the model.

Step 2: Experimental setup Each model will be connected to a single mooring line attached to an anchor at the flume bed. The load cell will be placed in line with the mooring rope to measure dynamic tension during testing.

Additional setup for the sub-experiment: Cameras should be positioned on stable tripods at the front, side, and top of the flume. Before testing, calibration frames and lighting conditions must be checked to ensure clear marker tracking during wave action.

Step 3: Test conditions Five environmental conditions should be tested based on the scenarios in Table 5.5, varying wave height, wave period, and current direction to simulate different sea states.

Step 4: Data collection The load cell will record continuous tension data throughout each run. Wave probes will measure the incident wave height, and currents will be calibrated at the start of each session.

Additional recording: All cameras will record simultaneously during each test. Each video should include a visible reference grid for motion calibration.

Step 5: Data processing The tension data will be processed to extract peak and RMS mooring loads. The results for the circular and vessel-shape designs will be statistically compared and validated against numerical AquaSim results.

Additional processing for sub-experiment: Video analysis software will be used to track marker motion and quantify horizontal and vertical displacements of the cage. The stability of both designs can then be compared based on average movement amplitude and recovery response.

E.6. Expected Results

Based on prior simulations and literature, the following outcomes are expected:

- The vessel-shape cage will experience lower maximum mooring line tension than the circular cage under identical wave conditions.
- Mooring tension will increase proportionally with wave height but be less affected by wave period.
- Longer mooring lines will further reduce dynamic loading.
- The flexible vessel-shape structure is likely to exhibit smoother motion and reduced peak responses compared to the rigid circular model.

If the sub-experiment is performed, it is expected to reveal that the vessel-shape cage shows improved directional alignment and smaller lateral excursions, confirming enhanced stability.

F

Data Analysis

F.1. Introduction

This appendix presents the data analysis underlying the environmental design conditions for offshore aquaculture near Sisal, Yucatán. The focus is on waves and currents, which are the main hydrodynamic factors controlling cage stability, mooring loads, fish welfare and operational safety [H. Cheng et al., 2020; Klebert et al., 2013]. The analysis combines direct measurements from the Acoustic Doppler Current Profiler (ADCP) deployed offshore Sisal with statistically downscaled long-term wave data, providing both local accuracy and historical context.

Over the past twelve years (2014 to 2025), UNAM has collected continuous ADCP measurements of waves and currents at a site located approximately ten kilometers offshore. These observations capture the full seasonal cycle and a wide range of oceanographic conditions representative of the local marine environment. The extended record strengthens the empirical basis for estimating design conditions for aquaculture systems located eight kilometers from the coast.

Previous work by Bakker et al., 2024 established the first design parameters for the Sisal site by combining a ten-year ADCP record with nearly four decades of ERA5 reanalysis data. This hybrid approach allowed Extreme Value Analysis (EVA) to be performed on the long ERA5 record while scaling results to local conditions using the shorter in-situ dataset. For currents, where no global reanalysis product exists, Bakker et al. defined design values based on the 95th percentile of measured speeds. Their methodology is summarized in Section F.1.2.

The present study expands on that framework using an updated twelve-year local record and a forty-seven-year downscaled wave dataset. The latter, produced through a RBF downscaling of ERA5, provides a long-term wave record equivalent to the ADCP location but contains wave parameters only (significant wave height, period and direction). No current information is available in the RBF dataset.

Although a record length of twenty to thirty years is generally recommended for robust extreme value estimation [Det Norske Veritas, 2014], the twelve-year continuous ADCP dataset substantially reduces statistical uncertainty compared with shorter records. This is important because uncertainties in wave data sources can propagate into vessel response and fatigue analyses, influencing structural safety and operational durability [Schirmann et al., 2020].

Building on Bakker et al., this analysis has two objectives. The first is to re-evaluate design wave and current conditions using the extended ADCP dataset, ensuring that the results reflect the actual site-specific environment. The second is to apply the same statistical framework to the long-term RBF wave record to assess how extended temporal coverage affects the estimation of extreme conditions. Together, these analyses provide a comprehensive and internally consistent basis for the environmental design of offshore fish farming systems near Sisal.

F.1.1. Acoustic Doppler Current Profiler

An ADCP measures water velocity profiles by transmitting short acoustic pulses into the water column and recording the Doppler shift of sound scattered back by suspended particles. Using a four-beam configuration, the instrument resolves three-dimensional velocity components within discrete depth cells, producing a vertical profile of currents throughout the water column. Bottom-mounted, upward-looking ADCPs are widely used in coastal and offshore studies because they provide stable, long-term measurements while remaining protected from surface exposure. The broadband ADCP design reduces velocity variance and enables finer vertical resolution, which is advantageous for energetic environments such as the offshore region near Sisal [Brumley et al., 1991].

In addition to currents, an upward-looking ADCP can also estimate bulk wave parameters and even directional wave properties. Under the assumptions of linear wave theory, orbital velocities in the upper water column and surface-tracking returns can be inverted to derive the wave elevation spectrum, from which significant wave height (H_s), spectral peak period (T_p) and mean and peak direction (D_p) are computed. Field comparisons have shown that ADCP-derived wave energy and directional statistics correspond closely with wave buoy measurements, confirming that a single bottom-mounted instrument can simultaneously capture both current profiles and wave parameters over extended deployments [Herbers and Lentz, 2010].

In this study, the ADCP was deployed on the seabed at an approximate depth of 10 m, oriented upward. The processed data files report the instantaneous water depth at the transducer, meaning that the instrument's height above the seabed is already accounted for. The dataset provides hourly records of H_s, T_p and wave direction (D_p), as well as depth-resolved current velocities, which together form the basis for the analyses presented in the following sections.

F.1.2. Bakker et al.

The research by Bakker et al, conducted last year, established the first set of design values for the offshore site near Sisal. To achieve this, two main datasets were used: local ADCP measurements (waves and currents, 2014–2023) and ERA5 reanalysis data (waves, 1985–2024). The combination allowed the researchers to balance the long historical record of ERA5 with the site-specific observations of the ADCP.

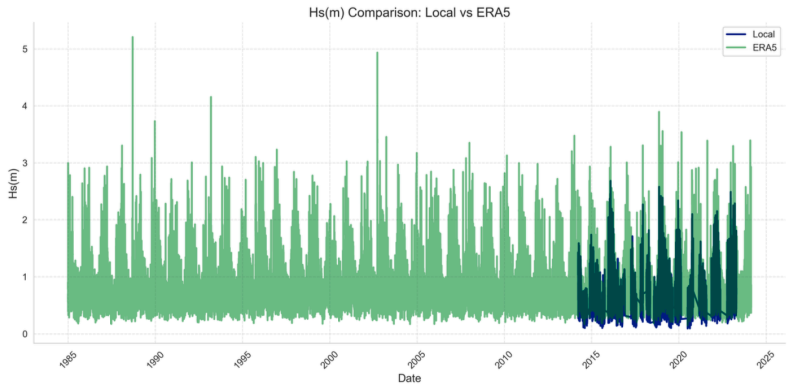

Figure F.1: Comparison of ERA5 and local ADCP wave data using Weibull fits. The difference in distribution tails motivated the application of a scaling factor ($k = 0.815$) to adjust ERA5 extremes to local conditions.

For the waves, an EVA was performed on the ERA5 dataset using the Peaks Over Threshold (POT) method with a threshold of 2.70 m. To ensure that successive storm peaks were treated as independent events, a declustering window of four days was applied. This Means that if multiple exceedances occurred within four days, only the highest value was retained. The exceedance were fitted with a Generalized Pareto Distribution (GPD) to estimate return levels. For a 20-year return period, the design wave height at the ERA5 location was found to be 4.19 m. To adjust this to local conditions, a scaling factor was calculated by comparing the Weibull scale parameters of ERA5 and ADCP wave records. Applying this factor reduced the design wave height to 3.40 m. The corresponding wave period was

derived through a power-law regression, resulting in a design wave period of 8.01 s.

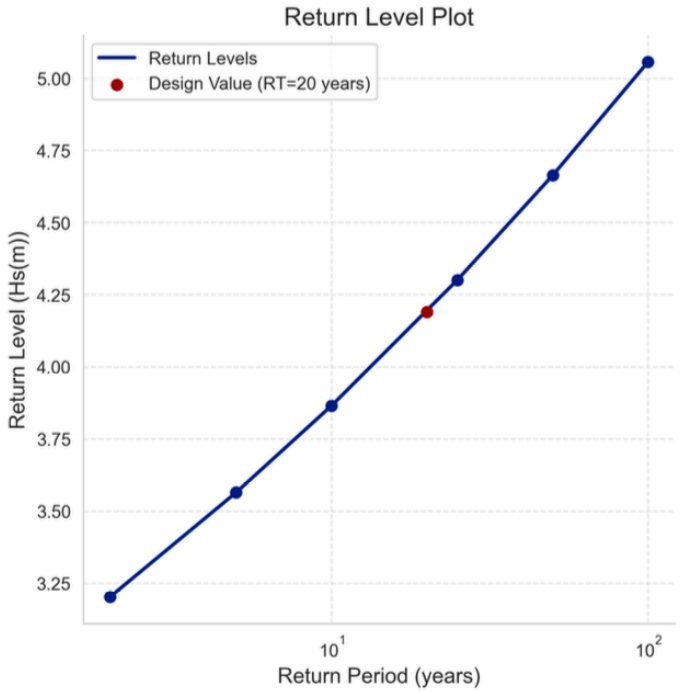

Figure F.2: Return level plot from ERA5 wave data using POT and GPD fitting. The estimated 20-year return value ($H_s = 4.19$ m) is indicated with a marker.

For the currents, EVA was not considered reliable due to the limited time span of observations. Instead, the 95th percentile of current speeds was used as the design value across depths. Polynomial regression was applied to extrapolate values closer to the surface, leading to a maximum design current speed of 0.50 m/s at −0.5 m depth.

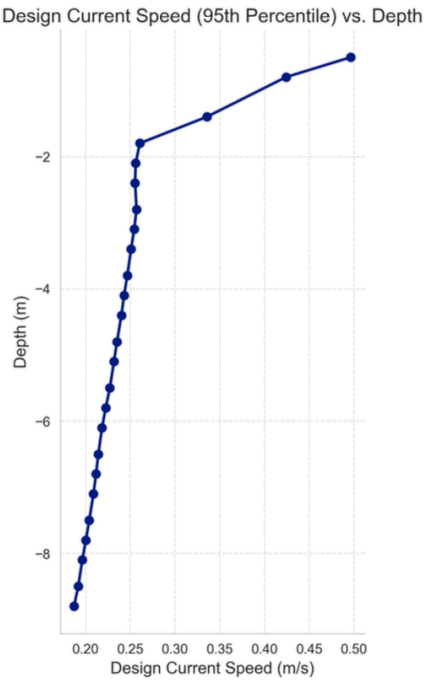

Figure F.3: Vertical profile of design current speed based on 95th percentile values and polynomial extrapolation. The maximum current speed of 0.50 m/s occurs near the surface.

Finally, directional analyses of both waves and currents showed that extreme waves predominantly came from the north to northeast, while the strongest currents were aligned east–west (70° and 250°). Importantly, waves and currents often reached extremes at the same time but from different directions, underlining the need for robust cage and mooring designs.

F.2. ADCP Data

F.2.1. Introduction

With an additional two and a half years of measurements now available, the local dataset has grown to twelve years in length. While this record alone does not yet reach the 20 to 30 years often recommended for extreme value estimation, it does provide a 20 percent longer site specific basis than was available previously. The ERA5 reanalysis remains valuable because of its multiple decade coverage, combined with the local data it will give a broad view of the conditions. By placing the ERA5 reanalysis and the twelve year observational record measured 10 km offshore side by side, the present study establishes design values that are both locally representative and supported by long term context. This dual approach reduces reliance on scaling factors and provides a more transparent and robust foundation for the site specific design of fish farms located eight km off the coast of Sisal. This location was chosen based on the research of Bakker et al., 2024, who identified it as the most suitable suitable area for offshore aquaculture.

To allow direct comparison the structure of Bakker et al., 2024 is used. Firstly, the wave dataset is examined, followed by the current dataset. Finally both wave and current data are considered together through directional and joint occurrence analysis.

F.2.2. Waves ADCP Data

An Extreme Value Analysis was carried out using the twelve year wave dataset (2014–-2025).

1. **Data cleaning:** The raw dataset was cleaned to remove outliers and inconsistencies.
2. **Extreme Value Analysis:** A POT method with Generalised Pareto fitting was applied to H_s. Return levels for 10 and 20 year periods were estimated, with the 20 year condition taken as the design wave height.

3. **Wave height–period relationship:** A power law regression was used to determine the relation between H_s and T_p. From this, the design period corresponding to the 20 year design wave height was estimated.

Data cleaning

In Bakker et al., 2024, the local record was cleaned by comparing it to ERA5 and removing points where the difference exceeded four standard deviations. That approach assumes ERA5 is an appropriate reference for every timestamp. In the present study, the twelve year local record is treated as the primary source for design and ERA5 is used later only for side by side comparison. Trial filters showed that a global σ rule tended to shave real storm peaks in this dataset, because the variance of the local series is smaller compared to the reanalysis.

To preserve genuine extremes while still removing obvious errors, a conservative site based procedure was used:

1. **Physical bounds.** Keep values within realistic limits for the site. For significant wave height this means $0 \leq H_s \leq 3$ m, which removes two isolated spikes above 3 m. Visual inspection of the raw time series revealed that one of these spikes was a clear measurement fault, showing an isolated jump inconsistent with surrounding values, while the other reached nearly 6 m without any corresponding storm event in regional meteorological records. Given the 10 m water depth at the site, such a wave height would imply a breaking ratio of $H/h \approx 0.3$, well below the classical Miche limit of $H_b/h \approx 0.78$ for regular waves [Miche, 1944] and near the lower range observed for random seas in intermediate depths [Goda, 2010]. This limit is also consistent with theoretical transformations of wave height distributions under depth-limited conditions, which show truncation of the upper tail as H_{rms}/h approaches 0.2–0.3 [Mendez et al., 2004]. The chosen threshold therefore removes implausible outliers while preserving genuine extreme events.
2. **Consistency of T_p with H_s.** Period spikes were screened using the local relation between height and period. The data was binned by H_s in steps of 0.20 m. Within each bin the median and the median absolute deviation of T_p were computed and values outside median ± 4 MAD were discarded. This removes implausible periods while keeping broad storm events.
3. **Resolution.** The record is already hourly, so no resampling was required.

This procedure removes only a small number of clearly erroneous points and retains the upper tail that is needed for the extreme value analysis. The resulting timelines are shown below.

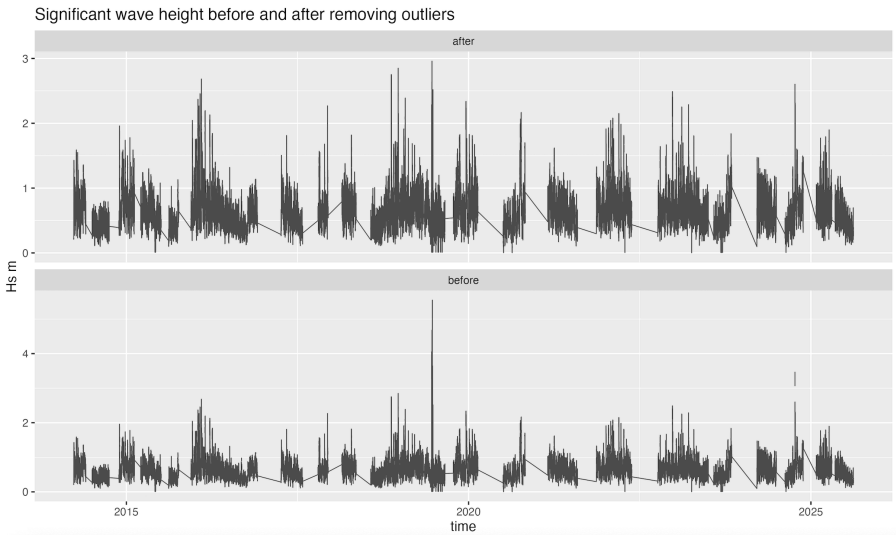

Figure F.4: Significant wave height H_s before and after cleaning.

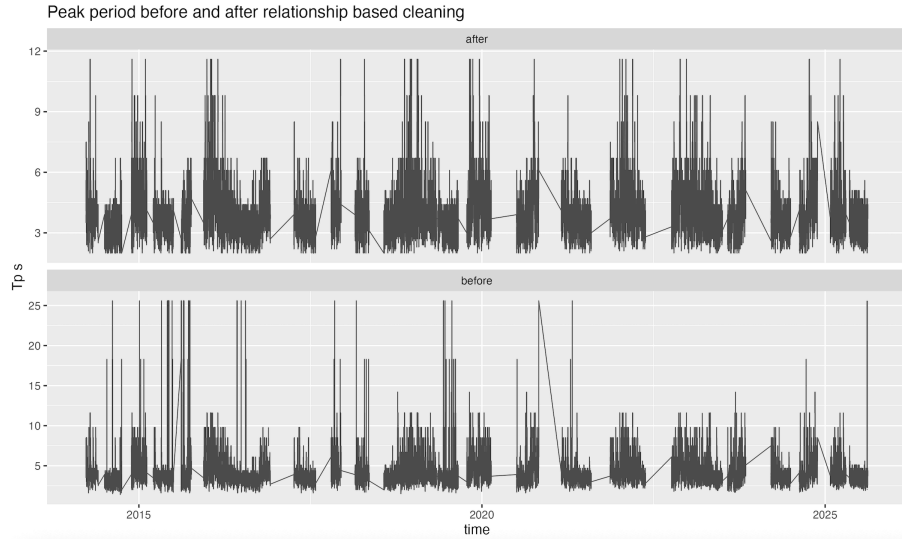

Figure F.5: Peak period T_p before and after cleaning.

EVA ADCP data

An important step in the POT method is the selection of a suitable threshold. The threshold must be sufficiently high to focus on extreme events, but not so high that the number of available peaks becomes too small for reliable statistical analysis. Candidate thresholds are evaluated using three diagnostic indicators:

1. **Chi-square statistic:** evaluates how well the exceedances follow a Poisson process, with lower values representing a better fit.
2. **p-value:** indicates whether the fit is statistically significant. A p-value greater than 0.05 suggests that the Poisson assumption is reasonable.
3. **Number of peaks:** represents the count of independent exceedances above the threshold. A sufficient number of peaks is required for robust estimation, but too many peaks may dilute the focus on truly extreme events.

In Bakker et al, the ERA5 dataset was used and yielded a threshold of 2.70 m. Figure F.6 illustrates the exceedances obtained from that dataset, which suggested that 2.70 m was an appropriate compromise between capturing extreme events and maintaining a sufficient number of peaks.

However, when applying the same 2.70 m threshold to the local ADCP dataset (Figure F.7), the results are not consistent with the ERA5-based analysis. Only a very small number of exceedances are detected locally, which does not align with the expected statistical behavior of extreme waves. This discrepancy highlights that the previously selected threshold does not reflect the characteristics of the local conditions. To address this, the threshold range was expanded and re-evaluated between 2.0 m and 2.8 m. This broader assessment ensures that the frequency and distribution of extreme wave events in the local dataset are properly captured, leading to a more robust and representative threshold selection.

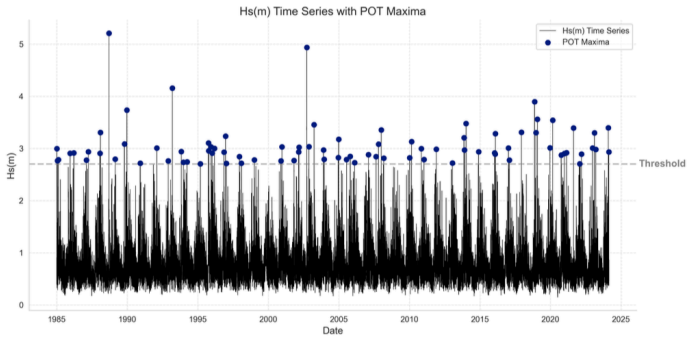

Figure F.6: Hs(m) Time Series with POT Maxima using ERA5 data at a Threshold of 2.70 m and a De-clustering Time of 4 days.

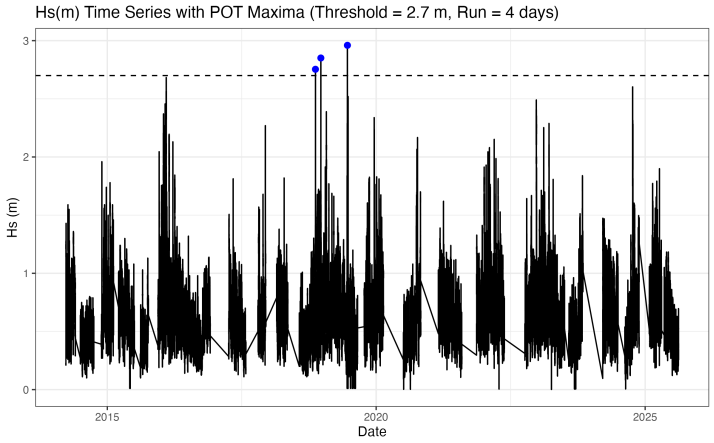

Figure F.7: Hs(m) Time Series with POT Maxima using local ADCP data at a Threshold of 2.70 m and a De-clustering Time of 4 days. The results show that the threshold of 2.70 m is not representative of the local conditions.

Figure F.8 shows the results of the diagnostic tests conducted over the range 2.0–2.8 m. The chi-square statistic (solid black line) and scaled p-value (dashed red line) are plotted against the threshold. The figure indicate that thresholds around 2.55 m and 2.60 m provide the strongest statistical support, with very low chi-square values and high p-values, while still retaining a sufficient number of peaks for robust estimation.

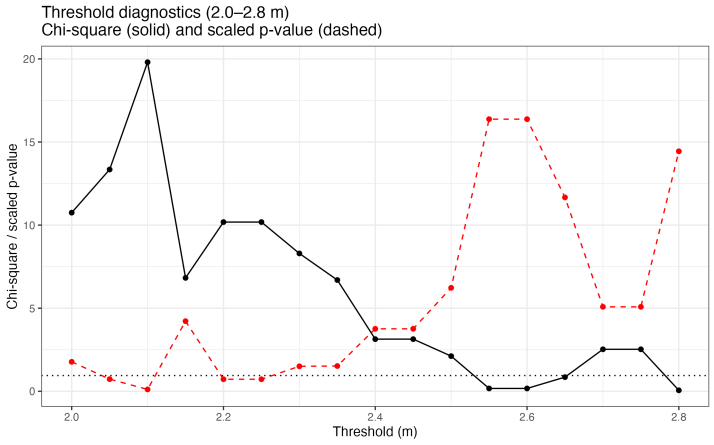

Figure F.8: Threshold diagnostics for POT analysis on the local ADCP dataset. The chi-square statistic (solid black line) and scaled p-value (dashed red line) are evaluated for thresholds between 2.0 m and 2.8 m.

Table F.1 summarizes the chi-square statistic, p-value and the corresponding number of peaks for thresholds in this range. Based on these results, a threshold of 2.55 m is selected, as it provides the best balance between statistical fit (lowest chi-square, highest p-value) and a sufficient number of exceedances for extreme value modeling.

Table F.1: Number of peaks, chi-square statistic and p-value for thresholds in the range 2.0–2.8 m based on the local dataset.

Threshold (m)	Chi-square	p-value	Number of Peaks
2.45	3.14	0.208	8
2.50	2.12	0.347	6
2.55	**0.17**	**0.918**	**5**
2.60	0.17	0.918	5
2.65	0.85	0.653	4
2.70	2.53	0.283	3
2.75	2.53	0.283	3
2.80	0.06	0.809	2

Once the threshold was selected, a declustering procedure was applied to ensure that the exceedances represent distinct and independent storm events. Without this step, multiple hourly observations from the same storm system could artificially inflate the number of extremes, leading to biased return level estimates. A declustering interval of four days was chosen, consistent with the methodology applied in the previous study. This means that any exceedance occurring within four days of a previous peak is treated as part of the same storm, with only the maximum retained.

Figure F.9 shows the resulting time series of significant wave height together with the declustered POT maxima above the selected threshold of 2.55 m. The plot demonstrates that a small but sufficient number of independent extreme events remain in the record, providing a robust basis for the subsequent extreme value analysis.

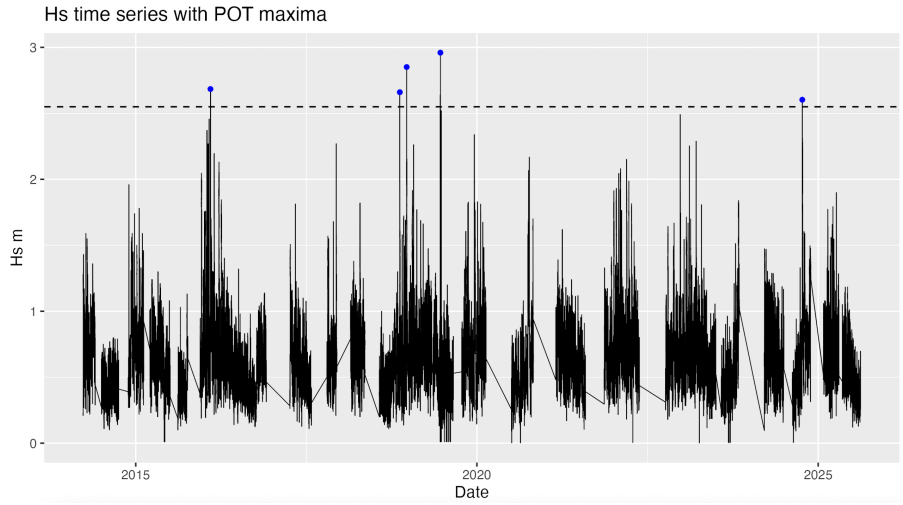

Figure F.9: Hs(m) Time Series with POT Maxima using local ADCP data at the selected threshold of 2.55 m and a de-clustering time of 4 days.

Figure F.10 highlights the annual frequency of extreme wave events exceeding the selected threshold of 2.55 m. The Probability Mass Function (PMF) shows that the majority of years experience zero to one independent extreme event, with very few years recording two or more events. This contrasts sharply with the outcomes of last year's analysis, where the 2.70 m threshold in the ERA5 dataset suggested a higher rate of exceedances. The discrepancy confirms that the ERA5 based threshold was not representative of the local conditions.

The Cumulative Distribution Function (CDF) further supports this conclusion. For the local dataset,

more than sixty percent of years show no extreme events above 2.55 m, while nearly tenty percent of years record one or fewer events. This distribution is consistent with the rarity of tropical storms and hurricanes in the region, which are the primary drivers of such extremes. In contrast, the ERA5 based analysis indicated more frequent exceedances at the higher 2.70 m threshold, which is inconsistent with the observed local record.

These results suggest that last year's threshold selection was more strongly guided by the ERA5 reanalysis, which reflects regional-scale conditions rather than site-specific dynamics. The extended twelve-year ADCP record offers a sharper picture of the local environment, indicating that extreme wave events are relatively rare and exhibit considerable year-to-year variability. By showing that the site experiences fewer exceedances than previously assumed, this analysis supports the adoption of a lower threshold while also highlighting the value of combining long-term reanalysis for context with direct observations for local design conditions.

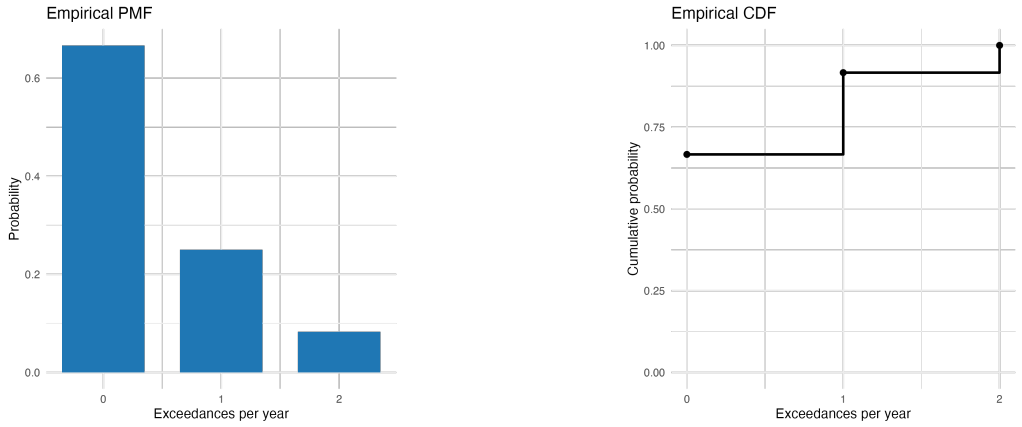

(a) Empirical PMF (b) Empirical CDF

Figure F.10: Empirical Probability Mass Function (PMF) and Cumulative Distribution Function (CDF) of exceedances per year based on the local ADCP dataset with a threshold of 2.55 m.

To verify that the frequency of exceedances can be described by a Poisson process, the annual counts of independent events above the 2.55 m threshold were compared to a fitted Poisson distribution. Figure F.11 shows the empirical cumulative distribution of exceedance counts alongside the fitted Poisson CDF. The close alignment of the two curves demonstrates that the Poisson model accurately captures the rarity and randomness of extreme wave events at the site.

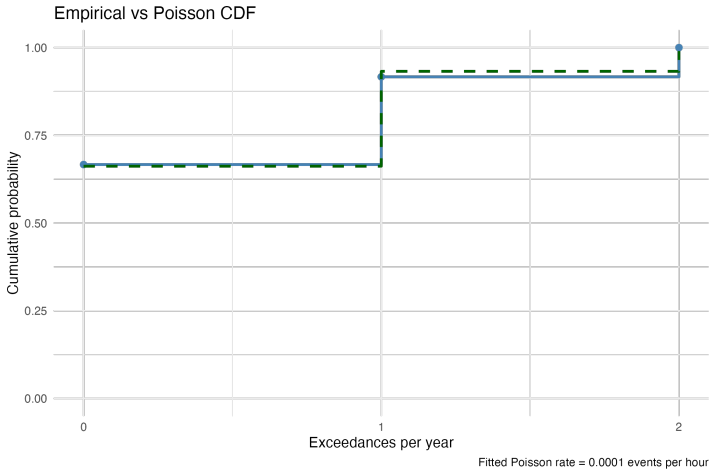

Figure F.11: Empirical CDF of annual exceedance counts above 2.55 m compared with the fitted Poisson CDF using a four day declustering interval. The close agreement supports the Poisson process assumption for event counts.

Return levels ADCP

Threshold diagnostics identified $u = 2.55$ m as the statistically optimal threshold for the POT analysis. However, at this level only five declustered exceedances remain, which makes GPD fitting unstable. To improve robustness while staying within the diagnostically supported range, the return level estimation is therefore carried out at a slightly lower working threshold of $u = 2.50$ m. This yields six independent peaks and provides a more stable fit. Sensitivity tests at $u = 2.45$ m and $u = 2.55$ m confirm that the results are not significantly affected by this adjustment.

Once the threshold was chosen, independent extreme events were selected using the four day separation rule so that closely spaced storms were not double counted. The peaks above this threshold were then modeled using the GPD, which is the standard method for extreme value analysis. The GPD provides a flexible statistical description of the upper tail and has two parameters: the scale parameter σ_u, which controls the spread of exceedances above the threshold and the shape parameter ξ, which determines whether the distribution has a finite bound or a heavy tail.

Suppose M independent exceedances are identified in a record of N observation hours, of which n_{th} lie above the threshold. If N_T denotes the number of observation hours in T years, the T year return level RL_T is given by

$$RL_T \;=\; u \;+\; \frac{\sigma_u}{\xi}\left[\left(\frac{n_{th}\cdot N_T}{M}\right)^{\xi} - 1\right].$$

In the special case where $\xi \to 0$, the GPD approaches an exponential distribution and the expression simplifies to

$$RL_T \;=\; u \;+\; \sigma_u \log\!\left(\frac{n_{th}\cdot N_T}{M}\right).$$

Diagnostic checks showed that the GPD provided a good fit to the highest values in the dataset. Since this POT approach models both how often and how large extremes are, it allows estimation of design return levels such as 10 year or 20 year waves even though the observational record itself is shorter than those return periods. However, the further we extrapolate beyond the available record, the larger the statistical uncertainty becomes. To reflect this, we present not only the point estimates but also two sided 95% confidence intervals around them.

Figure F.12 shows the histogram of exceedances with the fitted GPD probability density function (PDF) on the left and the exceedance probability plot on the right. Both plots demonstrate that the GPD provides an adequate description of the tail behaviour of the local dataset.

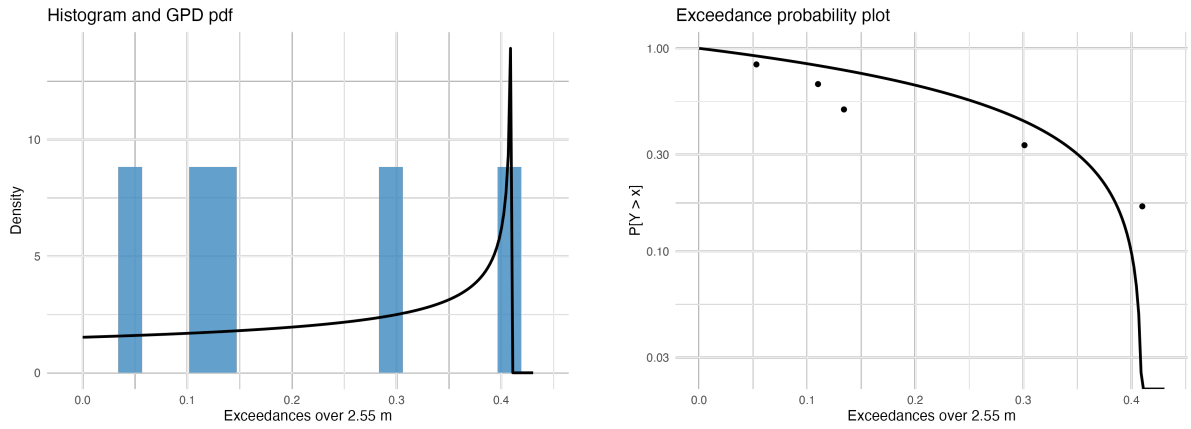

(a) Histogram with GPD PDF

(b) Exceedance probability plot

Figure F.12: Fitted GPD to local ADCP exceedances above 2.50 m. Left: histogram of exceedances with fitted PDF. Right: exceedance probability plot.

As a result of the fitted shape parameter being negative ($\xi < 0$), a finite upper bound to the distribution can be expected. Across thresholds from 2.45 m to 2.55 m, the implied endpoint is consistently close to $H_s \approx 2.96$ m. This result is identical to the values for the 10-year and 20-year return levels, both also at 2.96 m, with confidence intervals of [2.68, 2.96] m. The stability across thresholds is illustrated in Figure F.13.

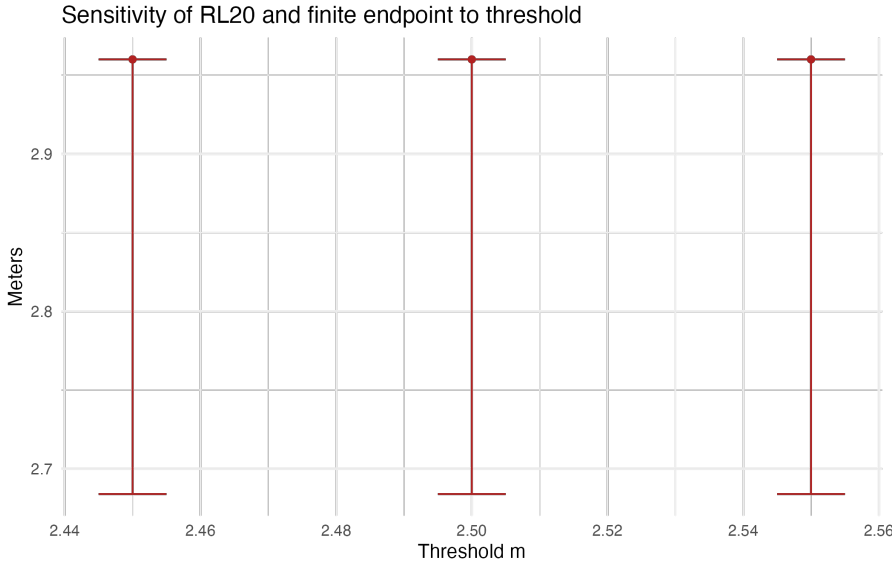

Figure F.13: Sensitivity of 20-year return level and finite upper endpoint across thresholds 2.45–2.55 m. The results confirm that the maximum significant wave height is bounded near 2.96 m.

These results show that the extreme wave conditions at the site are bounded at around 3.0 m. Since the fitted GPD shape parameter is negative, both the 10-year and 20-year return levels converge to approximately 2.96 m and the return level curve flattens at this ceiling (Figure F.14). This outcome differs from previous ERA5-based analysis. Which, using a threshold of 2.70 m and scaling to the local record, produced a 20-year design value of 3.40 m. The two perspectives are complementary: ERA5 provides a conservative regional upper bound, while the twelve-year site-specific ADCP record indicates a locally bounded extreme. Together they bracket the range of plausible design values, with the ADCP-based estimate forming the primary basis for fish cage design and ERA5 serving as a sensitivity check.

The negative shape parameter implies that the fitted distribution has a finite upper limit for wave height. In physical terms, such bounded behavior can occur when depth-limited breaking restricts wave growth, as shallow-water effects truncate the upper tail of the distribution. According to Mendez et al. [Mendez et al., 2004], this transformation becomes significant when the ratio of root-mean-square wave height to water depth (H_{rms}/h) exceeds approximately 0.2.

At the Sisal site, the effective water depth is about 10 m and the observed ratio H_{rms}/h is around 0.1, which is below this threshold. This suggests that the bounded tail observed in the statistical fit is not primarily a result of depth-induced wave breaking, but rather a statistical feature arising from the limited length of the available record.

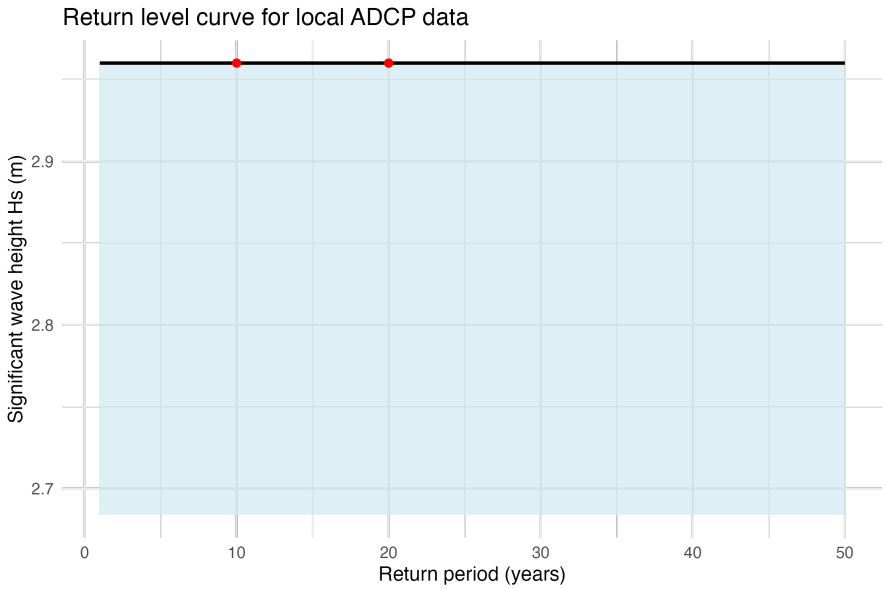

Figure F.14: Return level plot for the local ADCP dataset using a working threshold of 2.50 m. The fitted GPD has a negative shape parameter, leading to a finite upper bound near 2.96 m. Consequently, the 10-year and 20-year return levels coincide and the curve converges to this maximum value.

Wave Height and Period ADCP

This subsection examines the relationship between H_s and spectral T_p to understand how these parameters interact under the wave conditions relevant for offshore fish cage design.

In [Bakker et al., 2024], ERA5 reanalysis data were compared with a ten-year local ADCP record. The ERA5 dataset showed a smooth and continuous relationship between H_s and T_p, with a strong correlation ($R^2 \approx 0.75$), making it appear well suited for regression and design applications. In contrast, the local ADCP record exhibited distinct horizontal banding in T_p, a known effect of the instrument's spectral frequency resolution, which led to a weaker correlation. Consequently, ERA5 was used in last year's design estimates.

In the present study, the full twelve-year ADCP record (2014–2025) is reprocessed using only the T_p as the period variable. This parameter represents the dominant energy component in the measured spectrum and is the most relevant for characterizing structural loads on floating systems. Although the discrete spectral bins of the ADCP produce visible horizontal bands in the scatter, the extended record offers a more statistically robust and locally representative dataset for regression analysis.

Figure F.15 compares the previous ERA5-based results from [Bakker et al., 2024] with the updated twelve-year ADCP record. While ERA5 continues to exhibit a smoother and more correlated relationship, the locally measured ADCP data better capture the site-specific storm conditions that dominate the Sisal region.

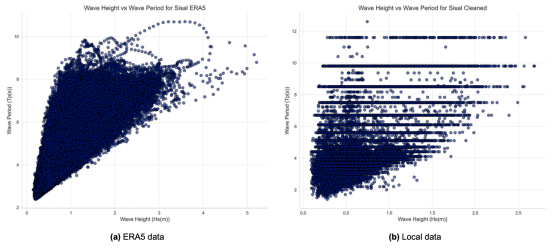

(a) ERA5 vs. 10-year ADCP (Bakker et al., 2024)

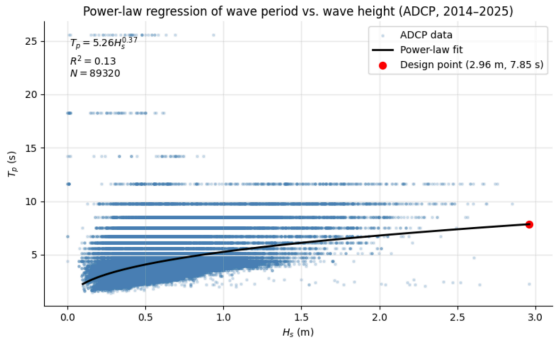

(b) Local ADCP (2014–2025) using T_p

Figure F.15: Comparison of H_s and T_p relationships. The ERA5 dataset (a) shows a smoother and more continuous trend, while the twelve-year ADCP record (b) captures the locally generated, short-period storm waves that dominate the site.

To estimate the wave period associated with the design wave height, a power-law regression was applied between H_s and T_p, following Equation F.1.

$$T_p = a\, H_s^b \tag{F.1}$$

Here, a and b are empirically derived coefficients: a represents a scaling factor, while b determines how strongly T_p increases with H_s. This relationship provides an efficient way to estimate the representative period for design conditions corresponding to the 20-year return height.

The results of the regression for the twelve-year ADCP record are shown in Figure F.16. The fitted parameters are $a = 5.26$, $b = 0.37$ and $R^2 = 0.13$, based on $N = 89,320$ paired observations. At the 20-year design wave height of $H_s = 2.96$ m, the corresponding design spectral peak period is $T_p = 7.85$ s. Although the correlation is moderate due to the discrete period resolution of the ADCP, the fitted trend provides a realistic, locally grounded representation of the wave conditions relevant to the site.

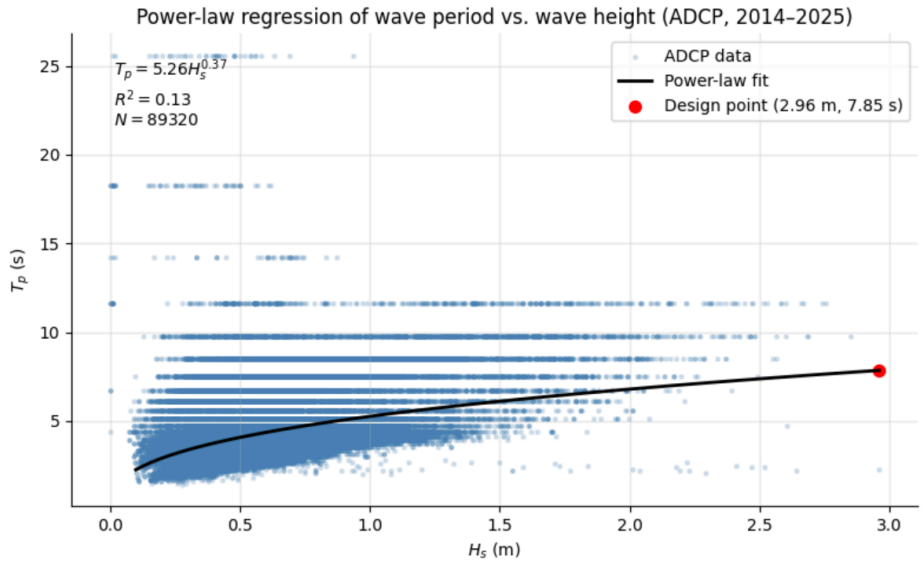

Figure F.16: Power-law regression of T_p versus H_s for the twelve-year ADCP dataset (2014–2025). The black line represents the fitted power-law trend, and the red marker indicates the 20-year design point ($H_s = 2.96$ m, $T_p = 7.85$ s).

The regression confirms that higher wave heights are generally associated with longer periods, but the relatively low R^2 reflects the dominance of short, storm-driven waves rather than long-period swell.

This supports the interpretation that the Sisal site is primarily influenced by locally generated wind seas, rather than the swell conditions captured by ERA5 reanalysis.

Conclusion on Waves

The extended twelve-year ADCP record indicates that extreme wave conditions at the Sisal site are both rare and bounded, with return levels converging to a maximum significant wave height of approximately 3.0 m and associated peak periods of about 7.8 s. In comparison, the ERA5-based analysis by Bakker et al., 2024 produced longer periods ($T_p \approx 8.0$–9.0 s) and a higher 20-year design height of 3.4 m. Taken together, these results highlight complementary perspectives: ERA5 provides a conservative regional upper bound, while the locally measured ADCP data offer a more representative description of site-specific storm conditions. For design purposes, the ADCP-based values are preferred, as they reflect the shorter, locally generated wave climate that the offshore fish cage will experience.

F.2.3. Currents

Currents are another key environmental loading factor for offshore fish cages. Bakker et al. [Bakker et al., 2024] analyzed a ten-year ADCP record but considered it too short for a reliable EVA. Instead, they used the 95th percentile of the measured current speeds as a practical indicator of extreme conditions. This provided a simple and robust measure, but it did not allow extrapolation to design return periods such as 10 or 20 years.

Data analysis

The current data was also obtained from an ADCP, which provides profiles of water velocity at multiple depth bins throughout the water column. Each data file contains time-stamped records of the horizontal and vertical velocity components:

- **U component:** East–West velocity, where positive values represent flow towards the East and negative values towards the West.
- **V component:** North–South velocity, with positive values indicating flow towards the North and negative values towards the South.
- **W component:** Vertical velocity, typically much smaller and less relevant for structural loading but included for completeness.

The velocity components are stored as matrices with dimensions of *time* × *depth*, allowing the construction of a vertical current profile for each hourly timestamp. Depth bins in the dataset range from approximately -9.6 m to -5.1 m, corresponding to measurement levels above the seafloor. In addition to the raw velocity components, the data files include derived quantities such as the mean current speed (`mcspd`) and mean current direction (`mcdir`), as well as measurement error estimates (`cerr`).

For the present analysis, the horizontal velocity magnitude is calculated from the u and v components using equation F.2.

$$\text{speed} = \sqrt{u_c^2 + v_c^2}, \tag{F.2}$$

Providing the total horizontal current speed at each depth and time step. This derived current speed is used in subsequent analyses of percentile values and extreme events.

Data Cleaning

Before any interpolation or extrapolation, the ADCP currents were quality controlled to remove outliers. A two-pass thresholding procedure was applied to the horizontal velocity components u and v. For each component, observations with an absolute deviation larger than 4σ from the component mean were flagged as outliers and removed, where σ denotes the sample standard deviation computed over the selected period. The means and standard deviations were recomputed after the first pass and the filter was applied a second time. This procedure preserves the bulk of the signal while eliminating isolated spikes that could dominate the color scale and distort subsequent interpolation. Only directly measured depth bins are retained at this stage, with no vertical interpolation or surface extrapolation.

Figure F.17 presents the cleaned data for September to December 2024. The panels display the ADCP's discrete depth bins from approximately $-1.1\,\mathrm{m}$ down to $-10\,\mathrm{m}$. Alternating red and blue bands indicate reversals in the horizontal flow, consistent with tidal modulation. Gaps between depth bins

remain visible because no depth filling is performed in this step; this highlights the information content of the measurements observed directly.

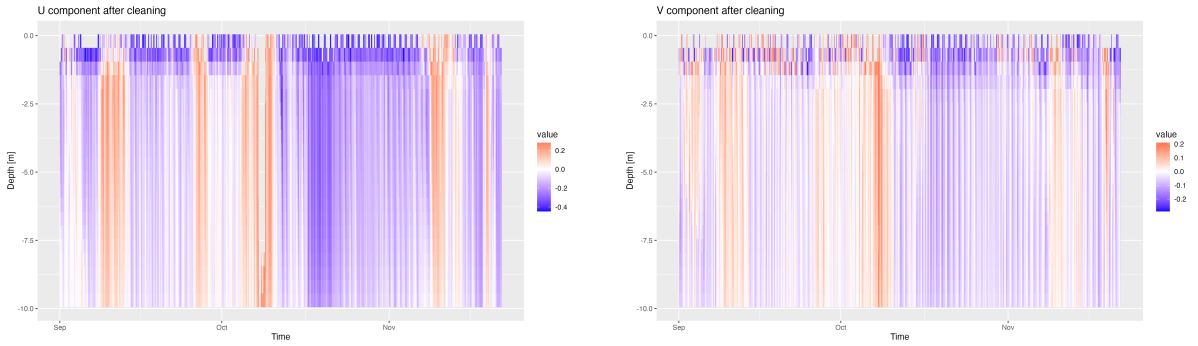

(a) U component — measured bins after outlier removal.

(b) V component — measured bins after outlier removal.

Figure F.17: Cleaned ADCP currents for Sep–Dec 2024. Panels show only directly measured depth bins, with no vertical interpolation or shallow-water extrapolation.

Interpolation and Extrapolation

The ADCP does not provide direct measurements in the upper water column shallower than approximately $-1.1\,\mathrm{m}$. To obtain continuous profiles, the measured velocities were interpolated between depth bins and extrapolated upwards to $-0.5\,\mathrm{m}$ using polynomial regression. A third–degree polynomial was fitted at each time step to the available depth bins for both horizontal components, which allows extension of the velocity field into the near–surface layer. This procedure follows the method used in previous analyzes of the same dataset and produces fields that are consistent with the measured structure below.

Figure F.18 presents the interpolated and extrapolated data for September to December 2024. The U and V components now show continuous velocity fields from the deepest measured bins up to the extrapolated surface layer, highlighting coherent banded patterns associated with tidal and tidal variability. The smoothing effect of the polynomial fit reduces the small–scale stripe patterns visible in the cleaned data and emphasizes the dominant temporal and vertical structures.

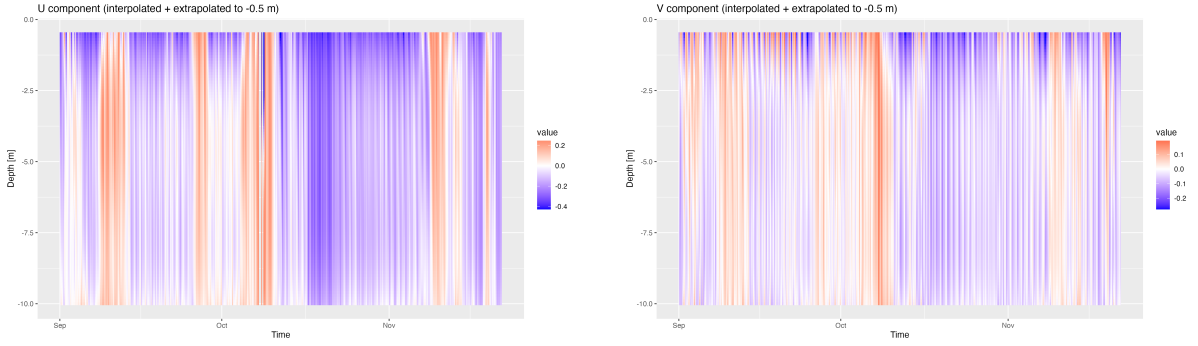

(a) U component — interpolated and extrapolated to $-0.5\,\mathrm{m}$.

(b) V component — interpolated and extrapolated to $-0.5\,\mathrm{m}$.

Figure F.18: Interpolated and extrapolated ADCP currents for Sep–Dec 2024. Velocities are shown as continuous fields from $-10\,\mathrm{m}$ to $-0.5\,\mathrm{m}$.

Current Speed Distribution

Figure F.19 compares the depth–speed distributions obtained in this study with those presented by [Bakker et al., 2024]. Both studies show that the strongest currents occur close to the surface, with current speed decreasing with depth. The general structure of the distributions is similar, although some differences are visible. In particular, the Bakker et al. data suggests the occurrence of speeds approaching $1\,\mathrm{m/s}$ at $-1.1\,\mathrm{m}$, while such extreme values do not appear in the present dataset.

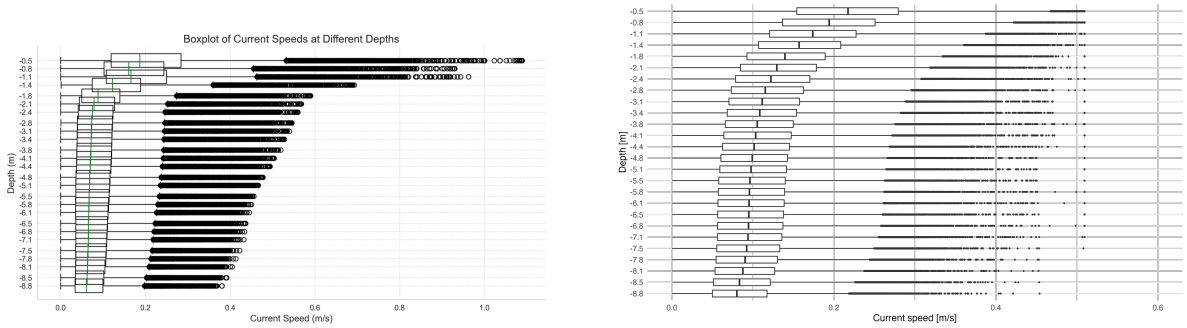

(a) [Bakker et al., 2024].

(b) Present study.

Figure F.19: Boxplots of current speed distribution by depth.

To further investigate this discrepancy, the uncleaned data at -1.1 m was extracted and analysed separately. Figure F.20a shows the histogram of current speeds at this depth, based on all available measurements. The maximum observed speed is 0.789 m/s and the 99.9th percentile equals 0.511 m/s. This confirms that the dataset used here does not include values near 1 m/s at -1.1 m, in contrast to [Bakker et al., 2024]. The discrepancy may originate from differences in cleaning methods, time period considered, or sensor calibration.

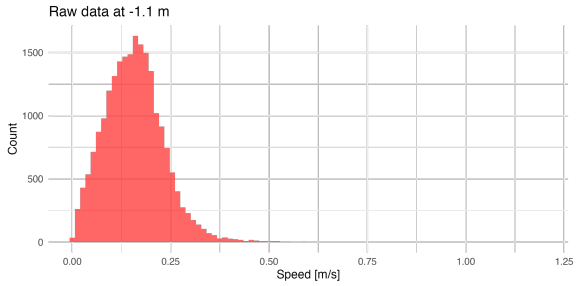

(a) Histogram of raw current speeds at -1.1 m.

Finally, figure F.21 presents the cleaned current speed distribution by depth, based on the full available dataset. The distribution shows that current speeds tend to decrease with depth, with the strongest and most variable flows observed near the surface. Importantly, the data demonstrate that currents between 0.2 and 0.4 m/s occur frequently across multiple depth layers, particularly in the upper 2–3 m. Such flow intensities are of practical relevance for aquaculture operations.

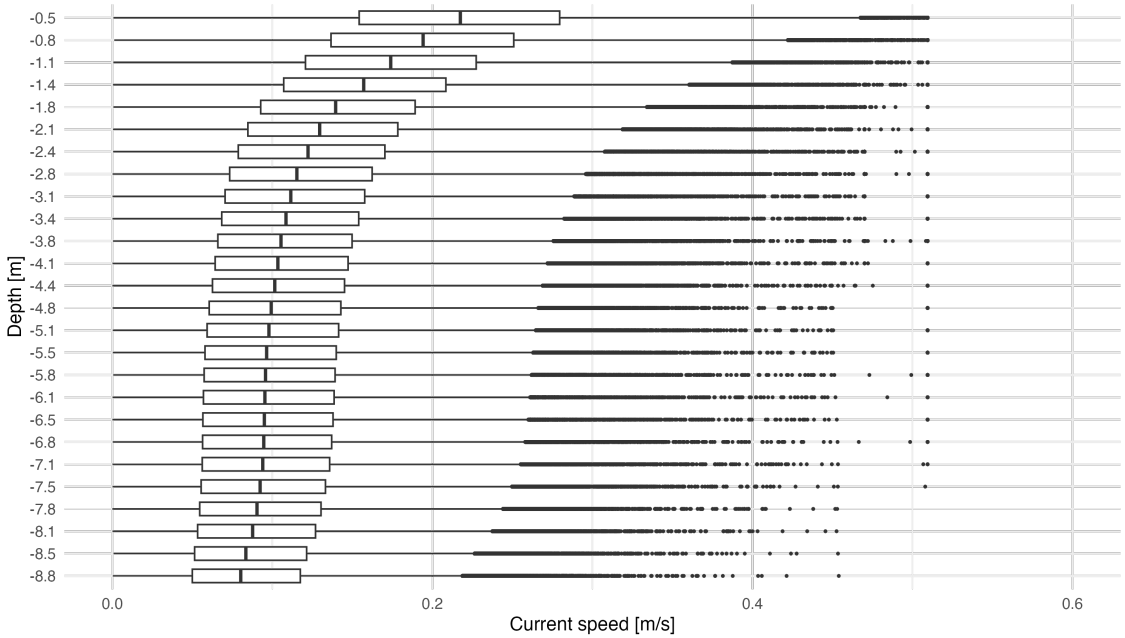

Figure F.21: Current speed distribution by depth based on the full cleaned dataset (all available years). Outliers are shown; x–axis limited to $0.5\,\mathrm{m/s}$.

Design Current Speed (95th Percentile)

To establish a representative design current speed, the 95th percentile of the current speed distribution was calculated for each measured depth bin. This approach captures the upper range of regularly occurring conditions, while filtering out rare extremes that may arise from instrument noise or infrequent events. The 95th percentile is widely used in aquaculture design guidelines as it provides a robust balance between structural safety and cost efficiency.

Figure F.22 presents the 95th percentile current speed profile across the water column. The results show that near-surface depths (-0.5 to $-1.5\,\mathrm{m}$) experience the highest design speeds, with values close to $0.4\,\mathrm{m/s}$. With increasing depth, speeds gradually decrease, stabilising around $0.2\,\mathrm{m/s}$ below $-6\,\mathrm{m}$. This vertical trend reflects the influence of surface forcing and turbulence in the upper layers, which is progressively damped with depth. The profile indicates that fish cages positioned closer to the surface are regularly exposed to stronger and more variable currents, emphasising the need for robust structural design in the upper part of the water column. At greater depths, where cages and mooring systems may also be located, the design loads are lower and more uniform.

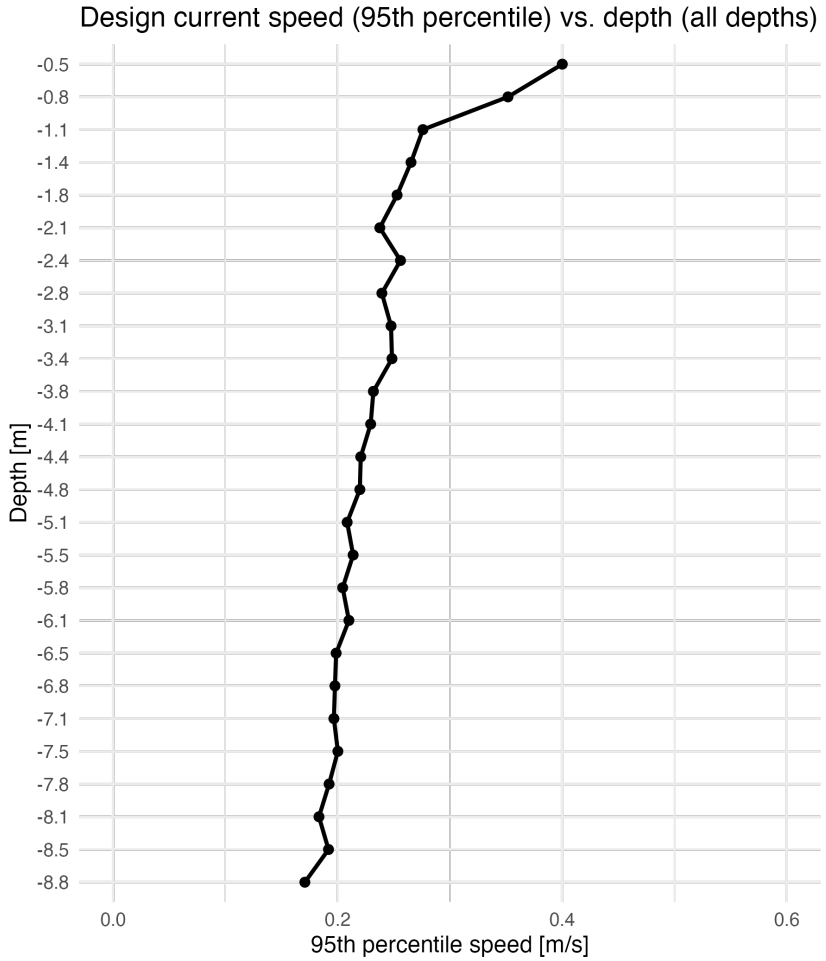

Figure F.22: Design current speed profile based on the 95th percentile of current speed at each measured depth (all available data).

When compared with the findings of [Bakker et al., 2024], the present results follow the same overall trend of decreasing current speeds with depth. Both studies show higher design speeds in the upper meter of the water column and more stable values at depth. However, the current dataset produces slightly lower near-surface values (peaking just below 0.45 m/s) compared to Bakker et al., where the 95th percentile approached 0.5 m/s. Below -6 m, both profiles converge to similar values around 0.2 m/s, underscoring the robustness of the observed vertical distribution of design currents.

Conclusion on Currents

The extended twelve-year ADCP record confirms that surface layers experience the strongest and most variable currents, with design speeds close to 0.4-0.45 m/s in the upper meter, decreasing to stable values near 0.2 m/s below 6 m. These results are consistent with earlier findings but provide greater robustness through the longer dataset and improved cleaning. The comparison indicates that extreme near-surface values approaching 1 m/s reported previously are not supported in the present record, suggesting that earlier differences may reflect methodological or calibration issues. Overall, the analysis shows that aquaculture must withstand larger current loading, while deeper structures are subject to lower and more uniform current forces.

F.2.4. The Relationship Between Wave and Current

Waves and currents interact to shape the flow conditions around aquaculture and their relative direction strongly influences the resulting loads. Aligned flows can increase inline drag, while cross-flow may produce large lateral stresses on moorings and cage structures. Building on the work of Bakker et al., 2024, who analyzed a 10-year record, the dataset is extended to 12 years to test the robustness of

earlier findings. In addition to directional statistics, attention is given to joint extremes where both wave height and current speed exceed their 95th percentiles. Specific time-stamped events with the highest combined stress are also highlighted. These cases are rare but represent critical design conditions, offering valuable insight into the most demanding environmental forces on aquaculture structures.

Wave direction

The wave roses based on the extended 12-year dataset in figure F.23 show a distribution that is very similar to the local measurements presented by Bakker et al. Both the full dataset and the 95th-percentile extremes confirm that waves predominantly come from the northeast sector. The small differences between the two studies can be explained by the inclusion of two additional years of data in the present study, which increases robustness and captures a wider range of storm events.

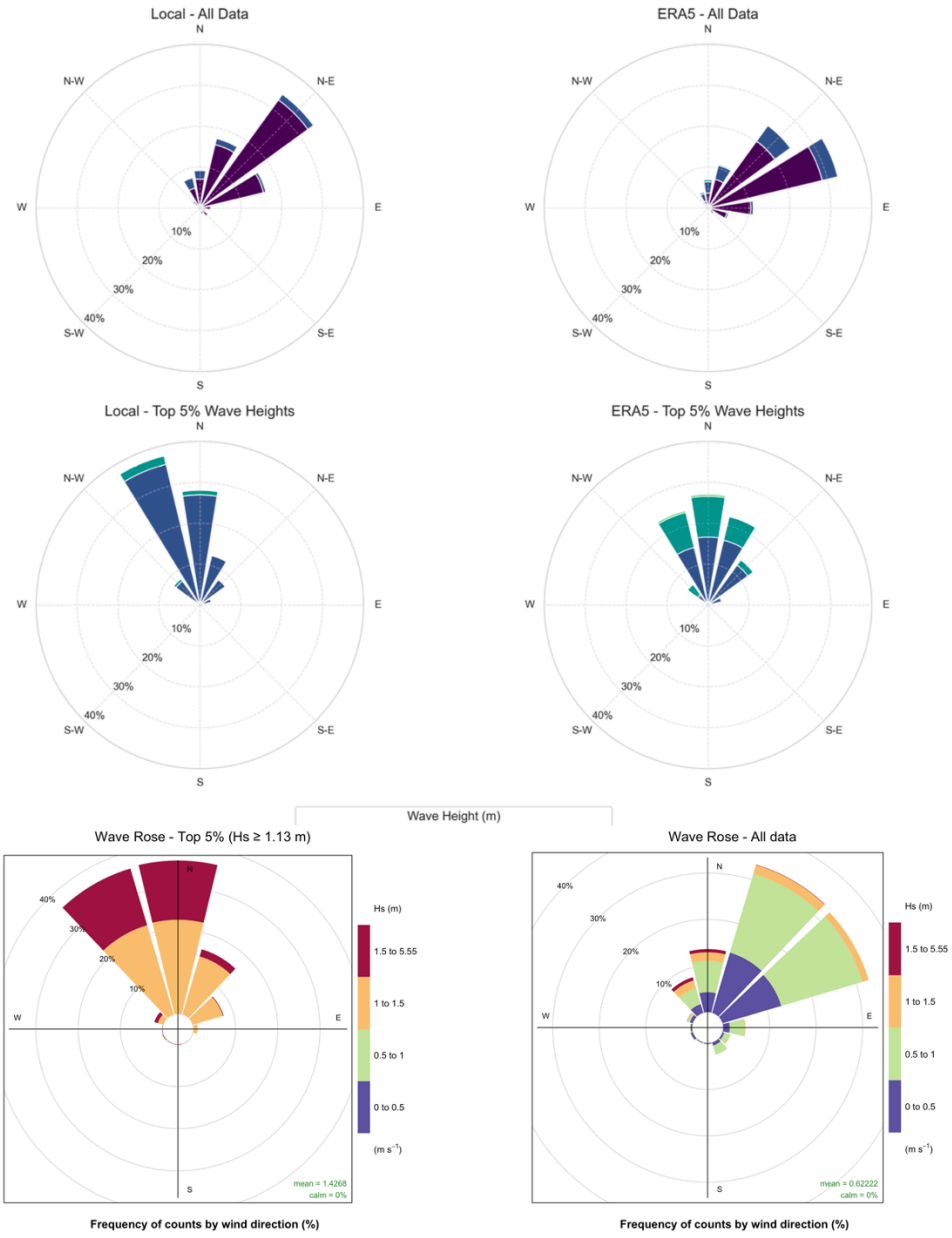

Figure F.23: Comparison of wave roses from [Bakker et al., 2024] (top) and the extended 12-year dataset (bottom).

Current direction

The current roses in figure F.24 are based on the extended dataset. They show a distribution that is consistent with the results of Bakker et al., 2024. Both the full dataset and the 95th-percentile extremes confirm that the currents are relatively stable in their direction, flowing predominantly from east to west throughout the water column. Minor variations with depth are present, but the overall stability of the current regime is clear. The similarity to the previous study supports the robustness of the extended analysis.

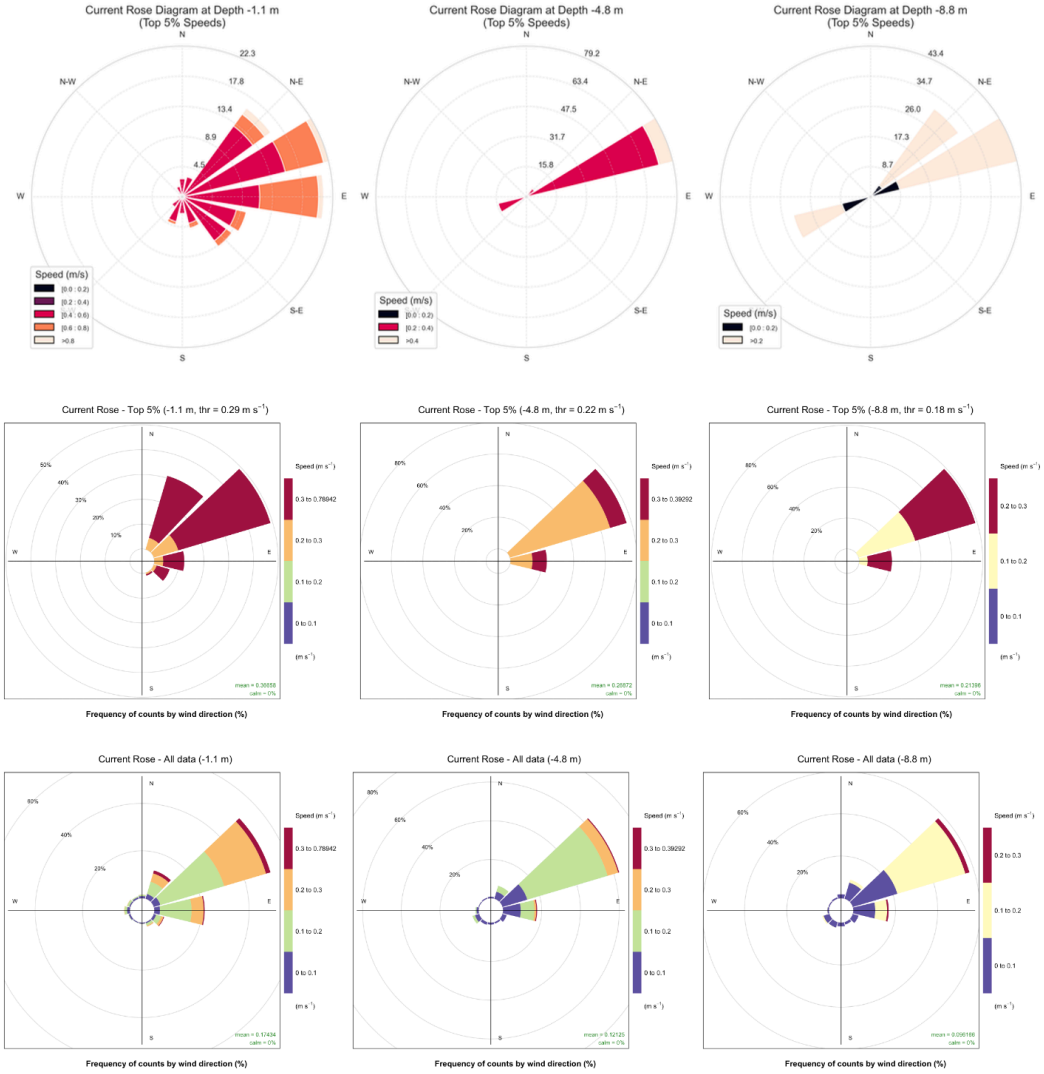

Figure F.24: Comparison of current roses from [Bakker et al., 2024] (top row) with the extended 12-year dataset (middle and bottom rows).

Wave and Current Interaction

Bakker et al. analyzed the wave and current roses by focusing on the directions associated with the 95th percentile values. Their approach provided a useful overview of dominant extreme directions but did not consider the specific time events when large waves and strong currents occurred simultaneously. In contrast, the present analysis places emphasis on identifying real occurrences of joint extremes, such as during storms, where both wave height and current speed were high at the same time. This event-based perspective highlights rare but critical situations that represent the actual maximum loading conditions experienced by the aquaculture.

Table F.2: Directional categorisation of wave-current combinations for all hourly cases by depth.

Depth (m)	Aligned	Cross	Opposing
-8.8	823	637	84
-4.8	821	650	52
-1.1	818	547	30

Table F.3: Directional categorisation after the joint 95th percentile filter ($H_s \geq Q_{95}$ and $U_c \geq Q_{95}$).

Depth (m)	Aligned	Cross	Opposing
-8.8	0	61	0
-4.8	0	66	0
-1.1	0	37	0

For each hour and depth, a relative stress index S is calculated using the quadratic drag law in equation F.3

$$F_d = \frac{1}{2}\rho C_d A v^2 \tag{F.3}$$

where u_r is the resultant flow speed, obtained by combining the wave orbital velocity vectors. Which are estimated from H_s and T_p using linear wave theory with depth decay and the measured current velocity. Due to the use of constants for seawater density (ρ), drag coefficient (C_d) and reference area (A), F_d should not be interpreted as an absolute force. Instead, it acts as a relative index proportional to V^2, ensuring consistent comparison and ranking of events. To prevent over-representation of single storms, declustering is applied so that only independent joint-extreme hours are considered.[1]

Figure F.25 summarizes the maximum and mean F_d per depth for these critical hours. A table of the op three highest-stress moments per depth, including wave and current directions and their mutual angle, is provided in Table F.4.

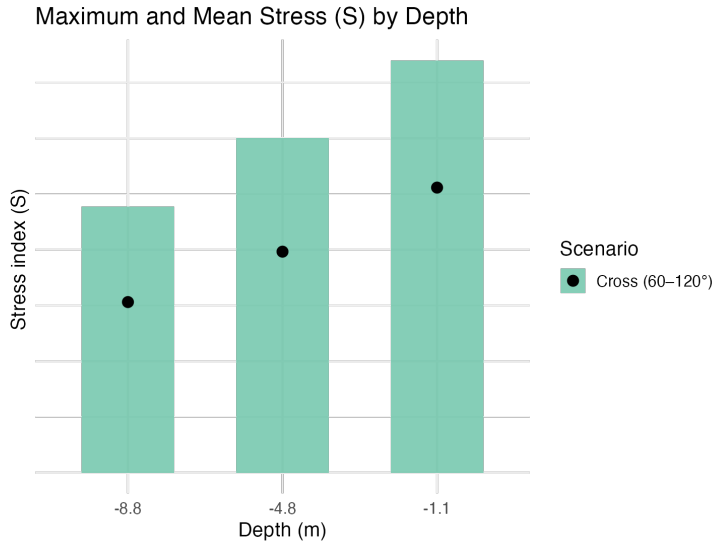

Figure F.25: Maximum ($S_{\max}$; bars) and mean ($\overline{S}$; points) stress index by depth for declustered joint-extreme hours. Counts are small, reflecting the rarity of such events; loads are largest near the surface.

[1]A typical value of seawater density is $\rho \approx 1025$ kg m^{-3} [National Oceanographic and Atmospheric Administration (NOAA), NESDIS, 2019]. The parameters C_d and A only rescale the magnitude of F_d and therefore do not affect the ranking of events.

Table F.4: Top three highest-stress joint-extreme events per depth, including wave height H_s, current speed U_c and the angle.

Depth (m)	Hs (m)	Uc (m/s)	Wave from (°)	Current from (°)	Angle (°)
-8.8	2.09	0.28	338	75	97
-8.8	1.98	0.25	354	83	89
-8.8	2.00	0.25	350	81	90
-4.8	2.09	0.37	338	74	96
-4.8	2.04	0.35	350	80	90
-4.8	2.00	0.32	350	80	89
-1.1	2.04	0.43	350	61	71
-1.1	2.03	0.31	355	68	73
-1.1	2.01	0.43	350	59	69

Conclusion on Wave–Current Interaction

The extended analysis confirms that waves at the site predominantly arrive from the northeast, while currents are consistently oriented east–west. This directional misalignment means that extreme wave and current conditions often occur at near-perpendicular angles, producing significant lateral stresses on aquaculture structures. The joint-extreme analysis shows that such high-loading cases are rare but critical, with the largest relative stresses concentrated near the surface. These findings highlight the importance of accounting for cross-flow loading scenarios in design, rather than assuming alignment of waves and currents. By focusing on real joint events rather than percentile directions alone, the present study provides a more realistic basis for assessing the most demanding hydrodynamic forces acting on offshore aquaculture systems.

F.3. RBF Data

F.3.1. Introduction

The previous EVA presented in Section F.2.2 was based on a 12-year ADCP record, which provided a reliable characterization of local nearshore conditions but was limited in temporal coverage. To extend the statistical robustness of the analysis, this chapter employs a 47-year Radial Basis Function (RBF)-downscaled ERA5 dataset provided by José Antolínez.

The RBF dataset was generated through a statistical relationship between offshore ERA5 wave parameters and locally measured ADCP data. Through this bias-corrected mapping, offshore ERA5 conditions were transformed into nearshore-equivalent wave series representing the environmental forcing at the ADCP location.

In this chapter, the downscaled dataset is first introduced and its underlying methodology briefly explained to provide context on how the long-term series was obtained. Subsequently, the RBF dataset is compared to the local ADCP observations to assess the consistency between both sources. Finally, an EVA is conducted using the extended 47-year dataset, following the same procedure described in Section F.2.2, to evaluate how the longer temporal record influences the estimation of design wave conditions.

F.3.2. Downscaling Methodology

Adaptation for the Sisal Case Study

For the Sisal site, the hybrid downscaling approach described by [Antolínez et al., 2018] was adapted to generate a long-term nearshore wave dataset. This method combines statistical and empirical techniques to relate large-scale offshore conditions to local measurements, offering an efficient way to reconstruct nearshore wave climates without the need for numerical wave modeling.

The procedure begins with offshore wave parameters from ERA5 (longitude = −90.5°, latitude = 21.5°), representing deep-water conditions in the Gulf of Mexico. These parameters: H_s, mean wave period (T_m) and mean direction (θ_m), are statistically linked to simultaneous measurements from the ADCP located near Sisal at a water depth of approximately 10 m. By establishing this relationship, the method

learns how offshore conditions are modified locally, accounting for the site's depth and directional characteristics.

Once trained, the statistical mapping was applied to the full ERA5 record to generate a 47-year time series of nearshore-equivalent wave conditions. The resulting dataset reproduces how offshore waves would have been observed at the ADCP site if measurements had been available for the entire period. As an empirical model, it integrates both bias correction and nearshore transformation in a single step, capturing realistic local behavior without the computational cost of a physical wave model.

Model Configuration and Sensitivity

The statistical downscaling was implemented using a RBF interpolation, following the framework described by [Camus et al., 2011]. The RBF model defines a multivariate relationship between offshore and nearshore wave conditions by interpolating in a multidimensional space defined by the input parameters H_s, T_m and θ_m. This approach effectively represents non-linear relationships, allowing complex wave transformations to be captured without requiring a physical model.

To evaluate model robustness, a sensitivity analysis was performed by varying the number of sea states used for training. Two configurations were tested: one with 100 randomly selected samples and another with 500. The larger sample size captured a wider range of variability in the ADCP record while maintaining numerical stability and was therefore adopted for the final downscaled dataset.

The resulting time series provides hourly values of H_s, T_m and peak direction (D_p) covering the period 1979–2025. To optimize storage, the data were archived as integer values scaled by a factor of 1000. For analysis in this study, the values were converted back to physical units (meters, seconds and degrees). No further transformations were applied, as the downscaling already reproduces the nearshore, depth-dependent patterns observed in the ADCP record.

Methodological Context and Limitations

The hybrid downscaling applied here represents a statistical implementation of the nearshore transformation process. Because high-quality ADCP data were available, it was unnecessary to perform additional numerical simulations with spectral wave models. Instead, the transformation between offshore and nearshore conditions was derived empirically from the observed data, enabling a computationally efficient reconstruction of long-term nearshore wave conditions.

A limitation of this method is that it does not explicitly simulate physical processes such as shoaling, refraction and depth-induced breaking. These nonlinear mechanisms are only implicitly represented through the statistical correspondence between ERA5 and ADCP measurements. Consequently, extreme offshore waves in the ERA5 record exceeding 4–5 m are downscaled to approximately 3 m at the nearshore site. This attenuation reflects both the depth constraint at 10 m water depth and the limited range of the observed ADCP data, where the highest recorded waves reached 2.63 m. Such constraints are typical of empirical downscaling based on observational data; a process-based numerical model would provide deeper insight into the underlying transformation dynamics.

Despite these limitations, the downscaled dataset reproduces the local wave climatology with high fidelity. The long-term record captures the frequency, directionality and magnitude of nearshore conditions consistent with in-site measurements, providing a robust foundation for the extreme value analysis presented in F.3.4

F.3.3. Historical Comparison of Wave Data

The locally downscaled RBF time series (1979–2025) was compared with the ADCP measurements (2014–2025) to assess its ability to represent site-specific wave conditions.

Time Series Comparison

Figure F.26 shows the complete RBF record (gray) and the overlapping ADCP data (blue). Both datasets exhibit similar seasonal variability, with higher wave heights typically occurring during the winter months when northerly cold fronts and occasional cyclonic systems influence the region. The long-term RBF record highlights interannual fluctuations in wave energy and confirms that the ADCP measurements fall within the historical range represented by the downscaled dataset.

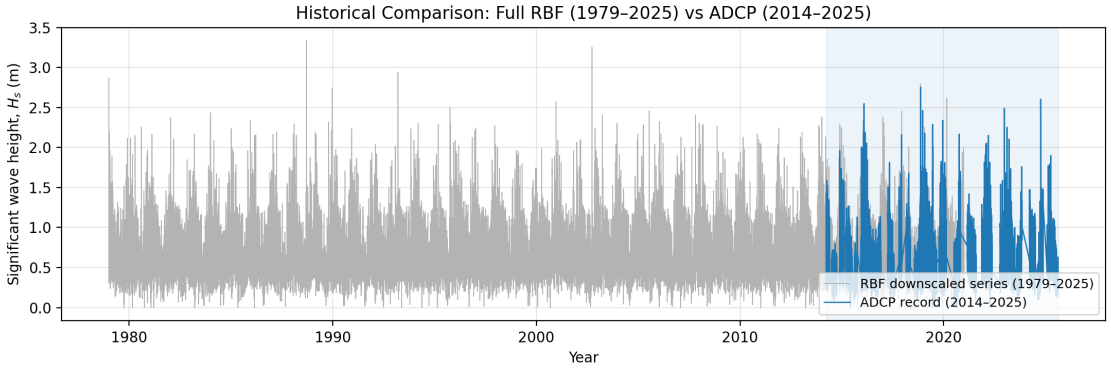

Figure F.26: Historical comparison between the full RBF downscaled series (1979–2025) and the ADCP record (2014–2025). The shaded blue region indicates the overlapping period where both datasets are available.

Significant Wave Height Correlation

A direct comparison of H_s values is presented in Figure F.27. The comparison was performed only for the time periods where both the ADCP and RBF datasets overlap. The data points cluster closely around the 1:1 line, indicating a strong correlation in both magnitude and variability of H_s. Minor deviations at higher wave heights are expected due to measurement uncertainty and temporal resolution differences. Overall, the RBF downscaling effectively reproduces the range and distribution of observed sea states, confirming that the transformation successfully transfers offshore ERA5 wave energy to nearshore conditions at the fish-farm site.

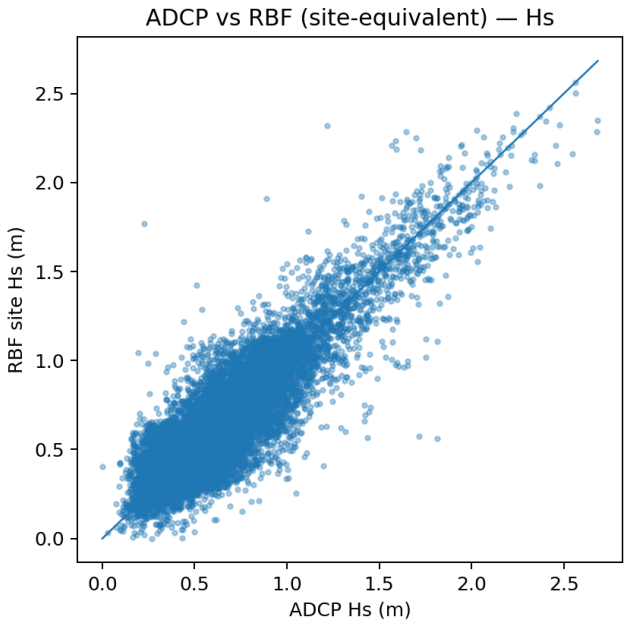

Figure F.27: Scatter plot comparing concurrent significant wave heights H_s from ADCP and RBF datasets during the overlapping period (2014–2025). The RBF data are site-equivalent, downscaled using the ADCP as reference.

Wave Direction Comparison

The comparison in wave direction is presented in Figure F.28. Each point represents a simultaneous directional observation from the ADCP and RBF datasets, with the color scale indicating the corresponding H_s. The comparison was restricted to periods where both datasets were available. The overall alignment of points along the 1:1 line indicates that the two datasets are generally consistent in their mean wave direction.

To quantify this agreement, the absolute directional difference was computed for each overlapping timestamp while accounting for the circular nature of wave direction data, using:

$$\Delta_i = \min\left(|D_{\text{ADCP},i} - D_{\text{RBF},i}|,\ 360 - |D_{\text{ADCP},i} - D_{\text{RBF},i}|\right) \tag{F.4}$$

where Δ_i is the absolute difference in mean direction for each time step i. From the resulting series of Δ_i values, two summary statistics were calculated: the mean absolute error (MAE) and the 90th-percentile deviation (P90):

$$\text{MAE} = \frac{1}{N}\sum_{i=1}^{N}\Delta_i, \qquad \text{P90} = \text{percentile}_{90}(\Delta_i) \tag{F.5}$$

The obtained values, MAE = $32.5°$ and P90 = $75.1°$, indicate that the RBF-downscaled data reproduces the directional variability of the ADCP record well, with most differences falling below $75°$.

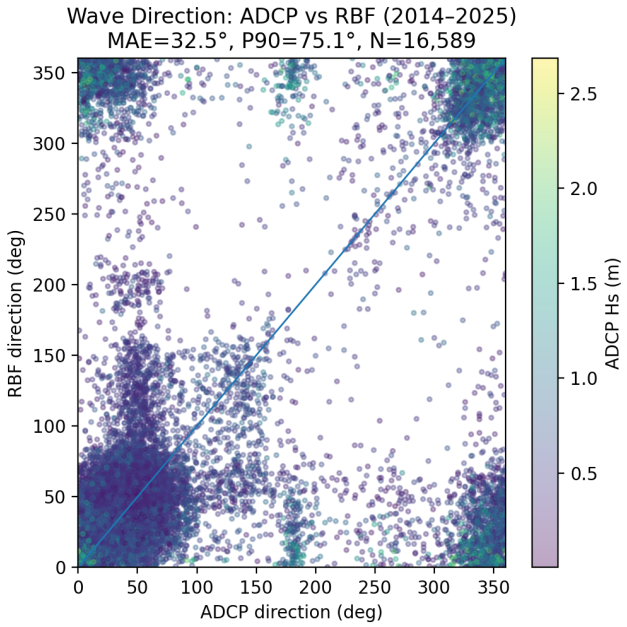

Figure F.28: Wave direction comparison between ADCP and RBF datasets (2014–2025). Each point represents a concurrent measurement, colored by ADCP H_s magnitude.

Interpretation

The comparison of the RBF and ADCP datasets demonstrates that the downscaled RBF series accurately represents both the magnitude and directional characteristics of locally measured waves. The RBF series therefore provides a reliable long-term extension of the short ADCP record, allowing for EVA. In the following section, the validated RBF dataset is used to estimate return wave heights through the same POT and GPD methodology applied earlier to the ADCP data.

F.3.4. Waves RBF data

EVA RBF data

Building upon the validated RBF dataset described in Section F.3.3, the same POT methodology introduced in Section F.2.2 is applied here to estimate long-term extreme wave conditions. The previous analysis based on the twelve-year ADCP record provided a detailed view of local extremes, but its limited duration constrained the stability of the statistical fit.

The analytical procedure follows the same main steps as in Section F.2.2: (1) threshold selection through diagnostic tests of the chi-square statistic, p-value and number of peaks; (2) declustering of

independent storm events; (3) verification of the Poisson process assumption; (4) fitting of a GPD to the exceedances; and (5) computation of return levels for selected design periods.

The only methodological differences are that the RBF dataset provides a longer record and that the threshold selection is re-evaluated to reflect the expanded statistical base. The four-day declustering interval used for the ADCP analysis is retained to ensure methodological consistency. The following subsections present the diagnostic results, GPD fit and return level estimates obtained for the long-term RBF dataset.

The threshold selection for the long-term RBF dataset follows the same diagnostic procedure described in Section F.2.2. The goal is to identify a threshold that is high enough to isolate extreme wave events, while retaining a sufficient number of independent peaks for robust statistical fitting. Candidate thresholds were evaluated using the chi-square statistic, the p-value and the number of exceedances, following the same diagnostic indicators applied in the ADCP-based analysis.

The results of these diagnostic tests are shown in Figure F.29. The chi-square statistic (solid line) and p-value (dashed line) are plotted as functions of the threshold for the RBF dataset covering 1979–2025. The p-value indicates the goodness of fit of the Poisson model to the exceedance counts, while the chi-square statistic measures the deviation between the observed and expected number of events. As with the ADCP analysis, the ideal threshold is characterized by a low chi-square statistic, a high p-value (typically above 0.05) and an adequate number of independent peaks.

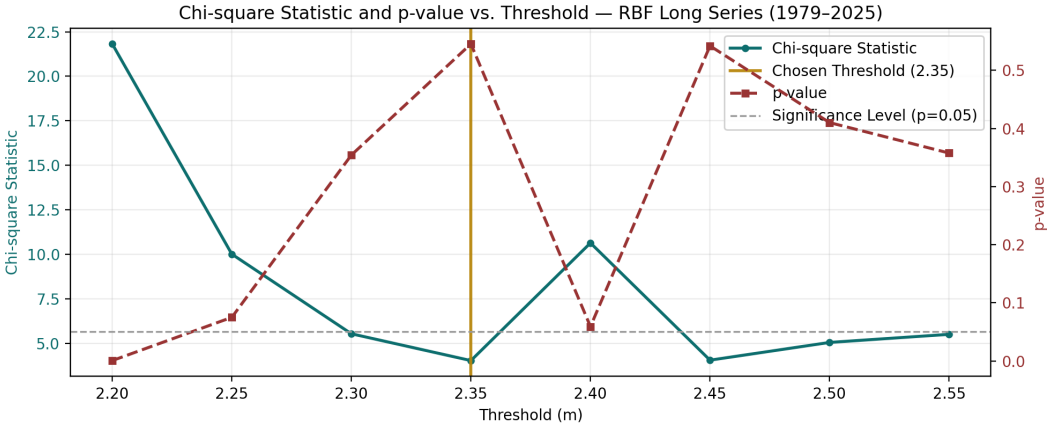

Figure F.29: Threshold diagnostics for POT analysis using the long-term RBF dataset (1979–2025). The chi-square statistic (solid teal line) and p-value (dashed red line) are plotted against the threshold. The vertical yellow line marks the selected threshold at 2.35 m.

Table F.5 summarizes the diagnostic results across the tested thresholds. The table shows that chi-square values decrease sharply up to approximately 2.35 m, where they reach their minimum, while the corresponding p-values remain high and the number of peaks is still sufficient for statistical stability. Based on these indicators, a threshold of $u = 2.35$ m was selected as the optimal working threshold for the RBF dataset.

Table F.5: Summary of diagnostic results for threshold selection using the RBF dataset (1979–2025). The selected threshold at $u = 2.35$ m provides the best statistical balance between model fit and number of peaks.

Threshold (m)	Chi-square	p-value	Number of Peaks
2.20	21.82	0.001	84
2.25	10.01	0.075	68
2.30	5.53	0.354	49
2.35	**4.03**	**0.545**	**25**
2.40	10.64	0.059	21
2.45	4.05	0.542	17
2.50	5.05	0.410	13
2.55	5.50	0.358	11

The chosen threshold of 2.35 m ensures that the selected exceedances represent independent storm events without including too many moderate waves. Compared to the ADCP-based analysis, the lower diagnostic variability observed here reflects the larger sample size and longer observation period of the RBF dataset. This threshold is used in the following steps of the POT analysis to identify independent extreme events and fit the GPD.

Figure F.30 illustrates the full RBF time series together with the declustered POT maxima identified above the selected threshold of 2.35 m. A declustering interval of four days was applied, consistent with the previous ADCP-based analysis, to ensure that consecutive peaks within the same storm system are treated as a single independent event. The resulting plot shows that the selected threshold effectively isolates a limited number of distinct extreme wave events while maintaining a sufficiently long time base for reliable statistical analysis.

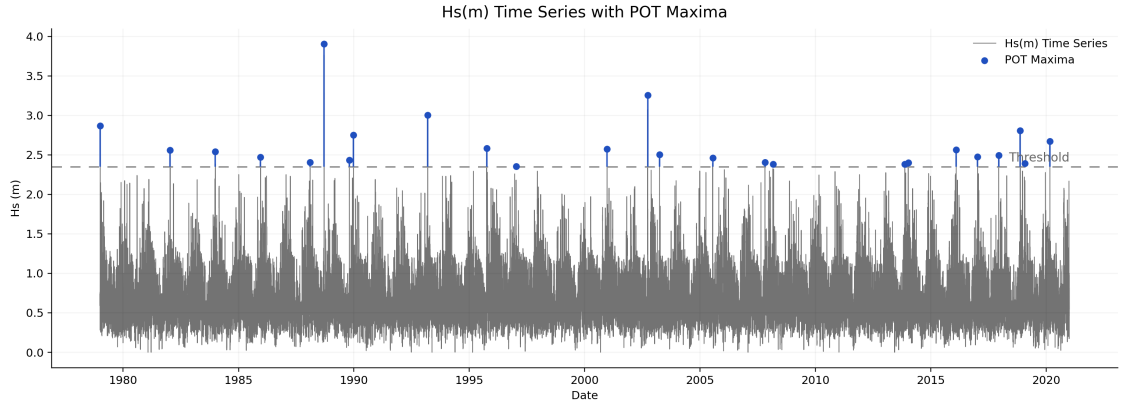

Figure F.30: Time series of significant wave height from the long-term RBF dataset (1979–2025) with declustered POT maxima above the selected threshold of 2.35 m. The dashed line marks the chosen threshold and the blue markers indicate independent extreme events.

To verify that the frequency of extreme wave events above the selected threshold of 2.35 m can be described by a Poisson process, the annual counts of independent exceedances were analysed over the full RBF record. Each year was assigned the number of events that exceeded the threshold after applying the four-day declustering interval. The resulting distribution of exceedance counts is shown in Figure F.31.

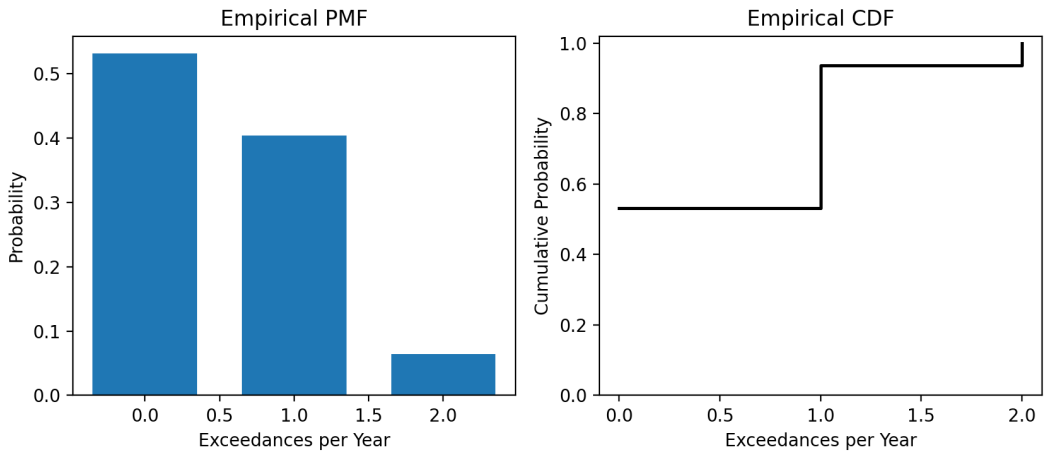

Figure F.31: Empirical Probability Mass Function (PMF, left) and Cumulative Distribution Function (CDF, right) of annual exceedance counts for the RBF dataset with a threshold of 2.35 m. The PMF shows that most years contain zero or one independent extreme event, while the CDF confirms the rarity of multiple occurrences within a single year.

The PMF indicates that more than half of the years have no exceedances, while roughly 40% contain a single independent extreme event and only a few years record two or more. This pattern is consistent with the expected rarity of severe storm events in the region. The corresponding CDF demonstrates a near-monotonic increase, supporting the assumption that exceedance counts are random and independent between years.

To further test this assumption, the empirical CDF of exceedance counts was compared with a fitted Poisson distribution using a mean rate parameter of $\lambda = 0.53$ events per year, corresponding to the long-term average occurrence rate derived from the dataset. Figure F.32 shows the comparison between the empirical and theoretical CDFs. The close alignment of the two curves indicates that the annual occurrence of extreme wave events can be represented by a Poisson process, validating the use of the POT–GPD framework for subsequent return level estimation.

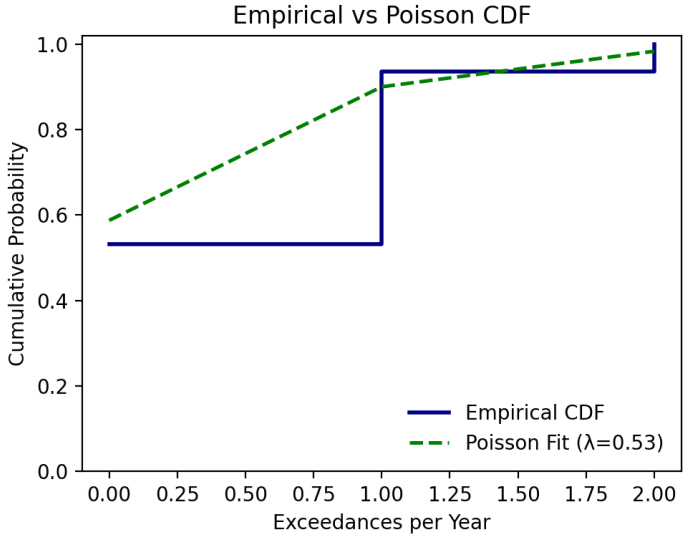

Figure F.32: Comparison between empirical and fitted Poisson CDFs of annual exceedance counts for the RBF dataset (1979–2025) with $\lambda = 0.53$. The close match confirms that exceedance arrivals follow a random Poisson process.

Return level RBF

Once the threshold of $u = 2.35$ m was selected (Section F.3.4), independent extreme events were identified using the four-day declustering rule to ensure that consecutive peaks belonging to the same storm were not double-counted. The resulting exceedances above this threshold were then modelled using the GPD, as introduced in Section F.2.2. The GPD provides a flexible statistical description of the upper tail of the distribution and is defined by two parameters: the scale parameter σ_u, which controls the spread of exceedances above the threshold and the shape parameter ξ, which determines whether the distribution has a finite or unbounded upper tail.

For the RBF dataset, diagnostic checks confirmed that the GPD provides an adequate fit to the upper tail. Figure F.33 presents the fitted probability density function (PDF) and exceedance probability plot. Both plots demonstrate that the GPD accurately reproduces the empirical distribution of extremes, validating its use for return level estimation.

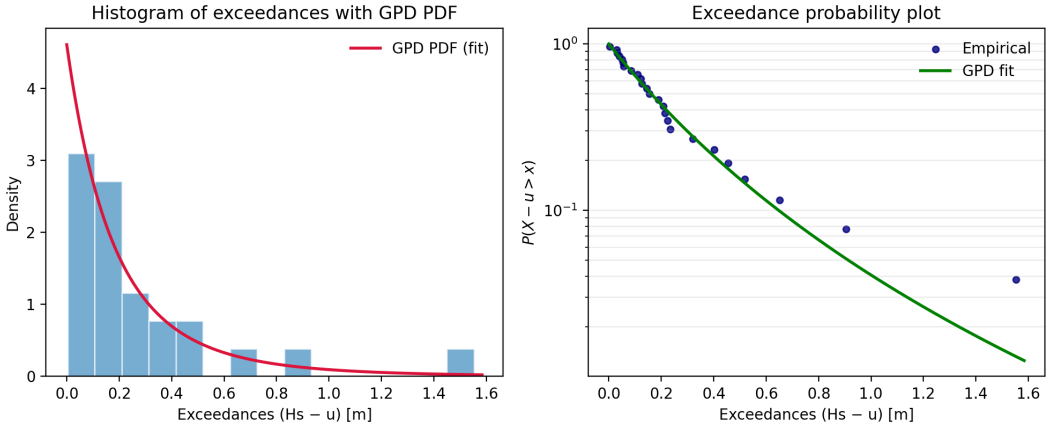

Figure F.33: GPD fit for exceedances in the RBF dataset above $u = 2.35$ m. Left: histogram of exceedances with fitted PDF. Right: exceedance probability plot showing agreement between empirical and modelled probabilities.

The return level (RL_T) for a given return period T was estimated using the same formulation as in Section F.2.2, which relates the magnitude of the T-year event to the exceedance rate and the fitted GPD parameters:

$$RL_T = u + \frac{\sigma_u}{\xi}\left[\left(\frac{n_{th} \cdot N_T}{M}\right)^{\xi} - 1\right],$$

where u is the selected threshold, σ_u and ξ are the GPD parameters, M is the total number of observations and n_{th} is the number of peaks above the threshold. For the RBF dataset, the fitted parameters were $\sigma_u = 0.217$ and $\xi = 0.216$, indicating a moderately heavy-tailed distribution with no finite upper bound. The parameters σ_u and ξ were estimated from the exceedances above the threshold using maximum likelihood estimation (MLE), which identifies the parameter values that maximise the likelihood of observing the dataset under the GPD model.

This procedure follows the standard approach for extreme value analysis in Python. The fitted parameters for the RBF dataset were $\sigma_u = 0.217$ m and $\xi = 0.216$, indicating a moderately heavy-tailed distribution with no finite upper bound.

Using these parameters, return levels were estimated for the 5- and 20-year return periods. Figure F.34 shows the fitted return-level curve based on a threshold of $u = 2.35$ m. The 5-year and 20-year return levels correspond to $H_s = 2.62$ m and $H_s = 3.06$m, respectively, both of which are shown in the figure. The 20-year value aligns with the typical operational lifespan of offshore fish farms of approximately 20 years [Bakker et al., 2024]. The curve shows a smooth increase in return level with return period, consistent with a weakly positive shape parameter and contrasts with the bounded behaviour observed in the ADCP-based analysis.

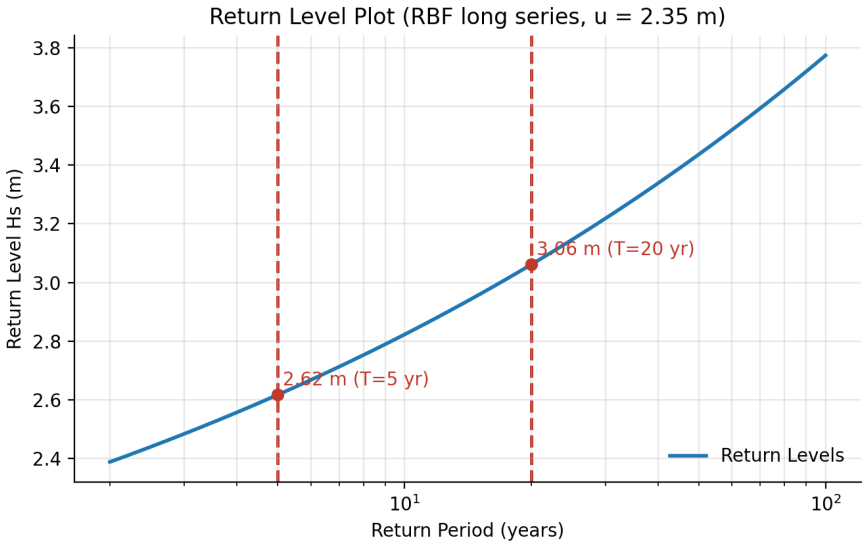

Figure F.34: Return level plot for the RBF long-term dataset ($u = 2.35$ m). The 5-year and 20-year return levels correspond to $H_s = 2.62$ m and $H_s = 3.06$ m, respectively. The positive shape parameter ($\xi = 0.216$) indicates an unbounded tail, resulting in a gradual increase of return levels with return period.

The longer RBF record allows for a more stable estimate of extreme wave heights than the shorter ADCP series. The design wave height of 3.06 m falls within the same range as the 20-year value derived from the ADCP data, but the positive shape parameter implies a heavier tail and higher extremes for longer return periods. This result reflects the advantage of combining long-term reanalysis with local calibration: the RBF dataset improves statistical stability while maintaining local accuracy, providing a robust and reliable basis for design applications.

Wave Height and Period RBF

This subsection extends the analysis of the relationship between H_s and T_p using the long-term RBF downscaled dataset. The objective is to obtain representative T_p values corresponding to the design wave heights identified from the RBF extreme value analysis in Section F.3.4, and to compare the resulting relationship with the locally measured ADCP data presented in Section F.2.2.

Following the same procedure applied to the ADCP dataset, a power-law regression of the form

$$T_p = a\, H_s^b \tag{F.6}$$

was fitted in log–log space using all hourly data from 1979 to 2025. The analysis uses the newly provided RBF dataset, which includes the downscaled T_p derived from ERA5 and statistically transformed to the local ADCP site. The regression provides a compact representation of how the dominant wave period scales with height across the full long-term record.

Figure F.35 presents the scatter of T_p versus H_s for the complete RBF record, together with the fitted power-law curve. The regression parameters are $a = 4.94$ and $b = 0.48$, with a coefficient of determination of $R^2 = 0.21$ based on approximately 259,000 paired observations. At the 20-year design wave height of $H_s = 3.06$ m, the fitted relation yields a corresponding peak period of $T_p = 8.42$ s. This trend is consistent with the ADCP-based analysis (Figure F.16), which produced a slightly shorter design period of $T_p = 7.85$ s at $H_s = 2.96$ m. The difference between the two datasets reflects the longer averaging period of the RBF reanalysis, which incorporates a greater number of moderate to long-period events.

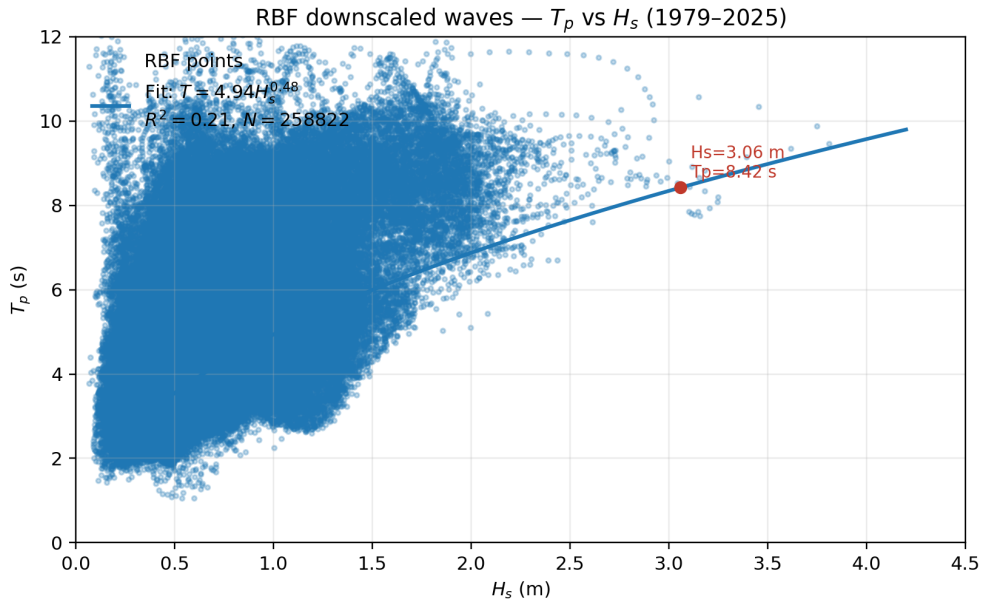

Figure F.35: Power-law regression of T_p versus H_s for the RBF downscaled dataset (1979–2025). The blue line represents the fitted power-law relation ($a = 4.94$, $b = 0.48$, $R^2 = 0.21$), and the red marker indicates the 20-year design point ($H_s = 3.06$ m, $T_p = 8.42$ s).

To further relate the regression to the extreme value results, two design heights were evaluated on the fitted curve corresponding to the 5-year and 20-year return levels identified in Section F.3.4. These values, $H_s = 2.62$ m and $H_s = 3.06$ m, correspond to peak periods of $T_p = 7.82$ s and $T_p = 8.42$ s, respectively. Both points are shown in Figure F.36. The smooth increase in T_p with H_s confirms that larger waves are associated with longer periods, a trend characteristic of storm-driven seas in the region.

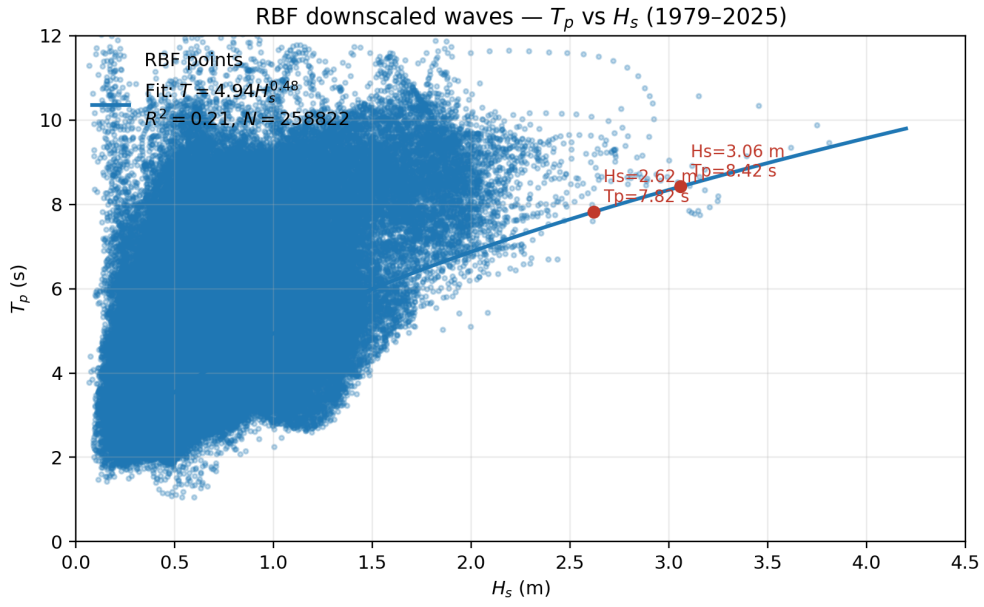

Figure F.36: RBF downscaled waves showing T_p versus H_s, with the fitted power-law curve and design points at 5- and 20-year return levels ($H_s = 2.62$ m, $T_p = 7.82$ s and $H_s = 3.06$ m, $T_p = 8.42$ s).

The regression for the long-term RBF record produces a stronger correlation ($R^2 = 0.21$) than the twelve-year ADCP dataset ($R^2 = 0.13$), reflecting the improved statistical stability from the extended record length and continuous offshore forcing. Nevertheless, both datasets show the same nonlinear trend with similar exponents ($b \approx 0.4$–0.5), indicating consistent behaviour between measured and downscaled data. The slightly longer peak periods in the RBF data suggest that the reanalysis captures more swell influence than the locally measured ADCP record, which is dominated by short-period storm waves. Together, these two datasets provide upper and lower bounds on the expected range of wave periods for the design wave heights at the Sisal site.

Normal wave conditions RBF

In addition to the extreme value analysis, the long-term RBF dataset (1979–2025) was analysed to characterise the most frequent, or normal, sea states. This analysis provides a statistical description of the dominant wave conditions represented in the full record.

Figure F.37 shows the occurrence distribution of H_s based on all RBF data points. The histogram indicates a right-skewed distribution, with the highest density of occurrences between 0.4 m and 0.8 m. The calculated mode of the distribution is $H_s = 0.61$ m, the mean value is $H_s = 0.66$ m and the 90th percentile is $H_s = 1.05$ m. These values define the typical range of wave heights observed at the site over the 47-year period.

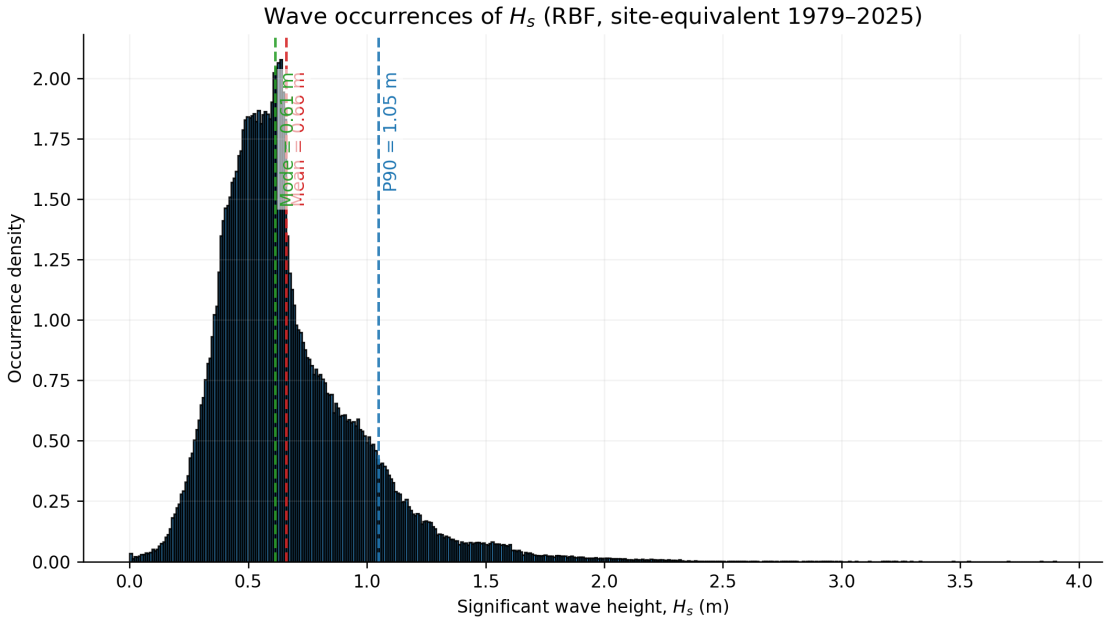

Figure F.37: Wave occurrence distribution of H_s from the RBF dataset (1979–2025). The mode (0.61 m), mean (0.66 m) and 90th percentile (1.05 m) are indicated by dashed lines.

The T_m provided in the RBF dataset (variable `mwp`) was then related to H_s to identify the representative period corresponding to the modal wave height. A power-law regression of the form $T_m = aH_s^b$ was fitted to the complete dataset, yielding parameters $a = 3.68$ and $b = 0.29$ ($R^2 = 0.50$, $N = 368{,}992$). The conditional mean period corresponding to the modal wave height ($H_s = 0.66$ m) was calculated as $T_m = 3.14$ s. The relationship between T_m and H_s, including the fitted power law and the identified normal condition, is shown in Figure F.38.

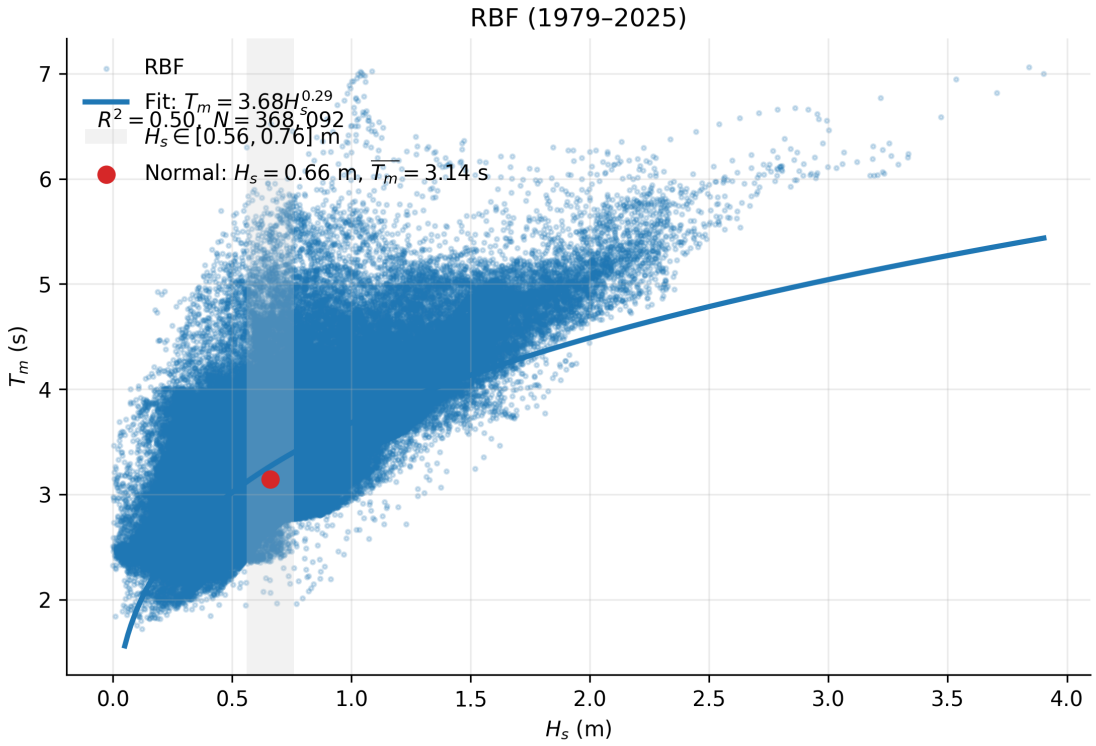

Figure F.38: Relationship between H_s and T_m from the RBF dataset (1979–2025). The fitted power-law $T_m = 3.68\, H_s^{0.29}$ is shown in blue, with $R^2 = 0.50$. The red marker denotes the mean wave period of $T_m = 3.14$ s corresponding to the modal height $H_s = 0.66$ m.

This statistical description provides a reference for the most typical wave height and corresponding mean wave period in the long-term RBF record. The results are based solely on direct calculations from the RBF dataset and the fitted H_s–T_m regression, without the use of any additional assumptions or scaling factors.